Deoxynucleotide biosynthesis and regulation

a study of deoxynucleoside kinases and deoxynucleotide pools

Skovgaard, Tine

Publication date:
2009

Document Version
Publisher's PDF, also known as Version of record

Citation for published version (APA):
Skovgaard, T. (2009). *Deoxynucleotide biosynthesis and regulation: a study of deoxynucleoside kinases and deoxynucleotide pools*. Roskilde Universitet.

Deoxynucleotide Biosynthesis and Regulation

A Study of Deoxynucleoside Kinases and Deoxynucleotide Pools

Tine Skovgaard

Roskilde University
Department of Science, Systems and Models

Ph.D. thesis
Roskilde 2009

PREFACE

This Ph.D. thesis is based on work carried out at the Department of Science, Systems and Models at Roskilde University under the supervision of Professor Birgitte Munch-Petersen. Crystallography was carried out at the Department of Molecular Biology, Swedish University of Agricultural Sciences, Uppsala Biomedical Centre in collaboration with Hans Eklund and Ulla Uhlin.

The aim of the present study has been to provide insight into regulation of deoxynucleotide pools and to obtain an increased understanding of important enzymes involved in nucleotide metabolism. The latter has been attempted by characterization of a new thymidine kinase from *Caenorhabditis elegans* and by a detailed structure-function study of human and *C. elegans* thymidine kinases.
Changes in deoxynucleotide pools as a consequence of DNA damage have been studied in different cell lines with the aim of elucidating the role of thymidine kinase 1 and mitochondrial function in deoxynucleotide damage response.

The main topics presented in this thesis include a presentation of thymidine kinase 1 and the importance of TK1 and other deoxynucleoside kinases in therapy. The regulation of some of the key enzymes involved in nucleotide biosynthesis is presented, and the consequences of imbalances in cellular and mitochondrial dNTP pools are discussed. Furthermore, I briefly summarize and discuss some of the results obtained during my work with deoxynucleotide metabolism.
The thesis includes two published papers (Papers I, II) and three unpublished papers (Paper III (submitted), IV (submitted) and V (in preparation)).

ACKNOWLEDGEMENTS

First and foremost, I would like to thank my excellent supervisor Birgitte Munch-Petersen for her never-ending optimism and for guiding me through this work, as well as for great discussions and for letting me work so independently.

Thanks to Lene Juel Rasmussen for guidance and support with the dNTP pool study and for encouraging conversations, and to Marianne Lauridsen for good laughs in the lab and for always being helpful.

In Uppsala, I would like to thank the crystallography group: Hans Eklund for letting me work there and Ulla Uhlin for helping with the crystal structure. Martin Welin, Nils Egil Mikkelsen and Urszula Kosinska for patiently answering all my questions and the rest of the lab for inviting me to the 'Thursday beer club' and for making me feel welcome.

My office mates: Peter Kristoffersen for always being helpful and kind, and Nicolai Balle Larsen for commenting critically on some of my papers and for cheering me up with champagne when my lab work failed.

Thank you, past and present lab members and colleagues: Maria Thunø for making me laugh then and now, Mesut Bilgin, Anne Lind Møller, Louise Slot Christiansen, Gabriella van Zanten and Claus Desler Madsen for being good sparring partners and creating a good working atmosphere, and all my former students for their ambitious work.

My sister for cheering me up with flowers and fruits when the writing was tough, and my parents for believing in me.

Finally, I am grateful to my husband Morten for correcting my hopeless English punctuation, but even more so for being behind me and supporting me through this work. Without his encouragement my work would have been much harder.

TABLE OF CONTENTS

ABBREVIATIONS

10-CHO-THF	10-formyltetrahydrofolate
ADP	Adenosine diphosphate
APC	Anaphase promoting complex
AraC	1-β-D-arabinofuranosyl cytosine
AraU	1-β-D-arabinofuranosyl uridine
ATP	Adenosine triphosphate
AZT	3'-azidothymidine
*Ba*TK	*Bacillus anthracis* thymidine kinase
*Bc*TK	*Bacillus cereus* thymidine kinase
*Ca*TK	*Clostridium acetobutylicum* thymidine kinase 1
Cdk1	Cyclin dependent kinase
CDP	Cytidine diphosphate
*Ce*TK1	*Caenorhabditis elegans* thymidine kinase
CMPK	Cytidine monophosphate kinase
dAdo	Deoxyadenosine
dADP	Deoxyadenosine diphosphate
dAMP	Deoxyadenosine monophosphate
dATP	Deoxyadenosine triphosphate
dCDP	Deoxyytidine diphosphate
dCK	Deoxyytidine kinase
dCMP	Deoxyytidine monophosphate
dCyd	Deoxyytidine
dGK	Deoxyguanosine kinase
dGuo	Deoxyguanosine
DHF	Dihydrofolate
DHODH	Dihydroorotate dehydrogenase
*Dm*dNK	*Drosophila melanogaster* deoxynucleoside kinase
dN	Deoxynucleoside
dNTP	Deoxynucleoside triphosphate
DNC	Deoxynucleoside carrier
dNK	Deoxynucleoside kinase
dThd	Thymidine
dTDP	Thymidine diphosphate
dTMP	Thymidine monophosphate
dTTP	Thymidine triphosphate

dUDP	Deoxyuridine diphosphate
dUMP	Deoxyuridine monophosphate
dUTP	Deoxyuridine triphosphate
FaraA	9-β-D-arabinofuranosyl-2-fluoroadenine monophosphate
GDP	Guanosine diphosphate
GVHD	Graft versus host disease
HSV1TK	Herpes simples virus type 1 kinase
HuTK1	Human thymidine kinase
MDS	Mitochondrial depletion syndrome
MNGIE	Mitochondrial neurogastrointestinal encephalomyopathy
mtDNA	Mitochondrial DNA
mtNOS	Mitochondrial nitrogen oxide synthase
NADH	Nicotinamide-adenine dinucleotide
NDK	Nucleoside diphosphate kinase
nDNA	Nuclear DNA
RNR	RIbionucleotide reductase
THF	Tetrahydrofolate
TK1	Thymidine kinase 1
TK2	Thymidine kinase 2
TMPK	Thymidine monophosphate kinase
*Tm*TK	*Thermotoga maritima* thymidine kinase
TP	Thymidine phosphorylase
TP4A	P1-(5′-adenosyl)P4-(5′-(2′-deoxy-thymidyl)) tetraphosphate
TS	Thymidine synthase
UDP	Uridine diphosphate
*Uu*TK	*Ureaplasma urealyticum* thymidine kinase

SUMMARY

Detailed knowledge of function and regulation of the key enzymes involved in deoxynucleotide metabolism is of utmost importance for understanding and treating a number of different diseases.

The key enzymes in the salvage of deoxynucleosides to deoxynucleoside triphosphates (dNTPs) are the deoxynucleoside kinases, and they have been found to be of major importance to the treatment of e.g. cancer and viral diseases by 'suicide' gene/chemo therapy. Along with the deoxynucleoside kinases the key enzyme in the *de novo* synthesis, ribonucleotide reductase, is playing a significant role in maintaining a constant and balanced supply of deoxynucleotides for DNA synthesis and repair.

Dysfunction of several of the enzymes in deoxynucleotide metabolism is known to cause imbalanced dNTP pools, a condition that can be severely mutagenic. Furthermore, mitochondrial DNA depletion is found to influence the dNTP pools and is associated with a mutator phenotype.

In the present thesis the structure-function relations of three different deoxynucleoside kinases are investigated in order to evaluate their possible role as candidates for 'suicide' gene therapy.

In a directed evolution study with the multisubstrate deoxynucleoside kinase from *Drosophila melanogaster* (*Dm*dNK) a double mutant, N45D/N64D, was created, with increased specificity toward several cytotoxic nucleotide analogues. Detailed kinetic and structural analysis revealed that the N64D mutation was responsible for the increased specificity towards the nucleoside analogue 3'-azidothymidine (AZT) (Paper I).

Characterization of a new thymidine kinase from *Caenorhabditis elegans* with high sequence similarity to human thymidine kinase 1 (TK1) led to a new mutation study (Paper II). By site-directed mutagenesis a number of amino acids were mutated in the active site of both human and *C. elegans* TK1 (HuTK1 and *Ce*TK1). By kinetic and structural analysis it was found that one HuTK1 mutant had increased specificity towards AZT and some *Ce*TK1 mutants had widened their substrate specificity to include deoxyguanosine and deoxycytidine, substrates not commonly phosphorylated by TK1-type enzymes (Paper VI).

In a study of human osteosarcoma cells subjected to UV-induced DNA damage, TK1 deficiency was found to increase the survival rate of the cells. Furthermore, it was shown that the thymidine triphosphate pools were lower in TK negative cells, emphasizing the importance of TK1 in maintaining balanced dNTP pools. The increased survival rate in TK1 deficient cells is suggested to be due to increased levels of thymidine absorbing some of the UV rays (Paper III).

UV-irradiation did not induce changes in dNTP pools in normal and TK1 deficient human osteosarcoma cells but when the TK negative cells are also deficient for mitochondrial DNA (mtDNA), all four dNTP pools were found to increase. A similar increase is also observed in yeast cells along with increased mutation frequencies, and it may explain the mutator phenotype of mtDNA deficient cells. The mechanism behind the UV-induced pool increase is suggested to be insufficient dATP feedback inhibition of DNA damage induced ribonucleotide reductase (Paper V).

SUMMARY IN DANISH

For at kunne forstå og behandle en række forskellige sygdomme er det yderst vigtigt at have et detaljeret kendskab til funktion og regulering af deoxynukleotid-metabolismens nøgleenzymer.

Deoxynukleosidkinaser er nogle af de vigtige enzymer i produktionen af deoxynukleosidtrifosfater (dNTPer) fra deoxynukleosider, og de har vist sig at være yderst vigtige i behandling af f.eks. cancer og virale sygdomme med 'selvmords'-genterapi/kemoterapi. Ud over deoxynukleosidkinaserne er ribonukleotidreduktase et af de centrale enzymer i *de novo* deoxynukleotid-metabolisme, og det spiller en vigtig rolle i opretholdelsen af en konstant og balanceret forsyning af deoxynukleotider til DNA-syntese og -reparation.

En defekt i et eller flere af enzymerne involveret i deoxynukleotid-metabolisme vides at kunne skabe ubalance i dNTP-niveauerne, en ubalance der kan være mutagen. Cellens dNTP-niveauer påvirkes desuden af manglen på mitokondrielt DNA, en tilstand der associeres med en øget mutationsfrekvens.

I denne afhandling undersøges sammenhængen mellem struktur og funktion for tre forskellige deoxynukleosidkinaser i et forsøg på at evaluere deres mulige rolle som kandidater til 'selvmords'-genterapi.

Et mutationsstudie med den multisubstrate deoxynukleosidkinase fra *Drosophila melanogaster* (*Dm*dNK) førte til produktionen af dobbeltmutanten N45D/N64D, som havde øget specificitet for flere cytotoksiske nukleosidanaloger. En detaljeret kinetik- og struktur-analyse viste, at mutatnonen N64D var ansvarlig for den øgede specificitet for nukleosidanalogen 3'-azidothymidin (AZT) (Artikel I).

Karakteriseringen af en ny deoxynukleosidkinase fra C*aenorhabditis elegans*, som har høj sekvenslighed med human tymidinkinase 1 (TK1), foranledigede et nyt mutationsstudie (Artikel II). I det aktive site i både human og *C. elegans* TK1 (HuTK1 og *Ce*TK1) blev flere aminosyrer muteret ved hjælp af 'site-directed' mutagenese. Ved strukturel og kinetikbaseret analyse fandt man en HuTK1-mutant med øget specificitet for AZT og nogle *Ce*TK1-mutanter, der havde øget deres substratområde til at inkludere deoxyguanosin og deoxycytidin – substrater, der ikke normal fosforyleres af TK1-lignende enzymer (Artikel IV).

I et studie med human osteosarcoma-celler, der blev udsat for UV-induceret DNA-skade, viste det sig, at celler, der manglede TK1, havde en øget overlevelsesrate. Desuden fandt man et lavere niveau af thymidintrifosfat i de TK-negative celler, hvilket understreger vigtigheden af en funktionel TK1 i opretholdelsen af balancerede dNTP-niveauer. Det blev foreslået, at den øgede overlevelsesrate i TK-negative celler skyldes et højere niveau af thymidin, der abosrberer nogle af UV-strålerne (Artikel III).

UV-bestråling havde ingen indflydelse på dNTP-niveauerne i normale og TK-negative human osteosarcoma-celler, men hvis de TK-negative celler også manglede mitokondrielt DNA (mtDNA), var der en stigning i alle fire dNTP-niveauer. En lignende stigning finder man også i gærceller, hvor den er sammenfaldende med en øget mutationsfrekvens. Dette kan måske forklare de øgede mutationsfrekvenser observeret i mtDNA-fri celler. Det foreslås, at mekanismen, der ligger bag den UV-inducerede stigning i dNTP-niveauerne, kan være utilstrækkelig 'feedback'-hæmning af ribonukleotidreduktasen, som induceres ved DNA-skade (Artikel V).

INTRODUCTION

Deoxynucleotide Metabolism – an Overview

Production of deoxynucleotides for DNA synthesis and repair is a complex and highly regulated metabolic system. Two major pathways are involved in deoxynucleotide metabolism, the *de novo* pathway, where the deoxynucleotides are synthesized from small inorganic precursors through many energy demanding enzymatic reactions, and the salvage pathway, where deoxynucleotides are synthesized from the salvage of deoxynucleosides. Some of the key enzymes in each pathway and the mechanism responsible for their regulation are described in more detail in the following sections. This section presents an overview of the two metabolic pathways and a short description of the enzymes involved.

De Novo Synthesis of Deoxynucleotides

DNA precursors synthesized by the *de novo* pathway are formed from ribonucleosides, and with the exception of dTTP they first appear at the diphosphate level. Purine ribonucleoside diphosphates are formed in a series of steps from 5-phosphoribosyl 1-pyrophosphate, and atoms in the purine base are donated from several amino acids, formate and CO_2. The atoms in the pyrimidine base originate mainly from aspartate and carbamoyl phosphate but like the purines the ribose and phosphate moieties originate from 5-phosphoribosyl 1-pyrophosphate.

Both purines and pyrimidines are reduced from nucleoside diphosphates to deoxynucleoside diphosphates by the key enzymes in the *de novo* pathway, ribonucleotide reductase (RNR) [Larsson & Reichard, 1966a; Larsson & Reichard, 1966b]. CDP, GDP and ADP are all substrates for RNR, and after reduction they are converted to deoxynucleoside triphosphates by nucleoside diphosphates kinase (NDK) Thelander & Reichard, 1979]. The route to dTTP formation is more complicated, and thymidine nucleotides can be formed either from uridine or cytidine nucleotides (figure 1).

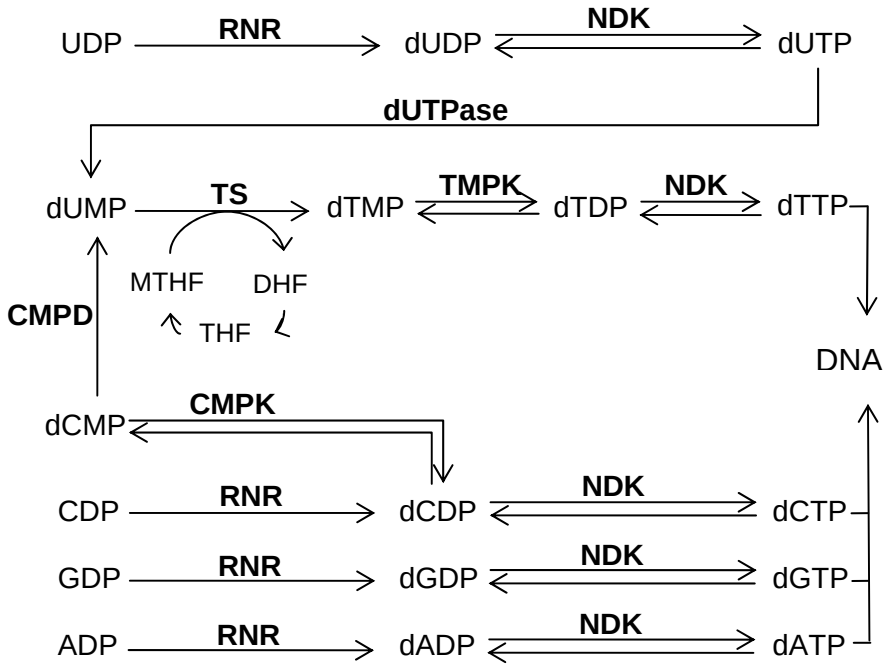

Figure 1
***De novo* production of deoxynucleotides for DNA synthesis in mammals**. Enzyme abbreviations: ribonucleotide reductase (RNR), nucleoside diphosphate kinase (NDK), cytidine monophosphate kinase (CMPK), thymidiylate synthase (TS), thymidylate kinase (TMPK). N^5, N^{10}-methylenetetrahydrofolate, dihydrofolate and tetrahydrofolate are abbreviated MTHF, DHF and THF, respectively.

Like CDP, GDP and ADP, UDP is also a substrate for RNR, and the reduced dUDP is also phosphorylated to dUTP by nucleoside diphosphates kinase. dUTP is subsequently dephosphorylated to dUMP by dUTPase, and dTMP is formed by methylation of dUMP. A methyl group is transferred from N^5, N^{10}-methylenetetrahydrofolate (MTHF) to the pyrimidine base by thymidylate synthase by simultaneous conversion of N^5, N^{10}-methylenetetrahydrofolate to dihydrofolate (DHF) [Reichard, 1988]. The tetrahydrofolate levels are maintained by dihydrofolate reductase that reduces dihydrofolate to tetrahydrofolate (THF), and tetrahydrofolate is subsequently remethylated by serine hydroxymethyl transferase. The dTMP produced by thymidylate synthase (TS) is subsequently phosphorylated in two steps, first by thymidylate kinase (TMPK) and then by nucleoside diphosphates kinase (NDK), and dTTP is ready for incorporation into DNA. The path from cytidine nucleotides to dTTP starts by dephosphorylation of dCDP to dCMP by cytidine monophosphate kinase and the subsequent deamination of dCMP to dUMP by cytidine monophosphate deaminase. The conversion from dUMP to dTTP follows the path described above (figure 1).

Extensive allosteric control is required in order to maintain a balanced supply of dNTPs for DNA synthesis and repair. The main key to this balance is RNR which up- and down-regulates reduction of the four NDPs upon binding of ATP and different dNTPs to two different allosteric sites. One site functions as an on/off switch where binding of ATP stimulates, and dATP inhibits enzyme activity. The other site, responsible for specificity regulation and binding of different (d)NTPs, up and down-regulates reduction of the four NDPs [Thelander & Reichard, 1979]. Yet, the pyrimidines are up and down-regulated simultaneously by RNR and instead, another allosteric enzyme, dCMP deaminase, regulates the balance between the dCTP and dTTP pools. dCMP deaminase is activated by dCTP and inhibited by dTTP [Ellims *et al.*, 1981].

Salvage of Deoxynucleosides by Deoxynucleoside Kinases

Deoxynucleotides can also be synthesized by a much shorter and less energy demanding way by salvage of deoxynucleosides (dN). The key step in deoxynucleoside salvage is the phosphorylation of deoxynucleosides to dNMPs catalyzed by deoxynucleoside kinases (dNKs). In two subsequent phosphorylation steps the dNMPs are phosphorylated to dNTPs by nucleoside monophosphate kinase and nucleoside diphosphate kinase.
In *de novo* synthesis of deoxynucleotides the key step is catalyzed by the multisubstrate RNR which is capable of reducing all nucleoside diphosphates with the exception of thymidine [Thelander & Reichard, 1979]. The first phosphorylation step in the salvage pathway is catalyzed by four different dNKs with overlapping substrate specificities. TK1 and deoxycytidine kinase (dCK) are located in the cytosol whereas thymidine kinase 2 (TK2) and deoxyguanosine kinase (dGK) are located in mitochondria [Lee & Cheng, 1976a; Johansson *et al.*, 1997; Hatzis *et al.*, 1998; Jüllig & Eriksson, 2000].

All four dNKs have been cloned and expressed and are all kinetically characterized [TK1: Bradshaw & Deininger, 1984; Berenstein *et al.*, 2000; dCK: Chottiner *et al.*, 1991; TK2; Johansson & Karlsson, 1997; Wang *et al.*, 1999; dGK: Wang *et al.*, 1996; Johansson & Karlsson, 1996]. TK1 was found to have the most narrow substrate specificity and can only phosphorylate thymidine (dThd) whereas dCK phosphorylates deoxycytidine (dCyd), deoxyguanosine (dGuo) and deoxyadenosine (dAdo). Together, the two cytosolic dNKs phosphorylate all four deoxynucleosides. The same is the case for the two mitochondrial dNKs. TK2 is capable of phosphorylating dThd and dCyd whereas dGK phosphorylates dGuo and dAdo [Arner & Eriksson, 1995].

A comparison of the amino acid sequences of the dNKs reveals distinct evolutionary origins of the four kinases found in mammalia. TK2, dCK and dGK have the same evolutionary origin and are more closely related to the multisubstrate insect dNKs than to mammalian TK1 [Piskur *et al.*, 2004]. This has been confirmed by three dimensional crystal structures showing very similar structures for human dCK, dGK and also for *Drosophila melanogaster* deoxynucleoside kinase (*Dm*dNK) but a radically different structure of TK1 [Sabini *et al.*, 2003; Johansson *et al.*, 2001; Welin *et al.*, 2004].

A simplified overview of both *de novo* and salvage pathways including the cellular localization of some of the key enzymes is presented in figure 2. The overview does not include the more complex metabolic paths of thymidine nucleotide synthesis but summarizes the key points in the *de novo* and salvage pathways described above.

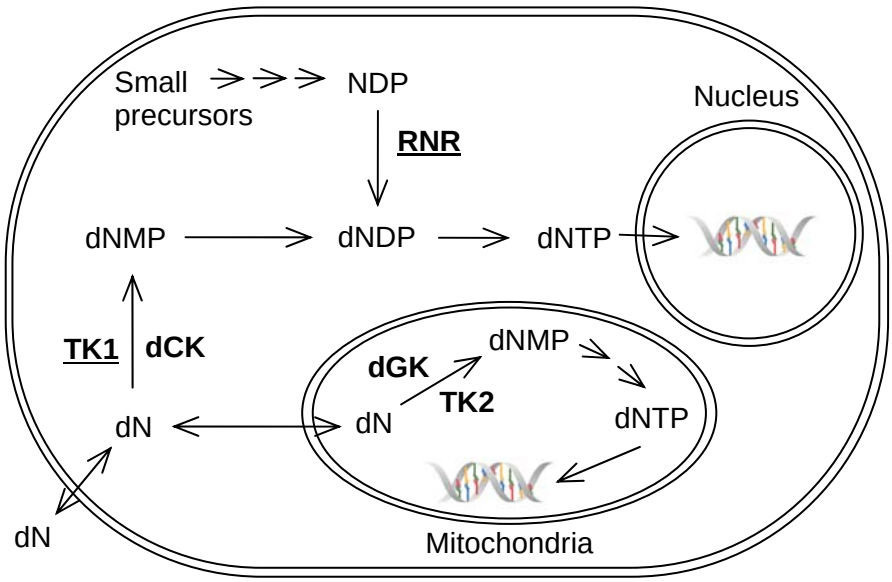

Figure 2
Overview of deoxynucleotide metabolism. Representation of the key enzymes in the *de novo* and salvage pathways. RNR, ribonucleotide reductase; TK1, thymidine kinase 1; dCK, deoxycytidine kinase; dGK, deoxyguanosine kinase; TK2, thymidine kinase 2. The underlined enzymes TK1 and RNR are only expressed in S-phase.

TK1 from the salvage pathway and RNR from *de novo* pathway are both strictly cell cycle regulated and are only expressed in S-phase. The regulation mechanisms are very complex and will be described in more detail in the following sections. The combination of having two pathways for deoxynucleotide synthesis and the complex regulation pattern of some of the key enzymes in both pathways enables the cells to adjust to the changing demands for deoxynucleotides during cell cycle.

Deoxynucleoside Kinases and Nucleoside Analogues in Therapy

The applications of deoxynucleoside kinases are many. TK1 has been the key player in HIV therapy for years where it activates the nucleoside analogue 3'-azidothymidine (AZT). AZT, also known as zidovudine, is part of the first-line therapy for HIV-1 infection. AZT is active in its triphosphorylated form where it is incorporated into viral DNA by HIV reverse transcriptase. Due to the lack of a 3'-hydroxyl group incorporation of AZT induces DNA chain termination and prevents viral proliferation. Prior to DNA incorporation by reverse transcriptase AZT must be phosphorylated by TK1 followed by thymidylate kinase and nucleoside diphosphate kinase [Furman *et al.*, 1986]. The fact that TK1 is of major importance for efficient AZT incorporation has been demonstrated recently by the correlation between inter-individual differences in the rate of TK1 induction and variability in AZT/DNA incorporation [Olivero *et al.*, 2008].

dCK plays a similarly important role in anti-cancer therapy. Patients suffering from leukaemia are typically treated with the nucleoside analogue 1-β-D-arabinofuranosyl cytosine (AraC) which is cytotoxic in its triphosphate form as well as other forms [Rustum & Raymakers, 1992]. AraC is phosphorylated to the monophosphate level (AraCMP) by dCK and to the di- and triphosphate levels by nucleoside monophosphate and diphosphate kinases, respectively. AraCMP can also be deaminated and form AraUMP which can be converted to AraUDP and AraUTP [Braess et al, 1999]. AraCMP and AraCTP exert their cytotoxic effects by competitive inhibition of DNA polymerase α and β. Furthermore, AraCMP is also incorporated into DNA where it leads to chain termination in replicating cells. Phosphorylated AraU can also be incorporated into RNA [Braess et al, 1999]. Several factors have been demonstrated to influence the toxicity of AraC, and one of them is the level of dCK activity. In a study on AraC resistant cells it was found that the resistance correlated with low dCK activity, low levels of intracellular accumulation of AraCTP and a low level of AraC incorporation in DNA [Riva & Rustum, 1985].

Some anti-cancer nucleoside analogues are administered in the monophosphate form due to the increased solubility. One example is the adenine analogue 9-β-D-arabinofuranosyl-2-fluoroadenine monophosphate (FaraA, Fludarabine) used for lymphoma treatment which is dephosphorylated in the extracellular environment by serum phosphatases and then rephosphorylated by dCK and dGK after cellular import [Hochster

et al., 2000]. Chemical synthesis of drugs is often more complicated and less efficient than enzymatic production, and using dCK or dGK as phosphorylation catalysts in the production of FaraA would most likely improve the efficiency and reduce both time and cost of production.

Deoxynucleoside kinases can also play a role in cancer diagnostics. Proliferation of cancer cells can be visualized by positron emission tomography using the thymidine analogue 3'-[18F]fluoro-3'-deoxythymidine [Shields *et al.*, 1998]. The thymidine analogue is specifically phosphorylated in proliferating tissues by cellular TK1. The phosphorylation leads to intracellular trapping, and the [18F] atom serves as a tracer for positron emission tomography and provides a measure of cellular TK1 activity. TK1 is S-phase specific and functions as a reporter of cellular proliferation status and thus as a measure of cancer cell proliferation.

Even though nucleoside analogues are widely used as chemotherapeutic agents, they do have some disadvantages. One major disadvantage is that not only cancer cells but all replicating cells are targeted. Tissues like marrow, skin and gastrointestinal cells are proliferating rapidly and are therefore compromised as a side effect of this type of therapy. By applying deoxynucleoside kinases as 'suicide' genes in gene therapy, attempts have been made to direct the treatment and only target selected cells.

One of the most well-characterized systems in 'suicide' gene therapy is one combining Herpes simplex type 1 thymidine kinase (HSV1TK) with the nucleoside analogue ganciclovir. This system was shown to be successful in mice several decades ago and has later been applied in clinical trials against several solid tumours [Moolten, 1986, Ram *et al.*, 1997, Klatzmann *et al.*, 1998a; Klatzmann *et al.*, 1998b]. Typically, a solid tumour is injected with cells producing a retroviral vector carrying the HSV1TK gene. The gene is subsequently transduced from the host cells to the surrounding tumour cells in which HSV1TK protein is produced. Ganciclovir is an acyclic deoxyguanosine analogue which is efficiently phosphorylated in the cancer cells by HSV1TK to the monophosphate form and subsequently by cellular kinases to the toxic triphosphate form. Apart from causing chain termination and single strand breaks by incorporation into DNA, the toxic triphosphate form also triggers tumour cell death by apoptosis [Beltinger *et al.*, 1999].

Other deoxynucleoside kinases have also been evaluated as candidates for 'suicide' gene therapy. The multisubstrate *Drosophila melanogaster* dNK (*Dm*dNK) [Munch-Petersen *et al.*, 1998] induced increased cell killing in human cancer cell lines treated with (E)-5-(2-bromovinyl)-2'-deoxyuridine and other nucleoside analogues [Zheng *et al.*, 2000; Zheng *et al.*, 2001]. Mutations in both *Dm*dNK and HSV1TK have been made in attempts to improve nucleoside analogue phosphorylation and thereby cell cytotoxicity.

Mutations were created with random [Knecht *et al.*, 2000] or semi-random mutagenesis [Black *et al.*, 2001], and mutants displaying increased cell killing in combination with selected nucleoside analogues were chosen for further analysis. Two such HSV1TK mutants were found to render several human cell lines more sensitive to ganciclovir, and another acyclic nucleoside analogue, acyclovir, and animal studies showed tumour growth inhibition with one or both analogues [Black *et al.*, 2001; Wiewrodt *et al.*, 2003]. Several *Dm*dNK mutant candidates were found but one *Dm*dNK double mutant in particular displayed highly increased sensitivity to several analogues in transformed bacterial cells and increased analogue specificity as determined by kinetic analysis. Furthermore, the cytotoxic effect of several nucleoside analogues on human cancer cell lines transduced with this double mutant was increased manifold compared to parental cells and cells transduced with wild type *Dm*dNK [Knecht *et al.*, 2000; Knecht *et al.*, 2007]. Further investigations revealed that only one of the mutations was responsible for the increased specificity towards the nucleoside analogue AZT. The crystal structure of the *Dm*dNK single mutant revealed that a shift in orientation of a single amino acid preventing a hydrogen bond in the active site was responsible for the increased AZT specificity [Welin *et al.*, 2005 (Paper I)]. This emphasizes the fact that detailed knowledge of enzyme substrate interactions is important in the development of new enzyme/drug combinations.

Creation of mutant deoxynucleoside kinases with improved nucleoside analogue activities has also been attempted with site-directed mutagenesis. Recently, a new thymidine kinase from *C. elegans* was characterized [Skovgaard & Munch-Petersen, 2006 (Paper II)]. It was found to be a TK1-type kinase with a weak ability to phosphorylate deoxyguanosine. Based on the existing structure of human TK1 (HuTK1) [Welin *et al.*, 2004], a detailed mutation study involving amino acids in the active site of both HuTK1 and *C. elegans* TK1 (*Ce*TK1) was carried out using site-directed mutagenesis [Skovgaard *et al.*, submitted (Paper IV)]. The mutant enzymes were tested for activity with different natural and analogue substrates. *Ce*TK1 and HuTK1 were equally efficient at phosphorylating the nucleoside analogue AZT but it was found that substitution of a single amino acid in HuTK1 with the amino acid in the corresponding position in *Ce*TK1 increased the specificity towards AZT 70-fold [Skovgaard *et al.*, submitted (Paper IV)]. The advantage of developing mutated human deoxynucleoside kinases for use as 'suicide' enzymes is that the human kinases do not increase the risk of provoking an antigenic response.

'Suicide' gene therapy is also employed to combat graft versus host disease (GVHD) arising from allogenic haematopoietic stem cell transplantations [Cohen *et al.*, 1997; Quasim *et al.*, 2005]. Haematopoietic stem cell transplantations are used to treat a number of immunodeficiencies, and for

most patients haploidentical sibling or parental donors are available. GVHD arises from immunological discrepancies between donor and recipient, and even though the T-cells play an important role in restoring the immune system it is mostly treated by T-cell depletion. By modifying the donor T-cells by retroviral transduction of the HSV1TK gene they can be selectively eliminated by administration of ganciclovir, should serious GVHD arise [Quasim *et al.*, 2005]. By employing 'suicide' gene therapy the alloreactive T-cells responsible for GVHD can be eliminated while the nonalloreactive T-cells remain unharmed.

Due to the importance of deoxynucleoside kinases in a wide range of therapies they have been studied intensively for many years. The studies include mechanism regarding cell cycle regulation, cellular localization, substrate specificity and structural studies examining elements responsible for catalysis and substrate selectivity. A detailed knowledge of deoxynucleoside kinase is important in the development of new enzyme/drug systems for 'suicide' gene therapy and for the general application of deoxynucleoside kinases in therapy. Of the four human deoxynucleoside kinases TK1 is the one subjected to the strictest regulation, and it will be described in detail in the following section.

Reaction Mechanism and Regulation of Human Thymidine Kinase 1

Thymidine kinase 1 differs considerably from the other mammalian deoxynucleoside kinases with respect to sequence, structure, kinetics and cell cycle regulation. This section will focus on the kinetic reaction mechanism and feedback inhibition along with mechanisms involved in cell cycle regulation of TK1.

ATP Effect on Molecular Weight and Kinetics

A lot of discrepancies in molecular weight and kinetic parameters have been observed for human TK1 over the years. The TK1-gene encodes a 25 kDa polypeptide, and molecular weights of the active enzyme have been reported in the 56-200 kDa range. Some of the discrepancies can be explained by the enzyme's oligomerization abilities but some are also likely due to insufficient protein purity and different gel filtration techniques.

In the absence of ATP in the elution buffer TK1 elutes with molecular weights in the range 55-75 kDa, and in the presence of ATP it elutes with molecular weights in the 90-200 kDa range (table 1) [Lee & Cheng, 1976a; Munch-Petersen *et al.*, 1984; Munch-Petersen, 1993; Jensen & Munch-Petersen, 1994; Munch-Petersen *et al.*, 1995a; Berenstein *et al.*, 2000; Zhu *et al.*, 2006; Munch-Petersen, 2009]. One exception is a publication of a recombinant TK1 that only elutes at 150 kDa regardless of ATP exposure [Jensen & Munch-Petersen, 1994]. This has later been proven to be due to an error in the sequence of the recombinant gene that disables the proteins' ability to change oligomeric state [Bradshaw & Deininer, 1984; Berenstein *et al.*, 2000].

In 1993, it was discovered that ATP induces an oligomeric change in TK1, causing it to rearrange from a dimer form with a theoretical molecular weight of 50 kDa to a tetramer of 100 kDa [Munch-Petersen, 1993]. The oligomerization change is also accompanied by a 20-40-fold shift in K_m. Both the dimer and the tetramer have a maximum velocity of app. 10 µmol/min/mg at the saturating ATP concentration 2.5 mM but the dimer has K_m values in the 12-16 µM range, and the tetramer has the same V_{max} but a much lower K_m value in the 0.4-0.7 µM range (table 1) [Munch-Petersen, 1993; Jensen & Munch-Petersen, 1994; Munch-Petersen *et al.*, 1995a; Berenstein *et al.*, 2000; Zhu *et al.*, 2006; Munch-Petersen, 2009]. One

exception is presented in 1991 where an apparently non-ATP incubated TK1 was found to have a K_m of only 0.5 µM and a hill coefficient of 1.0 [Munch Petersen *et al.*, 1991]. This is most likely the result of a tetramer form of TK1 since ATP was commonly added as a stabilizer before 1993 when it was found to affect the K_m [Munch-Petersen, 1993].

ATP mM	MW kDa	K_m µM	V_{max} U	Hill n	Publication and source
0	90				Lee & Cheng, 1976a Acute myelocytic leukaemia
2		2.6			Lee & Cheng, 1976b Acute myelocytic leukaemia
0	92	3			Gan *et al.*, 1983 Placenta
0 2	70-75 170-200	3.18			Munch-Petersen *et al.*, 1984 Partly purified Lymphocytes
0 2	55 110	0.5	9.5	1.0	Munch-Petersen *et al.*, 1991 Lymphocytes
0 2	56 120	15 0.7		0.74 1.17	Munch-Petersen, 1993
0 2.5	70 150	12 0.5	9.5	0.7 1.25	Jensen & Munch-Petersen, 1994 Lymphocytes
0 2.5	150 150	0.4 0.4	10	1.4 1.5	Jensen & Munch-Petersen, 1994 Recombinant
0 2.5	55 110	14 0.6	9.5		Munch-Petersen *et al.*, 1995a Lymphocytes (Pure fractions)
0 2.5	50 Tet	15 0.6		0.4 1	Berenstein *et al.*, 2000. Recombinant
0 2.5	60 100	16 0.7	15.7 17.3		Zhu *et al.*, 2006 Recombinant
0 3	57.5 115	16.4 0.51		0.75 1.04	Munch-Petersen, 2009 Recombinant

Table 1
Overview of molecular weight (MW) and kinetic properties of human TK1 with the substrate dThd. The concentration of ATP denoted in the first column is ATP present during TK1 pre-incubation. All assays were performed at saturating ATP concentration (2.5 mM or more). One Unit (U) is one µmol/min/mg. Tet: TK1 was found to be a tetramer but the molecular weight is not presented.

This dimer/tetramer transition is dependent not only on ATP but also on enzyme concentration. At enzyme concentrations below 10 ng/ml ATP does not appear to induce tetramerization [Munch-Petersen, 1993; Munch-Petersen, 2009]. The enzyme concentration at assay conditions is below this

level which explains why it is possible to obtain linear progress curves for non-ATP incubated enzymes despite the presence of 2.5 mM ATP during the assay. However, since the velocity at saturating dThd concentrations is the same for ATP and non-ATP incubated TK1 it is believed that high dThd concentrations can induce tetramerization even at low enzyme concentrations [Munch-Petersen *et al.*, 1993]. A more detailed reaction mechanism is described in the following section.

Cooperativity and Reaction Mechanism

With ATP as the varied substrate a positive cooperative pattern is observed (table 2). At a wide range of fixed dThd concentrations K_m for ATP shows only minor variations in the 31-59 µM range, and hill coefficients were nearly unchanged in the range of 2.0-2.4 [Munch-Petersen *et al.*, 1984]. An early study on acute myelocytic cells also found positive cooperativity with ATP but with a K_m of 220 µM at saturating dThd concentration [Lee & Cheng, 1976b]. In that study the storage buffer contained 2 mM ATP, and the difference in K_m between the two studies could be misinterpreted as an effect of tetramerization. This is not the case, however. In 1995 it was shown with lymphocyte TK1 of very high purity that ATP incubation does have an effect on K_m [Munch-Petersen *et al.*, 1995a]. At a 10 µM fixed dThd concentration the K_m for non-ATP incubated dimer TK1 is 140 µM, and the hill coefficient is 1.6. The ATP incubated tetramer TK1 has a highly increased catalytic efficiency as a result of a low K_m of 10 µM and increased positive cooperativity exemplified by a hill coefficient of 2.2.

ATP mM	MW kDa	K_m µM	Hill n	dThd µM	Publication and source
2		220			Lee & Cheng, 1976b acute myelocytic leukaemia
0	70-75	59	2.0-2.4	1.9	Munch-Petersen *et al.*, 1984 Partly purified Lymphocytes
		50	-	11.5	
		50	-	25	
		43	-	50	
		31		100	
0	55	140	1.6	10	Munch-Petersen *et al.*, 1995a
2.5	110	10	2.2	10	Lymphocytes (Pure fractions)

Table 2

Overview of molecular weight (MW) and kinetic properties of human TK1 with the substrate ATP. The concentration of ATP denoted in the first column is ATP present during TK1 pre-incubation.

The tetramer form of TK1 displays classical Michaelis-Menten kinetics with dThd as denoted by a hill coefficient of 1 or just over 1 for a few purifications. However, the non-ATP incubated dimer form of TK1 is more complex and exhibits apparent negative cooperativity with dThd as denoted by reported hill coefficients in the range of 0.4-0.7 (table 1) [Munch-Petersen *et al.*, 1991; Munch-Petersen, 1993; Jensen & Munch-Petersen, 1994; Berenstein *et al.*, 2000; Munch-Petersen, 2009]. For the tetramer TK1, the reaction mechanism has been shown to be ordered sequentially with the formation of a ternary complex where ATP binds before dThd [Lee & Cheng, 1976b; Munch-Petersen, 1993]. The apparent negative cooperativity observed for non-ATP incubated TK1 is believed to be due to a simultaneous presence of both dimer and tetramer, and a more complex model of reaction mechanism has been proposed for the non-ATP incubated enzyme where equilibrium between the dimer and tetramer form plays an important role [Munch-Petersen, 1993; Munch-Petersen *et al.*, 1995b]. The equilibrium between dimer and tetramer is believed to be established prior to steady-state and is maintained during the time frame of initial velocity measurements [Munch-Petersen *et al.*, 1993]. The model is based on the following assumptions quoted from Munch-Petersen *et al.* [1995b]:

1) *TK1 is active as a dimer as well as a tetramer.*

2) *The dimer has higher K_m and lower k_{cat} values than the tetramer.*

3) *The rate of tetramerization is proportional to the concentration of complex(es) between dimer and ATP or both substrates.*

4) *Tetramerization cannot take place with the dimer alone or in complex with thymidine.*

5) *A ternary complex is formed between TK1 and the two substrates with ATP as the first bound substrate.*

At saturating ATP concentrations and variable dThd concentrations the following model describes the reaction mechanism of non-ATP incubated TK (figure 3).

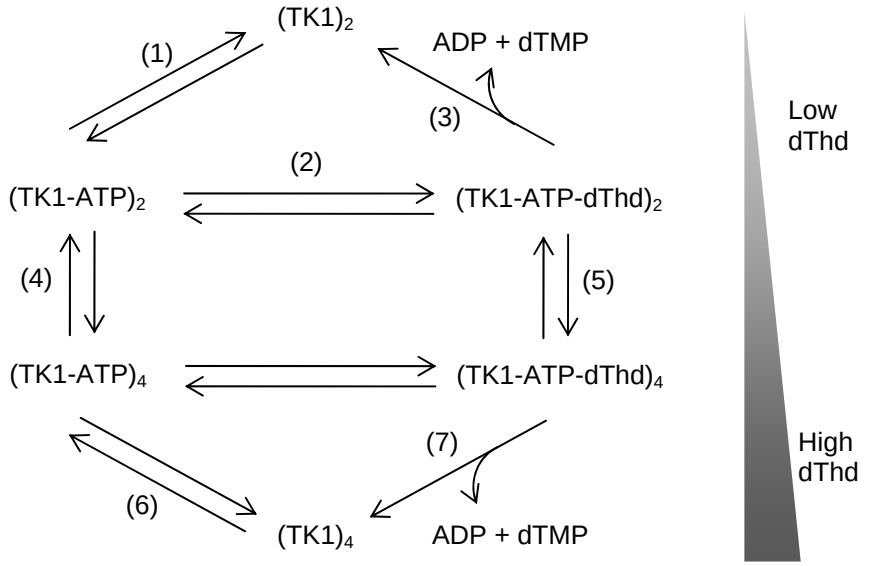

Figure 3
Model of the reaction mechanism for TK1 with saturating ATP and variable dThd concentrations. Dimer and tetramer forms of TK1 are denoted by suffices 2 and 4, respectively, and different enzyme-substrate complex forms are denoted within parentheses. Product is only released from the ternary complexes of either dimer or tetramer in the reactions 3 and 7, respectively. The figure is modified from [Munch-Petersen *et al.*, 1995b].

At low dThd concentrations the slow dimer-tetramer transition (reactions 4 and 5) are the rate-limiting reactions, and the majority of the enzyme is in the dimer forms, $(TK1\text{-}ATP)_2$ and $(TK1\text{-}ATP\text{-}dT)_2$, and product is formed via reaction 3. At higher dThd concentrations the concentrations of dimer complex will increase, and reaction 3 will become rate-limiting and tetramerization will occur at a rate depending on the concentrations of the dimer complexes, $(TK1\text{-}ATP)_2$ and $(TK1\text{-}ATP\text{-}dT)_2$ (reactions 4 and 5). At saturating dThd concentrations the majority of the enzyme will be on the tetramer forms and the products will be released via reaction 7.

Feedback Inhibition by dTTP

The end product of thymidine salvage, dTTP, has been found to be a feedback inhibitor of TK1. For TK1 purified from acute myelocytic leukemic cells, dTTP was shown to be a competitive inhibitor with a K_i value of 0.6 μM when the concentration of dThd was varied at a fixed ATP concentration. When ATP was varied at a fixed dThd concentration the

inhibition mechanism was more complex, and dTTP increased the sigmoid character of the velocity vs. [ATP] plot [Lee & Cheng, 1976b].

TK1 purified from phytohemagglutinin-stimulated lymphocytes showed a different inhibition pattern [Munch-Petersen *et al.*, 1984]. At varied dThd concentrations and a fixed ATP concentration, micro molar amounts of dTTP induce a change from Michaelis-Menten kinetics to biphasic kinetics. The K_m for dThd changed drastically from 1.6 μM to 600 μM when the concentration of dTTP was increased from 0 to just 30 μM. When ATP was varied at a fixed dThd concentration the cooperative kinetic with ATP was retained in the presence of 0-20 μM dTTP with Hill constants for ATP in the range of 2.3-2.8. dTTP also has a drastic impact on K_{50} for ATP. An increase in dTTP from 0 to 20 μM results in an increase in K_{50} from 43 to 5400 μM.

When the dTTP concentration was varied at different combinations of fixed dThd and ATP concentrations, the inhibition mechanism was shown to be cooperative with respect to both ATP and dThd with hill coefficients for dTTP in the range of 2.0-2.5. The dTTP concentration required to obtain 50 % inhibition, I_{50}, varied from 9.3-21 μM when the dThd concentration was varied from 4-111 μM, and I_{50} varied from 3.3-36 μM when the ATP concentration varied from 0.2-5.3 mM [Munch-Petersen *et al.*, 1984].

These results were later confirmed with very pure lymphocyte TK1 [Munch-Petersen *et al.*, 1995a]. The effect of ATP pre-incubation upon dTTP inhibition was examined, and it was found that both the non-ATP incubated and the ATP incubated forms of TK1 displayed cooperative inhibition by dTTP with similar hill coefficients of 2.7 and 2.5, respectively. The I_{50} values for dTTP were in the 9-12 μM range at dThd concentrations from 1-10 μM. These results suggest that despite the fact that the dimer and tetramer forms of TK1 display very different affinities for dThd and ATP, they both share a high affinity for dTTP feedback inhibition.

Cell Cycle Regulation

Unlike other mammalian dNKs TK1 activity fluctuates during cell cycle, and the enzyme is mainly expressed during S-phase [Sherley & Kelly, 1988, Kauffman & Kelly, 1991]. Since TK1 in the cell has a half-life of about 40 hours [Sherley & Kelly, 1988] this limited period of activity must be partly due to an up-regulation prior to S phase and a down-regulation after S-phase.

Several reports show that mitogenic activation, like serum-stimulation or viral SV40-infection, of tissue culture cells is followed by a sharp simultaneous S phase increase in TK1 activity and mRNA levels [Stuart *et al.*, 1985; Stewart *et al.*, 1987; Sherley & Kelly, 1988]. For the serum-stimulated cells the increase is coinciding with an increased transcription

rate of the TK1-gene but this is not the case for the SV40-infected cells, suggesting different regulation mechanisms in the two systems [Stewart *et al.*, 1987]. These results indicate that the increase in TK1 activity is regulated at a transcriptional and/or post-transcriptional level. For cells that are not stimulated by a mitogenic activator this is not the case, however. In HeLa cells synchronized by centrifugal elutriation and mitotic selection a 15-fold increase in TK1 activity and protein levels is observed in S-phase cells but this is only accompanied by a 3-fold increase in TK1 mRNA levels [Sherley & Kelly, 1988]. This concludes that the mechanism regulating TK1 induction in serum-stimulated and SV40-infected cells is different from the one operating during normal cell cycle. Addition of [^{35}S]methionine at different points during the cell cycle revealed a 12-fold increased methionine incorporation in S and G_2 cells compared to cells in G_1, suggesting that the increase in TK1 protein levels beginning at the G_1/S transition is caused by an increased protein translation rate [Sherley & Kelly, 1988].

Around the time of cell division TK1 protein levels measured in vivo are dramatically down-regulated by a decrease in protein half-life from around 40 hours to less than 1 hour, resulting in a rapid depletion of TK1 in newly divided G_1 cells (figure 4) [Sherley & Kelly, 1988; Kauffman & Kelly, 1991]. This down-regulation of TK1 protein and activity begins between metaphase and cytokinesis and is abolished upon removal of the 40 C-terminal amino acids of TK1, resulting in a protein that is constitutively expressed during cell cycle. Fusion of β-galactosidase to the TK1 C-terminal also abolishes regulation whereas removal of the 10 C-terminal amino acids results in mitotic degradation like the wild type TK1 [Kauffman & Kelly, 1991]. Sequence analysis has revealed a motif, the KEN box, which is conserved in TK1 from human, chicken and Chinese hamster [Ke & Chang, 2004]. The KEN box is a recognition signal targeted by the ubiquitin ligase anaphase promoting complex (APC) [Pfleger & Kirschner, 2000]. APC in complex with either Cdc20 or Cdh1 is a well-known mediator of cell cycle regulated proteolysis, targeting proteins for degradation via the ubiquitin dependent pathway at certain points during the cell cycle [reviewed by Peters *et al.*, 1998] The KEN box is recognized by the N-terminal of the Cdh1 protein followed by association of Cdh1 with APC forming the active ubiquitin ligase complex [Pfleger & Kirschner, 2000; Pfleger *et al.*, 2001]. Ubiquitinylated TK1 is subsequently transported to the proteasomes for proteolysis.

Other cell cycle regulating proteins Cdk1 (synonymous to Cdc2) or Cdk2 are also involved in TK1 regulation [Chang *et al.*, 1998]. TK1 in HeLa cells has been shown to be hyperphosphorylated during M-phase resulting in a 10-fold decreased affinity for the substrate dThd [Chang *et al.*, 1994]. The phosphorylation of TK1 is believed to take place on Ser13 and to be carried out by the protein kinases Cdk1 or Cdk2 during M-phase [Chang *et al.*,

1998]. By mutating Ser13 to Asp, and thereby mimicking phosphorylation, it has been shown that phosphorylation at Ser13 inhibits the ATP induced tetramerization [Li *et al.*, 2004]. Hence, phosphorylation lowers the TK1 activity by preventing the formation of the high activity tetramer form of TK1. At cellular ATP concentrations TK1 is most likely present in the high activity form, and prior to protein degradation the activity is down-regulated during M-phase by Ser13 phosphorylation in a response to the decreased demand for dTTP (figure 4).

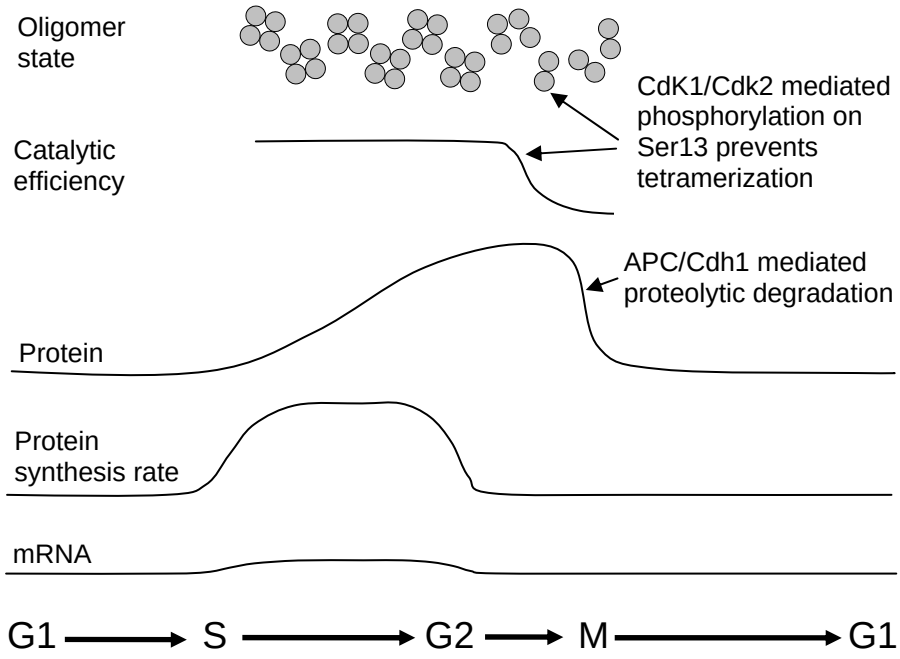

Figure 4
Schematic overview of factors affecting cell cycle regulation of TK1. Information about mRNA levels, rate of protein synthesis and protein levels is from [Sherley & Kelly, 1988], and APC/Cdh1 mediated proteolytic degradation is from [Pfleger & Kirschner, 2000; Pfleger *et al.*, 2001; Ke & Chang, 2004]. Research on catalytic efficiency, oligomeric state and Cdk1/Cdk2 mediated phosphorylation of Ser13 is done by [Chang *et al.*, 1994; Chang *et al.*, 1998¸Li *et al.*, 2004].

In G0 and G1 cells the physiological TK1 concentration is approximately 30-90 ng/ml (1.2-3.6 nM) but it is known to increase to approximately 4 µg/ml (160-240 nM) in S-phase cells [Munch-Petersen *et al.*, 1993]. Presuming equal distribution in the cytosol this means that in G1-phase and early S-phase, TK1 will mainly be in the dimer form regardless of the cellular ATP concentration since the TK1 protein concentration is low outside S-phase.

The dTTP pool in S phase cells is increased 20 times compared to resting cells correlating well with the tight regulation described for TK1 [Spyrou & Reichard, 1988]. Ribonucleotide reductase R2, which is another important player in the dNTP metabolism, has also been shown to be down-regulated by the APC/Cdh1 mediated pathway in late mitosis [Chabes *et al.*, 2003b]. The strict regulation of TK1 and ribonucleotide reductase is important for maintaining balanced dNTP pools which is again important for maintaining genomic stability [Daré *et al.*, 1995] and preventing unscheduled DNA synthesis. If, for instance, APC/Cdh1/Cdc20 mediated proteolysis of TK1 and thymidylate kinase is prevented, the result would be highly increased dTTP pools. Furthermore, the increased dTTP pool leads to a drastic dNTP pool imbalance due to the regulatory role of dTTP in *de novo* production of the other deoxynucleotides. Loss of proteolysis also leads to growth retardation and increased mutation rates [Ke *et al.*, 2005].

Thymidine Kinase 1 Structure and Structural Movement upon Substrate Binding

In order to compare information from different TK1 structures, amino acid numbering in this section will be from HuTK1 unless stated otherwise.

Tertiary Structure and Domains

The first structures that were solved for TK1 type enzymes were HuTK1 and a thymidine kinase from *Ureaplasma urealyticum* (*Uu*TK), both with dTTP bound in the active site [Welin *et al.*, 2004]. HuTK1 has subsequently been crystallized with dTTP again [Birringer *et al.*, 2005], and in order to elucidate substrate-protein interactions in the ATP binding site it was also crystallized with P1-(5′-adenosyl)P4-(5′-(2′-deoxy-thymidyl)) tetraphosphate (TP4A) [Segura-Peña *et al.*, 2007a]. They all revealed very similar structural folds. TK1 consists of two domains, both taking part in the active site.

The α/β-domain contains a central, six-stranded, parallel β-sheet surrounded by α-helices which, to some extent, is similar to that of other deoxynucleoside kinases but more so to enzymes in the RecA-F_1-ATPase family [Sawaya *et al.*, 1999; Bauer *et al.*, 2001]. Between β1 and α1 of this domain is the P-loop, a highly conserved phosphate binding motif (GXXXXGKS/T) found in both TK1 like and non-TK1 like kinases. The α/β-domain domain also contains a flexible β-hairpin that has proven to be untraceable in many of the solved TK1 structures [Welin *et al.*, 2004; Kosinska *et al.*, 2007; Segura-Peña et *al.*, 2007a; Segura-Peña et *al.*, 2007b].

The other domain, named the lasso-domain, is unique for TK1-like proteins and is so named due to a lasso-like loop closing down on top of the base of the phosphate acceptor. The lasso domain contains two perpendicular β-hairpins connected by the long flexible lasso loop. The structure of the lasso domain is stabilized partly by four cysteines coordinating a Zn^{2+} ion in one region of the domain and by the conserved amino acids Arg165 and Tyr181 making hydrogen bonds to main chain atoms in the loop region. [Welin *et al.*, 2004; Birringer *et al.*, 2005].

As described in the previous section, HuTK1 is a dimer of dimers and is known to exist as either a dimer or a tetramer in solution [Munch-Petersen, 2009]. The crystal structures of HuTK1 have either 2 tetramers or one dimer in the asymmetric unit [Welin *et al.*, 2004; Birringer *et al.*, 2005; Segura-Peña et *al.*, 2007a].

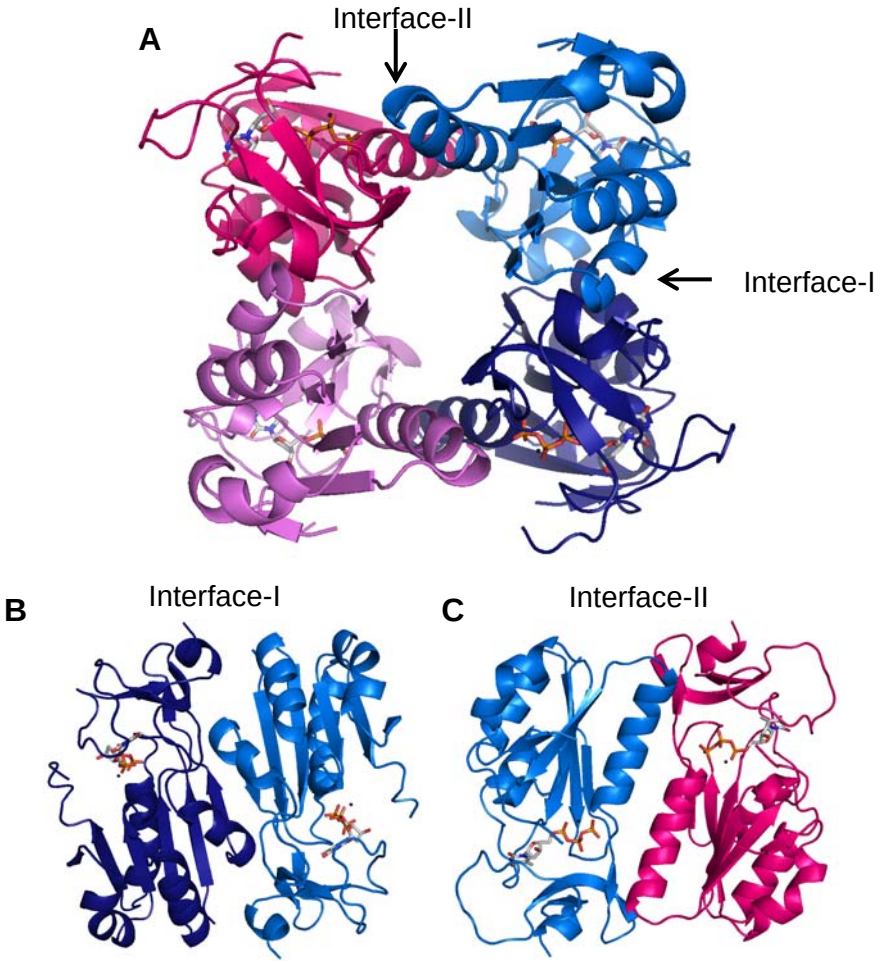

Figure 5
Structure of human thymidine kinase 1. A: HuTK1 tetramer showing the two types of interfaces (PDB id: 1xbt). B: Dimer one connected by Interface-I is the most stable of the two and is believed to be the active dimer. C: Dimer two connected by interface-II is the weak dimer, and interface-II separates upon dimerization of the tetramer [Welin *et al.*, 2004].

The tetramer structure has a 2-2-2-fold symmetry with two different subunit interfaces and a central channel exposing mainly polar or charged residues (figure 5). One subunit interface, here referred to as interface-I, is made up by the β-sheet from one subunit interacting with the antiparallel β-sheet from the neighbour subunit through water molecules. The other interface, referred to as interface-II, is dominated by the long α1-helices from neighbouring subunits interacting with each other in an antiparallel manner. The dimer connected by interface I is believed to be the active dimer found in solution [Welin *et al.*, 2004; Kosinska *et al.*, 2007; Segura-Peña *et al.*, 2007b].

Structural factors affecting the shift from dimer to tetramer will be discussed in one of the following sections.

Ligands in the Phosphate Acceptor Site are Affecting the Position of the Catalytic Glu98 and Lasso-loop Conformation

The phosphate acceptor is bound with the base moiety deeply buried in a deep hydrophobic pocket between the α/β-domain and the loop part of the lasso domain. In structures solved with the feedback inhibitor, dTTP, in the phosphate acceptor site, the phosphates extend into the P-loop where they are much more exposed than the thymine base. The structures of *Uu*TK [Kosinska *et al.*, 2005] and thymidine kinase from *Bacillus anthracis* (*Ba*TK) [Kosinska *et al.*, 2007] have been solved with the natural substrate dThd in the phosphate acceptor site, and the majority of the ligand/protein interactions are the same as for *Uu*TK and HuTK1 in complex with dTTP [Welin *et al.*, 2004].

The thymine base only forms hydrogen bonds to main chain atoms. O4 form bonds to atoms in the α/β-domain, and O2 and N3 form bonds to main chain atoms in the lasso-domain. The methyl group of thymine is pointing towards Thr163, and on the lasso-domain side the base stacks against the conserved Arg165 and Tyr181, and on the other side it stacks against Phe101 and Phe133 oriented perpendicular to the base plane.

The 3'-oxygen of the deoxyribose forms hydrogen bonds to the main chain of Gly176 and to the conserved Asp58 in the flexible β-hairpin.

The main difference between the dThd/TK1 complexes and dTTP/TK1 complexes is the position of Glu98 which is believed to act as a nucleophile subtracting a proton from the 5'-OH in the phosphate transfer reaction (figure 6). *Uu*TK has been crystallized with both dTTP and dThd in the active site [Welin *et al.*, 2004; Kosinska *et al.*, 2005]. In the structure with the natural substrate, dThd, in the active site the 5'-OH is hydrogen bonded to Glu98 [Kosinska *et al.*, 2005], and with the feedback inhibitor, dTTP, the Glu is repelled by the phosphates, and the side chain is twisted further away from the 5'-oxygen [Welin *et al.*, 2004]. *Thermotoga maritima* TK (*Tm*TK) has been crystallized in the apo form, with dThd, TP4A and as a ternary complex with dThd and the non-hydrolysable ATP analogue, AppNHp [Segura-Peña et *al.*, 2007a; Segura-Peña et *al.*, 2007b]. The latter revealed two different ternary complexes: one contained the expected ligands, dThd and AppNHp, and the other one the reaction products, TMP and ADP. In all the *Tm*TK structures, with the exception of the apo form, Glu98 is pointing towards the ribose but at different angles and distances. In the apo structure the side chain is pointing away from the ribose. The two ternary complexes and the complex with TP4A have the Glu in nearly the same position in a distance of app. 3.5 Å to the 5'-oxygen whereas it is

twisted slightly closer having a distance of only 2.8 Å in the dThd complex. These findings support the theory of Glu98 acting as the catalytic base.

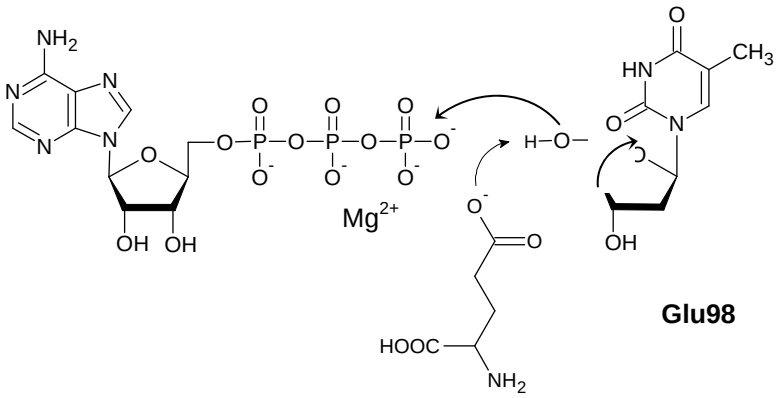

Figure 6
Catalytic mechanism of the phosphoryl transfer in TK1-type enzymes. The Glu98 acts as a catalytic base subtraction a proton from the 5-hydroxyl group of thymidine. Subsequently, the deprotonated 5'-oxygen makes a nucleophile attack on the γ-phosphate of ATP. The figure is modified from [Eriksson *et al.*, 2002].

Occupation of the phosphate acceptor site is not only affecting local amino acid arrangements but impacts the structure of the lasso-loop as well. In all the structures containing a thymidine or thymidine-like ligand in the phosphate acceptor site the lasso-loop is closed down on top of the thymine base. In structures without thymidine-like ligands in this site the lasso loop is in an open conformation or is too flexible to show traceable electron density (figure 7). One exception from this is the *Tm*TK structure with dThd (2QQE) which is lacking electron density for at few amino acids in the lasso-loop (Figure 7 F). The loop in *Tm*TK only becomes fully traceable upon occupation of the phosphate acceptor site also (figure 7 D and G) [Segura-Peña et *al.*, 2007a; Segura-Peña et *al.*, 2007b].

Ligands in the Phosphate Donor Site are Affecting Subunit-Subunit Interactions and the Flexible β-hairpin

The first TK1 structures with ligands in the phosphate donor site were HuTK1 and *Tm*TK in complex with TP4A [Segura-Peña et *al.*, 2007a] but the HuTK1 structure did not display electron density for the adenine and the neighbouring ribose (figure 7 C and D). Therefore, many of the ligand protein interactions in this region are only observed in different non-human thymidine kinases but will be described with HuTK1 numbering. *Tm*TK and a thymidine kinase from *Clostridium acetobutylicum* (*Ca*TK) have been solved with adenine nucleotides in the phosphate donor site (figure 7 G and L) [Segura-Peña et *al.*, 2007b; Kuzin *et al.*, 2004] and in an attempt to

crystallize the apo form of *Bacillus cereus* TK (*Bc*TK), the donor site was unexpectedly occupied by dTTP (figure 7 K) [Kosinska *et al.*, 2007].

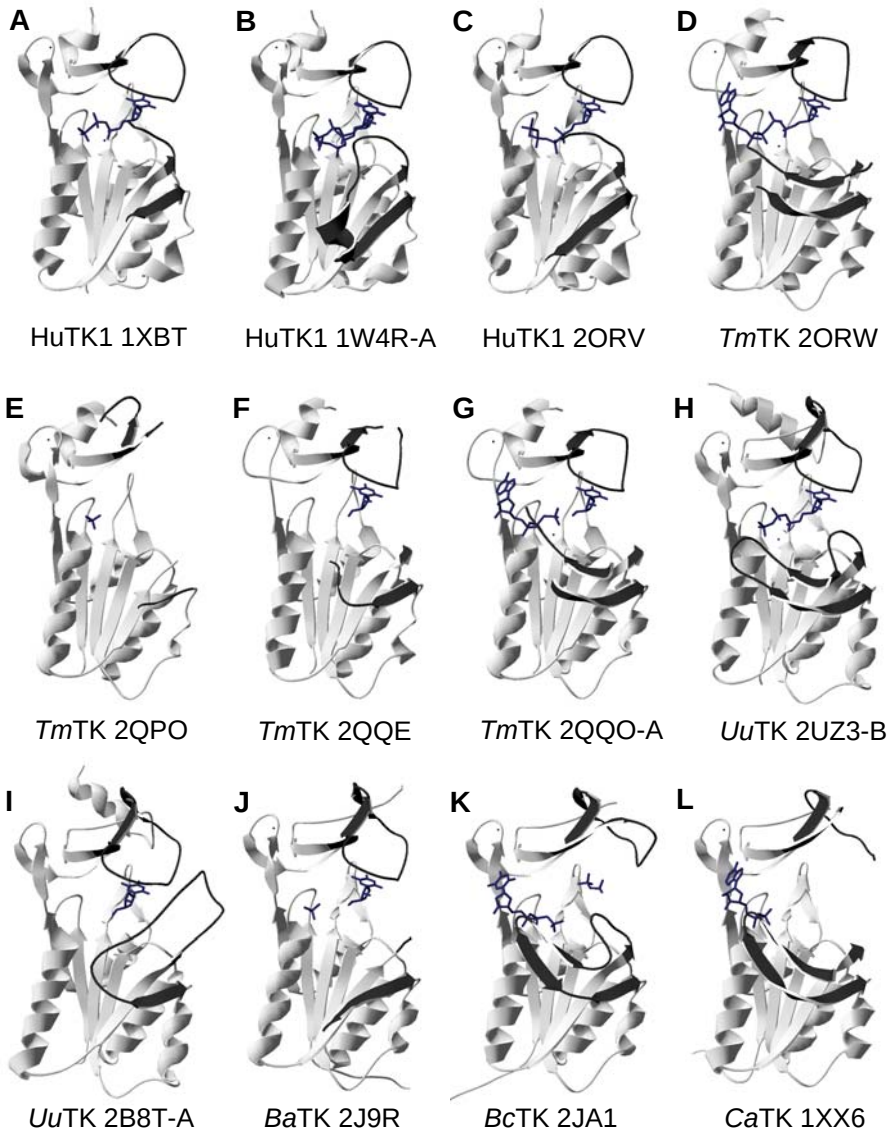

Figure 7
Overview of loop organization in TK1-type structures from different organisms with different ligands. The lasso-loop and β-hairpin are highlighted in black, and ligands are shown in dark grey. Enzyme name and PDB id are shown for each structure, and in structures where the subunits differ in traceability or ligand composition the subunit shown is designated by a letter after the PDB id (Ex. 2UZ3-B is subunit B of the structure with PDB id 2UZ3).

In the phosphate donor site the ligand phosphates are bound to the P-loop of the α/β-domain, and the ribose and the base moieties are bound in the dimer interface-II between the α1-helices of neighbouring subunits. In the *Tm*TK structure with TP4A two of the phosphates in TP4A are coordinating a Mg^{2+} ion along with the hydroxyl group of a Thr/Ser (Thr17 in *Tm*TK, and Ser33 in HuTK1) and the conserved Asp83 and Glu98 [Segura-Peña *et al.*, 2007a]. This Mg^{2+} ion is absent in the HuTK1 structure lacking electron density for the adenosine and ribose of TP4A, and the phosphates are oriented differently from those in the *Tm*TK structure. The HuTK1 structure has the TP4A β-phosphate in the place occupied by Mg^{2+} in the *Tm*TK structure, indicating that the conformation of TP4A observed in the HuTK1 structure is not compatible with binding of magnesium. Since Mg^{2+} is necessary for catalysis in both TK1-like and non-TK1-like kinases [Lee & Cheng, 1976b], this phosphate orientation is not expected to exist in the active enzyme.

The adenosine base is sandwiched between a Tyr/Phe from the P-loop (Tyr13 in *Tm*TK and Phe29 in HuTK1) and a Leu/Ile from the neighbouring subunit (Leu29 in *Tm*TK and Ile45 in HuTK1), and the main chain carbonyl oxygen of Val152 interacts with adenosine N6 [Segura-Peña et *al.*, 2007a]. The interaction between Val152 and N6 in adenosine explains why ATP is a better phosphate donor than GTP since the O6 in GTP may be repulsed by the carbonyl oxygen of Val152.

As mentioned previously, HuTK1 undergoes a reversible transition from a low activity dimer to a high activity tetramer upon ATP incubation, and this transition is believed to be important for the regulation of activity during cell cycle [Munch-Petersen *et al.*, 1993, Munch-Petersen, 2009] In one of the first publications of a HuTK1 structure it was suggested that dimer interface-II was the stronger interface and that interface-I fell apart upon transition from tetramer to dimer in solution [Birringer *et al.*, 2005]. Two later studies on bacterial TKs disagree and suggest that the dimer connected through interface-I is the active dimer [Kosinska *et al.*, 2007; Segura-Peña et *al.*, 2007b]. *Ba*TK and the nearly identical *Bc*TK have been crystallized with dThd in the phosphate acceptor site and dTTP in the phosphate donor site, respectively, and a comparison reveals a change in interface-II when the donor site is occupied compared to when it is unoccupied [Kosinska *et al.*, 2007]. An occupied phosphate donor site leads to a 3 Å dissociation of the α1-helices in interface-II of BcTK compared to the one observed in BaTK. Furthermore, fewer subunit-subunit interactions are present in the BcTK structure. A calculation of interaction areas reveals that interface-II interaction is reduced by over one third upon occupation of the phosphate donor site (790 $Å^2$ in *Ba*TK and 413 $Å^2$ in *Bc*TK) [Kosinska *et al.*, 2007]. This is supported by the structures of HuTK1 and *Uu*TK having empty phosphate donor sites and large interaction areas of 790-820 $Å^2$, and the

structure of *Ca*TK having ADP in the phosphate donor site and an interaction area of only 500 Å^2 [Kosinska *et al.*, 2007].

In order to compare different substrate-bound states in the same enzyme, *Tm*TK has been the subject of a thorough structural study on subunit interaction and substrate binding [Segura-Peña et *al.*, 2007b]. This study also supports earlier findings by showing that the apo and dThd bound proteins both have a tighter interface-II than the ternary *Tm*TK complex with dThd and AppNHp. In the loose confirmation the phosphate donor is involved in 260 Å^2 out of a total 630 Å^2 interaction area in the interface but the two tight conformations have interaction areas of 900-1030 Å^2. This proves that occupation of the phosphate donor site significantly stabilizes the loose conformation but the tight confirmation is still the more stable one. However, since none of the previously mentioned TK1 structures show electron density in the phosphate donor site in the tight conformation this form is likely to be inactive. This is confirmed by a double cysteine mutant of *Tm*TK (T18C/S22C *Tm*TK numbering) that has a disulfide bond across interface-II, locking the enzyme in the tight conformation in solution [Segura-Peña et *al.*, 2007b]. In this confirmation *Tm*TK has only 3.7 % activity compared to the free wild type enzyme. These findings provide an explanation for the positive cooperativity observed with ATP for both HuTK1 and *Tm*TK [Lee & Cheng, 1976b; Munch-Petersen *et al.*, 1984; Segura-Peña et *al.*, 2007a]. A model has been proposed where the tetramer is continuously oscillating between the tight and loose conformation [Segura-Peña et *al.*, 2007b].

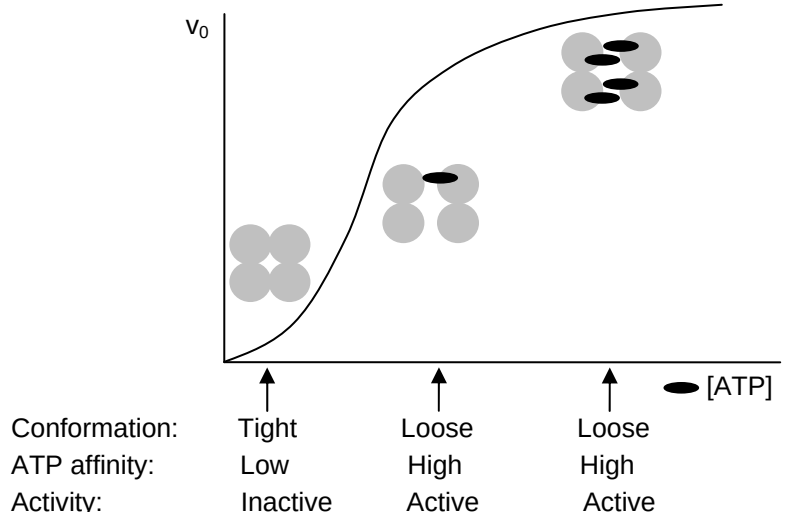

Figure 8
ATP induced tetramerization of TK1. The model shows the conformational change in TK1 interface-II upon ATP binding that gives rise to positive cooperativity.

Upon binding of ATP to one subunit the dimers connected by interface-II move apart, and the tetramer is transformed to the loose conformation. This results in increased ATP affinity for the remaining subunits due to the increased space in the phosphate donor binding site, giving rise to a sigmoid initial velocity curve (figure 8).

When comparing the structures of the *Tm*TKs (figure 7 D, E, F and G) the flexible β-hairpin also appears to be influenced upon binding of a ligand in the phosphate donor site. In structures without a ligand in the phosphate donor site the loop is disordered and untraceable (E and F) but when a ligand is bound, it folds up into an almost fully traceable ordered β-hairpin with the tip in close proximity to the phosphates of the ligand (D and G) [Segura-Peña *et al.*, 2007a; Segura-Peña *et al.*, 2007b]. By including the structures of the nearly identical *Ba*TK and *Bc*TK it is evident that this structural change is independent of the base of the ligand but responds to binding of a phosphate donor. *Ba*TK has a dTTP molecule in the phosphate donor site, and the β-hairpin is fully traceable whereas *Bc*TK has an empty phosphate donor site and an untraceable disordered β-hairpin loop (figure 7 J and K) [Kosinska *et al.*, 2007]. The exact role of the β-hairpin in ATP binding is unclear but fluorescence spectroscopy on tryptophan substituted *Tm*TK's confirms the link between β-hairpin reorganization and ATP binding [Segura-Peña *et al.*, 2007b]. Unfortunately, there is no HuTK1 structure in the loose conformation with a visible ligand in the phosphate donor site so it remains unclear whether the β-hairpin is displaying the same structural rearrangements upon ATP binding in the human thymidine kinase.

Ribonucleotide Reductase; the Key Enzyme in *De Novo* Synthesis of Deoxynucleotides

Ribonucleotide reductase (RNR) is a key regulator of DNA precursors and has been studied extensively for many years. Three different classes of RNR exist in nature, and they are all regulated by binding of nucleotides and deoxynucleotides to specific allosteric sites on the protein, enabling them to provide a balanced supply of deoxynucleotides for DNA synthesis. Here, the focus will be on Class I RNR.

Reaction Mechanism and Communication Between the (Deoxy)nucleotide Binding Sites

The Class I RNR, which is found in higher organisms and some microorganisms, like *E. coli*, is a tetramer consisting of two types of homodimers [Nordlund & Reichard, 2006]. The larger of the two dimers is denoted R1 whereas the smaller one is denoted R2.

The structures of the R1 and R2 subunits have been determined separately [Nordlund *et al.*, 1990; Uhlin & Eklund, 1994], and the active site is located in the R1 subunit not far from the R1-R2 interface. The R1 subunit contains two types of nucleotide binding allosteric sites R2 contains an iron center and a tyrosyl-free radical crucial for catalysis.

The R1 contains three domains, a helical N-terminal domain, an α/β barrel domain and a small C-terminal α+β domain (figure 9). The N-terminal domain is mainly helical and contains the activity regulating allosteric site. Adjacent to the helical domain is an α/β barrel domain, and in the cleft between the two domains is the active site [Uhlin & Eklund, 1994; Uhlin & Eklund, 1996]. Two cysteines (Cys225 and Cys462 in *E. coli*) from the α/β barrel domain extend into the active site, and this cysteine pair is responsible for reduction of the NDP bound in the active site during catalysis. Upon catalysis the cysteine pair in the active site is oxidized, and the subsequent reduction of the cysteines after catalysis involves an additional cysteine pair (Cys754 and Cys759 in *E. coli*) located in the more flexible C-terminal domain. The second cysteine pair is reduced on the protein surface by glutaredoxin or thioredoxin and is believed to move inward, reducing the two active site cysteines that are oxidized during catalysis [Åberg *et al.*, 1989; Mao *et al.*, 1992a; Uhlin & Eklund, 1994]. On a loop in the center of the barrel domain 6Å from Cys225 is another conserved cysteine residue (Cys439 in *E. coli*) which is essential for activity [Mao *et al.*, 1992c]. It is

believed to form a radical and abstract the 3'-hydrogen from the substrate ribose initiating the catalytic reaction.
The specificity regulating allosteric site is located in the dimer interface between the two α/β domains not far from the active site, and the effect of different (d)NTPs bound in the specificity site is mediated to the activity site by amino acids in three flexible loops in the dimer interface (figure 9) [Uhlin & Eklund 1994; Eriksson *et al.*, 1997].

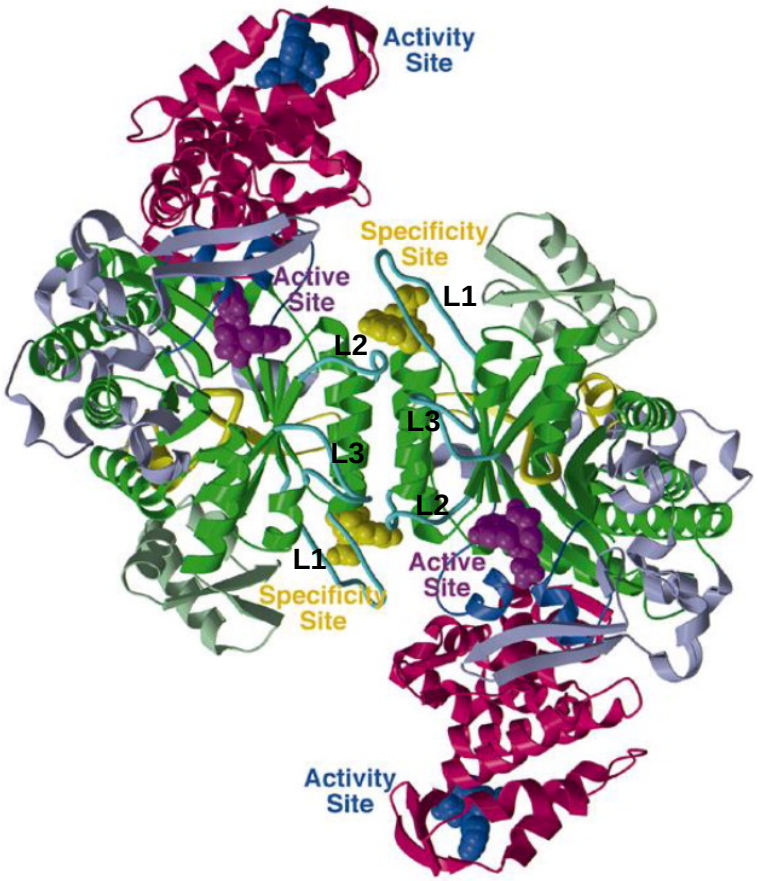

Figure 9
The ribonucleotide reductase R1 dimer. R1 contains three domains. In pink is the N-terminal helical domain containing the activity site, in green is the α/β barrel domain and in light blue is the smaller C-terminal α+β domain. The active site is located between the N-terminal domain and the α/β barrel domain and contains a GDP molecule (purple). The specificity site is located in the dimer interface and contains the ligand dTTP (yellow) while the activity site contains the ATP analogue AMPPNP (blue). In the center of the barrel is the loop entailing the Cys439 radical in light green, and the three flexible loops mediating contact between the specificity site and the active site are shown in cyan. [Eriksson *et al.*, 1997]

Structural analysis of class II RNR reveals that loop 2 changes conformation upon binding of the three effectors, dTTP, dGTP and dATP in the specificity site changing the amino acid interactions between loop 2 and the NDP bound in the active site. It is believed that the mechanism of substrate specificity regulation is the same in class I and class II RNR [Nordlund & Reichard, 2006]. Furthermore, structures of class I and class Ib RNRs show that the effectors binding to the specificity site are mediating changes in the active site mainly through structural changes in loop 2 (designated L2 in figure 9) [Eriksson *et al.*, 1997; Uppsten *et al.*, 2003].

The R2 subunit is constituted by a helix bundle consisting of 8 long α-helices surrounded by three smaller helices and a single antiparallel β-hairpin [Nordlund *et al.*, 1990]. The R2 dimer contains two iron centers 25 Å apart (in *E. coli* R2), each containing two iron atoms. The iron atoms are ligated by four α-helices, of which two are involved in the R2 dimer interface. The hydroxyl group of Tyr122 (*E. coli* numbering), which carries the free radical, is positioned at a 5.3 Å distance from one of the iron atoms buried 10 Å from the protein surface and far from the active site [Nordlund *et al.*, 1990, Uhlin & Eklund, 1994]. Between one of the iron atoms and Tyr122 is a binding pocket for oxygen species. This enables simultaneous oxidation of the iron atoms and generation of the oxidized tyrosyl radical necessary for catalysis [Sahlin *et al.*, 1989].The catalytic mechanism is complex and involves long distance electron transport between the tyrosyl radical in the R2 subunit and the Cys439 radical responsible for abstracting the 3'-hydrogen from the substrate in the active site in R1. The radical/electron-transfer has been suggested to go through several tyrosine residues and a tryptophan residue [Mao *et al.*, 1992a; Uhlin & Eklund, 1994, Ekberg, *et al.*, 1996]. When the cysteines 225 and 462 are in the reduced form, a NDP can bind in the active site and the Cys439 radical attacks the ribose forming a 3'-ribonucleotide radical. Subsequently, the 2'-hydroxyl is protonated by one of two cysteines in the active site and by the elimination of H_2O and formation of a cysteine disulfide bond between Cys225 and Cys462, the 2'-carbon is reduced by hydrogen transfer. Finally, the radical is transferred back to Cys439, forming the deoxynucleoside diphosphate reduced at the 2'-carbon [Mao *et al.*, 1992b; Eriksson *et al.*, 1997; Nordlund & Reichard, 2006].

Allosteric Regulation of Ribonucleotide Reductase

The strict allosteric regulation of RNR allows the enzyme to maintain a balanced dNTP pool and continuously adapt to the changing demands for dNTPs for DNA synthesis and repair. The substrates are all ribonucleoside diphosphates, and the effectors are (deoxy) ribonucleoside triphosphates. The triphosphate compounds change the affinity in the active site by binding

to two allosteric sites inducing conformational changes in the enzyme. The structural mechanism by which the allosteric effectors induce changes in the activity site has still not been elucidated but as described above, the change in substrate specificity upon effector binding is regulated through structural changes in loop 2 in the R1 dimer interface [Eriksson *et al.*, 1997; Uppsten *et al.*, 2003].

The activity site only binds two effectors, ATP and dATP. ATP is a positive effector that stimulates enzyme activity whereas dATP is a negative effector that inhibits enzyme activity (figure 10). If no effector is present in the activity site, RNR remains active but at slower reaction rates than the ATP stimulated enzyme [Brown & Reichard, 1969b; Eriksson *et al.*, 1979; Thelander & Reichard, 1979].

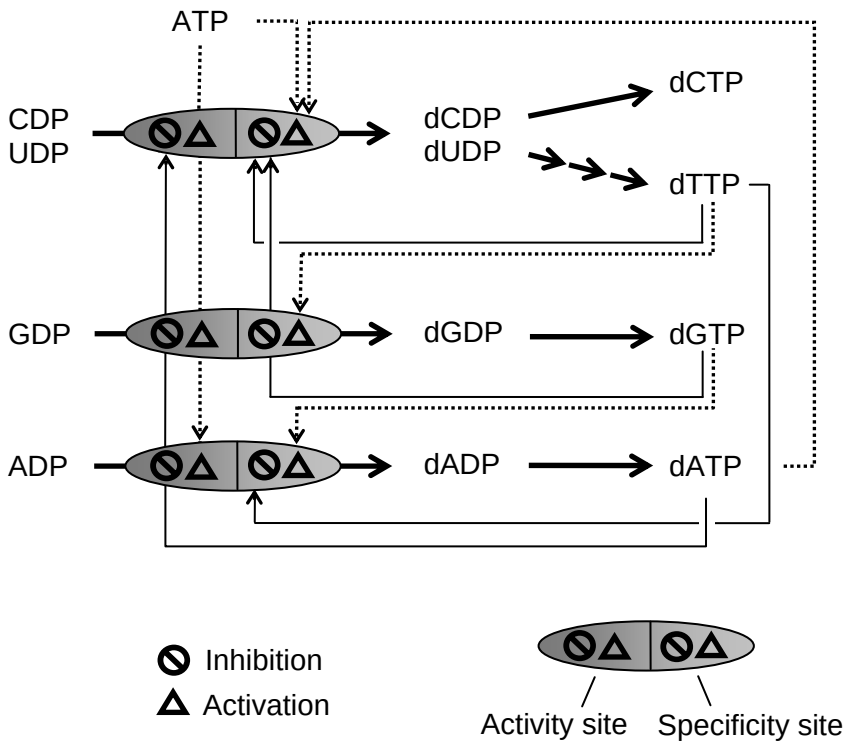

Figure 10.
Allosteric regulation of class I ribonucleotide reductase. The RNR enzyme is represented by a grey oval with the activity site on the left and the specificity site on the right. Feedback inhibition/activation by triphosphates compounds is symbolized by dotted arrows. Inhibitory and stimulatory binding is indicated by a crossed circle and a triangle, respectively. (Details are described in the text).

In early studies on *E. coli* RNR it was found that the protein formed heavy oligomeric complexes in the presence of the inhibitory effector dATP, and it

was suggested that dATP exerts its inhibitory effect by inducing protein aggregation [Brown & Reichard, 1969a; Thelander, 1973]. This was, however, not supported by later findings suggesting that binding of dATP in the activity site instead interferes with the long range electron transport from the tyrosyl radical in R2 to the active site cysteine radical 439 in R1. Binding of ATP to the activity site was suggested to promote electron transport [Ingemarson & Thelander, 1996].

The specificity site binds ATP and dATP like the activity site but it also binds dTTP and dGTP (figure 10).
Binding of ATP or dATP to the specificity site stimulates reduction of the pyrimidines CDP and UDP. dATP has a much higher affinity for the specificity site than for the activity site. Hence, the inhibition of enzyme activity only exerts its effect at higher dATP concentrations [Brown & Reichard, 1969b; Thelander & Reichard, 1979]. dUDP (and dCDP) can be converted to dTTP through several subsequent enzyme regulated steps (described in detail in figure 1), and dTTP can then bind to the specificity site and stimulate reduction of GDP. Besides from stimulating GDP reduction, binding of dTTP inhibits reduction of the other three substrates, CDP, UDP and ADP. The reduced GDP is phosphorylated to dGTP by nucleoside diphosphate kinase, and binding of dGTP to the specificity site stimulates the reduction of ADP while inhibiting reduction of the other substrates, CDP, UDP and GDP [Eriksson *et al.*, 1979]. Generally, ATP or dATP initiate up-regulation of pyrimidine deoxynucleotide levels whereas dTTP initiates up-regulation of purine deoxynucleotide levels.

In order to supply the cell with dNTP at the changing demands during cell cycle, RNR is the subject of other regulation mechanisms apart from allosteric regulation.

Cell Cycle Regulation and the Role of p53R2

Activity of the R1/R2 tetramer ribonucleotide reductase is limited to the S-phase of the cell cycle where DNA replication increases the demand for dNTP production. Outside S-phase dNTPs for DNA repair and mtDNA replication are supplied mainly by the salvage enzymes, TK2, dCK and dGK and by low levels of a more recently discovered version of RNR [Tanaka *et al.*, 2000; Nakano *et al.*, 2000]. Outside S-phase RNR comprises the R1 subunit in complex with the p53R2 subunit.

When the cells enter S-phase, both R1 and R2 are up-regulated at the transcriptional level. Studies with RNA antisense probes show an increase in R1 and R2 mRNA levels in synchronized mouse fibroblasts simultaneously with the cells' progression into S-phase [Björklund *et al.*, 1990]. R1 protein

levels remain high during all phases of the cell cycle but R2 protein is S-phase specific and thereby functions as the rate limiting factor. R2 only has a half-life of 3 hours [Eriksson *et al.*, 1984] whereas R1 is much more stable with a half-life of 15 hours [Engström *et al.*, 1985]. In late mitosis RNR activity is down-regulated by degradation of the R2 subunit. Like the salvage protein TK1, R2 protein is degraded due to an N-terminal KEN box that binds the anaphase promoting complex/Cdh1. Binding of the anaphase promoting complex/Cdh1 to R2 leads to ubiquitination and subsequent proteolysis [Chabes *et al.*, 2003b].

Resting cells contain no R2 protein, and the ribonucleotide reduction is performed by the p53R2 protein in complex with R1 [Tanaka *et al.*, 2000; Nakano *et al.*, 2000; Guittet *et al.*, 2001]. p53R2 and R2 are very similar but p53R2 lacks the N-terminal KEN box found in R2 and hence, low levels of p53R2 protein have been detected throughout the cell cycle [Håkansson *et al.*, 2006]. As the name indicates, p53R2 was first discovered as a p53 target gene, and transcription was found to be induced in a p53 dependent manner upon exposure to DNA damaging agents like γ-radiation (DNA strand breaks), adriamycin (inhibits topo II progression by DNA intercalation), camptothecin (inhibitor of topo I), actinomycin-D (transcription inhibitor) and UV-radiation (pyrimidine dimers) [Tanaka *et al.*, 2000, Nakano *et al.*, 2000].

DNA damage of human colon carcinoma p53(+/+) cells led to the induction of p53R2 protein and simultaneous reduction of R2 protein levels whereas in p53(-/-) cells no induction of p53R2 was observed, and an increase in the levels of R2 protein was observed instead [Lin *et al.*, 2004]. Unfortunately, the publication does not include measurements of cell cycle distribution after DNA damage in the two cell lines but the authors suggest that the decrease in R2 levels in p53(+/+) cells is simply due to a reduction in the percentage of cells in S-phase caused by a p53 induced G_1 arrest. Since the p53(-/-) cells do not undergo G_1 arrest the increased R2 protein levels in these cells are suggested to be due to an increased number of S-phase cells. It is very common for DNA damaging agents to interfere with cell cycle progression. Logarithmically growing human osteosarcoma cells have been shown to accumulate in S-phase in response to UV-irradiation [Skovgaard *et al.*, in preparation (Paper V)], and logarithmically growing mouse fibroblasts leave S-phase as a response to adriamycin treatment [Håkansson *et al.*, 2006]. Håkansson *et al.* [2006] also showed that R2 protein levels in adriamycin treated cells were reduced along with the reduction in number of S-phase cells.

Since the discovery of p53R2, its primary role and cellular location has been debated, and different studies have various suggestions to its regulatory role.

Immunofluorescent staining with R1 and R2 antibodies has shown that both the R1 and R2 subunits are localized to the cytoplasm of cells in

both culture and tissue [Engström *et al.*, 1984; Engström *et al.*, 1988]. Only 50 % of the cells in a logarithmically growing culture stained positive for R2 corresponding with the fraction of cells in S-phase [Engström and Rozell, 1988].

The first study on p53R2 showed that p53R2 protein translocates from the cytosol to the nucleus upon DNA damage with adriamycin [Tanaka *et al.*, 2000]. Results from a later study suggested nuclear translocation for the R1 and R2 subunits along with p53R2 in response to UV-irradiation [Xue *et al.*, 2003]. p53R2 was also believed to translocate to the nucleus at the time of transition from G_1 to S-phase and in contrast to the study by Engström and Rozell [1988], R2 was shown to also translocate to the nucleus during S-phase [Liu *et al.*, 2005]. Cellular localization of R1 was not addressed in this study and since RNR activity requires the presence of both R1 and one of the R2 or p53R2 subunits, it is not known whether the nuclear localization involves active enzyme complexes.

It has been suggested that the nuclear translocation functions as a regulatory mechanism. Due to the p53R2 up-regulation after DNA damage, the primary function of p53R2 was believed to be supplying dNTPs for DNA damage repair [Liu *et al.*, 2005; Xue *et al.*, 2003]. Very recently, this nuclear translocation upon DNA damage was disproven by three different localization methods. All three RNR subunits were shown to be exclusively cytoplasmic regardless of whether or not they were subjected to DNA damage by adriamycin [Pontarin *et al.*, 2008]. In another study, p53R2 was induced in S-phase cells despite the fact that the cells contained 30 times higher levels of R2 protein [Håkansson *et al.*, 2006]. Together, these results suggest that the primary function of p53R2 is not that of DNA repair.

Other recent discoveries link p53R2 with mitochondrial deoxynucleotide metabolism. Mutations leading to dysfunctional p53R2 protein were found in children with severe mtDNA depletions and besides, mtDNA depletion was proven in p53R2 deficient mice. These findings suggest an important role of p53R2 in maintaining dNTP pools for mtDNA synthesis outside S-phase [Bourdon *et al.*, 2007].

Lin and co-workers [2004] showed that reduction of R2 levels by siRNA increased the sensitivity of p53R2 deficient human colon cancer cells to the DNA damaging agent cisplatin (DNA crosslinker) and the RNR inhibitors Triapine® and hydroxyurea. The sensitization to cisplatin was reversed by ectopic expression of p53R2 in the R2 knock-down cells but p53R2 expression had no effect on sensitization to the RNR inhibitors. These findings support the hypothesis that p53R2 and R2 fulfill similar roles at different times of the cell cycle. When R2 is down-regulated outside S-phase, p53R2 takes over the responsibility of dNTP production for mtDNA synthesis and repair.

In this and previous sections the structure, function and regulation of the two key enzymes in nucleotide metabolism RNR and TK1 have been described in detail. The next section will focus cytosolic and mitochondrial dNTP pools, and how they are affected by dysfunction of one or more of the enzymes involved in nucleotide metabolism.

Consequences of dNTP Pool Imbalances in Mitochondria and Cytosol

The means by which the cells maintain balanced dNTP pools have been studied extensively for many years. But why is a balanced dNTP pool important, and what are the consequences if the pools are imbalanced? Some of the key enzymes responsible for regulating the cellular dNTP pools have been described comprehensively in the previous sections. This section will focus on some of the reasons for and consequences of imbalanced dNTP pools, particularly in connection with DNA damage and mitochondrial dysfunction.

dNTP Pools Sizes and Compartmentation

dNTP pool sizes vary greatly between different cell lines and even between different reports on the same cell line [Collins & Oates, 1987; Rampazzo *et al.*, 2004; Skovgaard *et al.*, in preparation (Paper V)]. This is to some extent due to the dNTP pool variations during the cell cycle. In S-phase, when the DNA is replicated, the dNTP pools increase drastically and after G_2/M-phase they decrease, and they are low in G_1-phase and G_0 cells [Skoog *et al.*, 1973; Munch-Petersen *et al.*, 1973; Tyrsted, 1975; Reichard, 1988]. Hence, even small changes in the percentage of S-phase cells present in a cycling culture influence the average dNTP levels of the cells. Even cells with the same doubling time and cell cycle distribution may vary in dNTP levels depending on the time after explantation. Still, the pyrimidine pools are usually greater than the purine pools, and dGTP are often the lowest while dCTP often is the highest pool. However, there are many exceptions from these generalizations [Reichard, 1988; Munch-Petersen *et al.*, 1973; Tyrsted, 1975; Skoog & Bjursell, 1974; Rampazzo *et al.*, 2004].

Several reports have presented evidence of separation between nuclear and cytoplasmic dNTP pools [Skoog & Bjursell, 1974; Leeds *et al.*, 1985; Bestwick *et al.*, 1982], and the separation has been suggested to be related to the "reptilase model" [Murthy & Reddy, 2006]. The "reptilase model" involves nuclear localization of RNR and other enzymes in dNTP metabolism in one large multiprotein complex responsible for the up-regulation of dNTP pools during S-phase. Several other older and newer reports present the evidence for a solely cytoplasmic localization of RNR and thymidylate synthase [Engström *et al.*, 1984; Leeds *et al.*, 1985;

Engström *et al.*, 1988; Pontarin *et al.*, 2008; Kucera & Paulus, 1986], and it is more likely that dNTPs diffuse from the cytoplasm to the nucleus across the permeable nuclear membrane. The differences in dNTP distributions observed between cytoplasmic and nuclear compartments may be explained by perturbation of the equilibrium across the nuclear membrane by different localizations of enzymes in nucleotide metabolism [Leeds *et al.*, 1985].

Contrary to the nuclear membrane, the mitochondrial membrane is not permeable to deoxynucleotides and hence, mitochondrial dNTP pools are separated from cytoplasmic pools. However, the pools are not entirely separated. Labeled thymidine has been shown to be phosphorylated in mitochondria by the mitochondrial thymidine kinase 2 in TK1 deficient cells, and subsequently labeled dTTP was observed in nuclear DNA. This suggests a transport of deoxynucleosides between the cytosolic and mitochondrial compartments [Pontarin *et al.*, 2003].

During the past decade, several mitochondrial (deoxy)nucleotide transport proteins have been investigated. One deoxynucleotide carrier (DNC) has a preference for transporting deoxynucleoside diphosphates across the membrane [Dolce *et al.*, 2001] and another, which is found both in mitochondria and in the nuclear envelope, is transporting deoxynucleosides [Lai *et al.*, 2004]. It has later been suggested that deoxynucleoside transport is not the primary function of DNC as it was proposed by Dolce and co-workers [Mathews & Song, 2007]. It is believed that the transport of dNDPs from the cytosol into mitochondria is most prevalent in dividing cells having highly active *de novo* synthesis whereas in resting cells, where mitochondrial deoxynucleosides are phosphorylated by the intra-mitochondrial salvage enzymes, TK2 and dGK, the deoxynucleoside transporter becomes important [Pontarin *et al.*, 2003; Rampazzo *et al.*, 2004]. None of the reported transport proteins are very specific for any particular deoxynucleotide but a recent report providing evidence of a highly specific mitochondrial import of dTMP suggests the presence of a more specialized thymidine nucleotide carrier [Ferraro *et al.*, 2006].

Consequences of dNTP Pool Imbalance

The enzymes responsible for maintaining balanced dNTP pools are of major importance for cellular stability and survival. The consequences of imbalanced dNTP pools are many, and a common trait between different imbalances is increased mutagenesis and increased sensitivity to DNA damaging agents.

The cellular balance among pyrimidine nucleotide levels is strongly affected by disruption of dCMP deaminase function. dCMP deaminase deficiency in mouse lymphosarcoma cells disrupts the dCTP/dTTP balance

by elevating the cellular dCTP levels and reducing dTTP levels, leading to an increased mutation rate [Weinberg *et al.*, 1981]. Likewise, high mutation rates have been observed in Chinese hamster ovary cells harbouring a dysfunctional dCMP deaminase and a mutated CTP synthase resistant to feedback inhibition by CTP. Like the lymphosarcoma cells, these cells also display highly elevated dCTP pools, and in addition they are thymidine auxotroph [Meuth *et al.*, 1979; Trudel *et al.*, 1984].

A reduction of dCTP pools is observed in Chinese hamster ovary cells deficient for the salvage enzyme deoxycytidine kinase [Meuth, 1983]. This is not lethal for the cells but they display increased sensitivity to DNA alkylating agents due to an imbalanced dCTP/dTTP pool. The decreased levels of dCTP relative to dTTP increase the risk of thymine to O^6-alkylguanine mispairing. Depletion of dCDP and increased mutation rates are also observed by addition of high concentrations of dThd to Chinese hamster ovary cells [Meuth, 1981]. The high dThd concentration results in increased dTTP levels which in turn lead to allosteric inhibition of RNR catalyzed CDP reduction. Consequently, the dCDP pool is depleted. Additionally, high thymidine concentration increases the number of single base pair substitutions and sister chromatid exchanges induced by DNA alkylating agents [Perry, 1983].

The other cytosolic deoxynucleoside salvage enzyme, TK1, is also important to maintaining balanced dNTP pools. In cell cultures TK1 is dispensable but TK1 knock-out mice are found to develop sclerosis of kidney glomeruli and die from kidney failure before reaching 298 days of age. Furthermore, serum thymidine levels were increased 2-3-fold in $TK1^{-/-}$ mice compared to homozygous ($TK1^{+/-}$) or heterozygous ($TK1^{+/+}$) mice [Dobrovolsky *et al.*, 2003]. Despite the severe effects of TK1 deficiency in mice it is noteworthy that no human disease is associated with this genotype. This indicates that TK1 deficiency in humans either has a phenotype with mild or no symptoms or that the phenotype is lethal. In vitro it was shown that TK1 deficient human osteosarcoma cells had decreased levels of dTTP but they also displayed increased survival following UV-irradiation compared to TK1 positive cells [Skovgaard *et al.*, submitted (Paper III)].

Thymidylate synthase deficiency results in thymidine deprivation which has severe consequences for cellular viability. It leads to depletion of dTTP and dGTP pools and expansion of dATP, dCTP and dUTP pools. Lethality associated with mutagenesis is observed if cells are not supplied with thymidine during growth [Kunz, 1982]. If thymidylate synthase is either inhibited or dysfunctional, the cells accumulate single and double strand breaks in DNA along with rapid cell death. On the genetic level the consequences of thymidylate synthase dysfunction is uracil incorporation into DNA, sister chromatid exchanges and gross chromosomal abnormalities [Meuth 1989; Li *et al.*, 2005].

Imbalances in purine deoxynucleotide pools also have consequences for cellular function. Chinese hamster ovary cells exhibiting purine starvation due to a defect in *de novo* purine synthesis display a rapid shutdown of DNA replication in the absence of exogenous addition of the purine precursor hypoxanthine. Furthermore, the cells exhibit increased UV-induced mutations and cell death, as well as the inability to repair UV-induced pyrimidine dimers [Collins *et al.*, 1988].

Likewise, simultaneous addition of deoxyadenosine and the adenosine deaminase inhibitor deoxycoformycin to resting lymphocytes results in disturbed DNA repair due to accumulation of dATP. The increased dATP level did not in itself induce DNA damage but it inhibited the repair of single strand damage induced by the alkylating agent N-methyl-N'-nitro-N-nitrosoguanidine [Cohen and Thompson, 1986]. Addition of all three but not of the single deoxynucleosides, dThd, dCyd and dGuo, prevented the effect of dAdo addition, suggesting that the imbalanced pools are responsible for inhibiting the DNA repair.

There can be no doubt that imbalanced dNTP pools can cause increased sensitivity to DNA damaging agents but some reports have also proven the reverse relation: that DNA damaging agent can induce changes in dNTP pools [reviewed by Kunz and Kohalmi, 1991]. Early reports showed increased dATP and dTTP pools in Chinese hamster fibroblasts following treatment with the DNA damaging agents MNNG, UV, mitomycin C and cytosine arabinoside [Das *et al.*, 1983]. Newman and Miller found rapid but short-term 5-fold increase in the dTTP pool along with an equally rapid but longer lasting 10-fold decrease in the dCTP pool as a consequence of UV-irradiation in Chinese hamster ovary cells [1983]. However, in a later study of Chinese hamster ovary cells and two human cell lines no significant change in dNTP pools was found after UV-irradiation. The same authors also make note of the large differences in dNTP pools measured in undamaged Chinese hamster ovary cells in different laboratories [Collins & Oates, 1987]. Recently, a report on mouse fibroblasts demonstrated that treatment with adriamycin decreased all four dNTP pools but consistent with the study on Chinese hamster and human cells [Collins & Oates, 1987], UV-irradiation did not affect the dNTP pools [Håkansson *et al.*, 2006].

Clearly, imbalances in cellular dNTP pools have been proven to have serious consequences but imbalances in the much smaller mitochondrial dNTP pools can be equally severe. In order to clarify the connection between imbalanced mitochondrial dNTP pools and their impact on mitochondrial function, we first need a detailed understanding of some of the key players involved in maintaining mitochondrial function.

Mitochondrial Function and Consequences of Mitochondrial dNTP Pool Imbalance

A large part of the energy-demanding reactions in our cells are driven by hydrolysis of ATP and consequently, a sufficient supply of ATP is of major importance for cellular function. One of the most important functions of mitochondria is production of ATP by oxidative phosphorylation. They are also the compartment of amino acid metabolism, the citric acid cycle and β-oxidation of fatty acids.

Mitochondria are double membrane organelles with an electrochemical gradient between the mitochondrial matrix and the inter membrane space. The electrochemical gradient is maintained by electron flow through the five enzyme complexes bound in the inner mitochondrial membrane. The five large complexes, along with the two electron carriers, cytochrome C and ubiquinone, constitute the electron transport chain. Complex I, III and IV maintain the electrochemical gradient by pumping protons from the matrix into the inter membrane space while complex V, also known as ATP synthase, catalyzes the production of ATP from ADP along with the reduction of O_2 to H_2O. ATP synthase is driven by the reverse flow of protons into the matrix.

Some of the characteristics of mitochondrial dysfunction can be depolarization or hyperpolarization of the inner mitochondrial membrane due to dysfunction of one or more of the protein complexes in the electron transport chain. Apart from mutations in nuclear DNA (nDNA) this can be caused by mutations in or the complete lack of mtDNA.

The mitochondrial genome resides in the matrix and encodes 37 genes, including several t- and r-RNAs. 13 of the genes encoded by mtDNA are protein components of complex I, III, IV and V of the electron transport chain and hence, mutations in the mitochondrial genome can have severe consequences. Mutations in one or more of the protein complexes in the electron transport chain can lead to reduced ATP production due to disruption of the electrochemical gradient across the inner mitochondrial membrane and is associated with a number of different diseases [reviewed by McKenzie *et al.*, 2004].

ND6 is a gene in the mitochondrial genome encoding a protein subunit in complex I of the electron transport chain. A heteroplasmic point mutation in the ND6 gene can, if present in low copy numbers, cause Leber hereditary optic neuropathy (LHON), characterized by blindness in early adulthood. If the same mutation is present in higher copy numbers it can result in the more severe disease dystonia, characterized by movement disorders, mental retardation, short stature and degeneration of the basal ganglia [Jun *et al.*, 1994]. A heteroplasmic mutation in the mitochondrial ATP6 gene encoding a protein in ATP synthase can cause equally severe diseases. The mutation blocks the F_0 proton channel, reducing the ADP/O

ratio, and in lower copy numbers it leads to neurogenic muscle weakness, ataxia and retinitis pigmentosa (NARP) associated with dementia and learning difficulty. If the mutation is found in high copy numbers (>95 %) it can cause the much more severe and often lethal Leigh's syndrome characterized by hypotonia, ataxia, spasticity, optic atrophy, opthalmoplegia and developmental delay [Tatuch *et al.*, 1992; Trounce *et al.*, 1994]. These diseases underline the importance of a fully functional electron transport chain.

Due to the role of mitochondria in cellular energy production, functional mitochondria are extremely important for cellular vitality. However, unlike nuclear DNA the mitochondrial DNA (mtDNA) is not protected by histones and has limited DNA repair [Larsen *et al.*, 2005], making it very sensitive to mutations and mtDNA depletion. Hence, imbalances in the mitochondrial dNTP pool can have severe consequences for the cells.

Mitochondrial DNA depletion can result from deficiency or malfunction of one of several enzymes involved in nucleotide metabolism. Some of the diseases caused by imbalanced dNTP pools in mitochondria and subsequent mutations and depletions of mtDNA are hepatocerebral and myopathic mitochondrial depletion syndrome (MDS) and mitochondrial neurogastrointestinal encephalomyopathy (MNGIE). As mentioned previously, the mitochondrial dNTP pools are maintained either by import of deoxynucleotides from the cytosol via nucleotide transporters or by intra-mitochondrial salvage of deoxynucleosides. The salvage enzymes TK2 and dGK residing in the mitochondria are encoded by nuclear genes and are the key players in mitochondrial dNTP salvage. In resting cells, when the cytosolic dNTP metabolic enzymes TK1 and RNR are not expressed, TK2 and dGK are pivotal to maintaining mitochondrial dNTP pools. Several mutations in the dGK and TK2 genes have been identified in patients suffering from mitochondrial depletion syndrome [Saada-Reisch, 2004].

A single nucleotide deletion resulting in a frameshift and premature termination of translation in dGK was identified in patients suffering from the hepatocerebral form of MDS in three Israeli-Druze kindreds. The majority of the affected individuals have mitochondrial DNA depletion (only 8-39 % mtDNA/nDNA ratio compared to normals) and reduced enzyme activity of the electron transport chain complexes I, III and IV in liver tissue. They die during the first year of age [Mandel *et al.*, 2001]. No mtDNA depletion is found in tissues from blood, skin and muscle, consistent with this form of MDS being characteristic by showing hepatic failure and neurological abnormalities. Several other mutations in dGK have been identified in patients suffering form hepatocerebral MDS, and enzymatic characterization of the mutant enzymes reveals that they all result in severely reduced or complete lack of enzymatic activity [Wang & Eriksson, 2003].

Likewise, several mutations in TK2 have been identified in patients suffering from a different form of MDS affecting muscle tissue (myopathic MDS) [Saada-Reisch *et al.*, 2004]. The first mutations were found in a study of four unrelated patients [Saada *et al.*, 2001]. Three Moslem-Arabs suffering from severe devastating myopathy all had a point mutation in the TK2 gene, resulting in the amino acid change, I212N (numbering is based on the full length TK2 sequence from Wang *et al*., 2003). In the same study another mutation resulting in the H121N amino acid change vas identified in an Ashkenazi Jewish patient, showing milder symptoms and later onset of myopathic MDS [Saada *et al.*, 2001; Nevo *et al.*, 2002]. Kinetic characterization of the mutant TK2 enzymes reveals that the I212N mutant had severely decreased activity with both dThd and dCyd whereas the H121N mutant had reduced capacity to phosphorylate dCyd due to inefficient binding and catalysis of ATP [Wang *et al.*, 2003]. These findings correlate well with the different severeness of the patient symptoms. Additionally, the connection between TK2 and mitochondrial function was demonstrated in a study of TK2 deficient mice showing growth retardation and premature death along with loss of mtDNA in several different tissues, including heart and skeletal muscle [Zhou *et al.*, 2008]. In another study, knock-in mice harboring the gene of the mouse homologue to H121N TK2 were created. The knock-in mice showed TK2 deficiency, unbalanced dNTP pools, mtDNA depletion and defects in electron transport chain enzymes, and they died within 2-3 weeks. Contrary to humans, the effects of TK2 deficiency in mice were most prominent in the central nervous system [Akman *et al.*, 2008].

Studies on mtDNA regulation suggest that mtDNA copy number is tightly regulated by mitochondrial dNTP pools [Tang *et al.*, 2000]. Dysfunctional TK2 is likely to result in decreased mitochondrial dTTP and/or dCTP pools whereas dysfunctional dGK will likely result in decreased dGTP and dATP pools. These pool imbalances may influence the mtDNA copy number and thereby lead to various versions of MDS.

The liver, brain, and muscle tissues are some of the most energy demanding tissues in the body, and it is not surprising that they are the tissues most affected by mtDNA depletion. It is comprehensible that mitochondrial depletion is not observed in replicating tissues and during fetal development since mtDNA pools can be maintained by cytosolic import of nucleotides. However, the tissue specificity displayed by TK2 dysfunction being characteristic of myopathic MDS and dGK dysfunction being characteristic of hepatocerebral MDS is not yet understood.

It has been suggested that dGK deficiency may be counterbalanced by dCK activity in some tissues since they have overlapping substrate specificities. In liver and brain tissues the dCK activity is low, explaining the hepatocerebral form of MDS as a result of dGK dysfunction [Saada-Reisch, 2004]. Sparing of liver and brain tissue in myopathic MDS caused by TK2 dysfunction is less obvious since the *de novo* pathway, TK1 and dCK are

low in liver tissue. On the other hand, the ratio of TK2 activity and mtDNA in healthy liver tissue is high relative to other tissues, suggesting that even low levels of TK2 activity is sufficient for maintaining mtDNA. In skeletal muscle the TK2 activity/mtDNA ratio is only 5 % of that in liver tissue, explaining the vulnerability of muscle tissue to TK2 deficiency [Saada-Reisch, 2004]. It is highly likely that small tissue specific changes in TK2 activity versus mtDNA content are responsible for the tissue specificity of myopathic MDS. In knock-in mice carrying the mouse homologue of the dysfunctional mutant H121N TK2 the brain was the most affected tissue having only 12.5 % mtDNA compared to litter mates. This correlates well with the finding that TK2 accounts for as much as 60 % of the thymidine kinase activity in the brain of wild type mice, suggesting that the central nervous system is more dependant on mitochondrial pyrimidine salvage than the other tissues in mice [Akman *et al.*, 2008]. Unfortunately, the actual levels of TK2 activity and mtDNA content were not reported so the TK2 activity /mtDNA ratio in the mice tissues is unknown, and it is unclear if the high percentage of TK2 activity is due to low TK1 or high TK2 activity.

Whereas dysfunction of the two mitochondrial enzymes dGK and TK2 is causing MDS correlated with a decrease in one or more of the mitochondrial dNTP pools, dysfunction in the cytoplasmic enzyme, thymidine phosphorylase (TP), results in increased blood thymidine levels. The high thymidine levels in the blood are associated with point mutations and long deletions in mtDNA [Marti *et al.*, 2002; Nishigaki *et al.*, 2003]. A number of different mutations in the nuclear TP gene have been identified in patients with mitochondrial neurogastrointestinal encephalomyopathy (MNGIE) [Nishino *et al.*, 1999]. TP is expressed in tissues of the brain, peripheral nerves, spleen, lung, bladder and the gastrointestinal system consistent with some of the clinical features of MNGIE being leukoencephalopathy, neuropathy and gastrointestinal dysmotility, but even skeletal muscle that has no TP activity is usually affected in MNGIE. TP catalyzes the breakdown of thymidine to free thymine and deoxyribose-1-phosphate and is an important regulator of cellular thymidine levels. TP deficiency leads to cellular thymidine export, and due to the high levels of blood thymidine (3-25 μM in plasma) it is also affecting dNTP pools in cells not expressing TP [Spinazzola *et al.*, 2002; Marti *et al.*, 2002]. The increased thymidine levels have a considerable impact on the mitochondrial dNTP pools since they rely mainly on the salvage pathway whereas the cytoplasmic dNTP pool is highly regulated by enzymes in the *de novo* pathway. The mitochondrial dNTP imbalance caused by TP deficiency is suggested to lead to mtDNA abnormalities including site-specific point mutations [Nishigaki *et al.*, 2003; Song *et al.*, 2003]

The connection between dysfunctional enzymes in the mitochondrial nucleotide metabolism and between imbalanced mitochondrial dNTP pools,

and their effect on mitochondrial function has been thoroughly studied for years. A less well-known but closely related phenomenon is the reverse connection between dysfunctional mitochondria and their effect on cellular dNTP pools.

Mitochondrial Dysfunction is Affecting Cellular dNTP Pools

It has recently been demonstrated that exponentially growing human cells depleted of mitochondrial DNA (termed ρ^0 cells) exhibit decreased cellular dNTP levels and dNTP imbalance. In human HeLa cells the dTTP and dCTP pools were decreased 4-5-fold whereas the dATP and dGTP pools were unchanged. In human breast cancer cells all four dNTP pools were equally 2-3-fold reduced. It was also found that dNTP imbalance results in genomic instability of nuclear DNA at that mitochondrial dysfunction leads to chromosomal instability [Desler *et al.*, 2007]. Additionally, another recent study on osteosarcoma cells found low dATP pool levels in ρ^0 cells compared to two ρ^+ cell lines. It was discovered that dNTP pools in ρ^0 cells respond differently to UV-induced DNA damage than the parental ρ^+ cell line. In the ρ^0 cells the levels of all four dNTPs increased 2-4-fold over 30 hours after the time of UV-irradiation [Skovgaard *et al.*, in preparation (Paper V)]. Furthermore, it was found that inhibition of the electron transport chain with the ATP synthase inhibitor oligomycin in the parental ρ^+ cells induced a similar response in dNTP pools after UV-irradiation as was observed in the ρ^0 cells. There was no direct link between changes in dNTP pools and changes in ATP pools, however. From these results, it is suggested that low initial levels of dATP in ρ^0 cells and oligomycin treated ρ^+ cells play a role in the dNTP pool increase after DNA damage. In normal cells dATP functions as a feedback inhibitor of ribonucleotide reductase, keeping RNR activity in check when it is induced upon DNA damage. In ρ^0 cells and ρ^+ oligomycin treated cells the low dATP pools are not capable of restraining RNR activity leading to increased dNTP production. A similar phenomenon is observed in yeast cells, displaying a relaxed feedback inhibition of RNR by dATP [Chabes *et al.*, 2003a]. But why are some of the dNTP pools lower in ρ^0 cells in the first place and, why are the same pools not affected in different cell types? A review by Desler [2009] suggests several factors that can connect mitochondrial dysfunction and cellular nucleotide metabolism. Some of the important elements are summarized below.

Dihydroorotate dehydrogenase (DHODH) is a mitochondrial flavoenzyme that links the electron transport chain to *de novo* pyrimidine synthesis. It is an integral membrane protein located in the inner mitochondrial membrane where it faces the inner membrane space [Rawls *et al.*, 2000]. DHODH catalyzes the oxidation of dihydroorotate to orotate (figure 11), and in multiple steps orotate is subsequently converted to UTP and CTP which are

finally converted to dTTP and dCTP. Dihydroorotate oxidation takes place by simultaneous reduction of ubiquinone to ubiquinol, with the immediate electron acceptor in DHODH being FMN and with ubiquinone as the final acceptor [Bader *et al.*, 1998]. From ubiquinol the electrons continue the path through the respiratory chain.

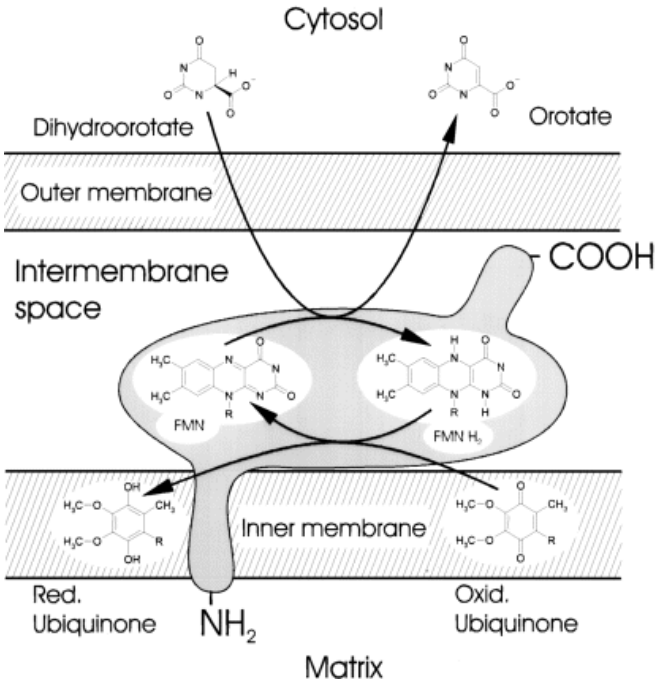

Figure 11
Schematic representation of the mitochondrial enzyme dihydroorotate dehydrogenase. DHODH is located in the inner mitochondrial membrane where it is responsible for dihydroorotate oxidation and ubiquinone reduction [Rawls *et al.*, 2000].

Import and correct positioning of DHODH into the inner mitochondrial membrane has been demonstrated to require a membrane potential and an input of energy in the form of ATP [Rawls *et al.*, 2000]. Hence, a decreased membrane potential or insufficient ATP production can influence DHODH localization to the mitochondria and thereby prevent pyrimidine biosynthesis.

Inhibition with chloramphenicol of mammalian mitochondrial protein synthesis and consequently impairment of the electron transport chain or impairment of the electron transport chain by oxygen deficiency inhibits DHODH activity and cell growth. However, the inhibition can be reversed by addition of pyrimidines to the growth media, indicating a close connection between mitochondrial function and pyrimidine metabolism [Löffler, 1980; Grégoire *et al.*, 1984].

Mitochondria are also indirectly involved in *de novo* purine biosynthesis through the involvement in one-carbon metabolism. Cytosolic 10-formyltetrahydrofolate (10-CHO-THF) is an important one-carbon donor in purine biosynthesis. It can be produced either from tetrahydrofolate (THF) and mitochondrially synthesized formate in a reaction catalyzed by 10-formyltetrahydrofolate synthetase or from 5,10-methenyltetrahydrofolate (5,10-CH=THF) catalyzed by cyclohydrolase. In figure 12 is an overview of cytosolic and mitochondrial one-carbon metabolism, and several studies demonstrate that the net flow of one-carbon units through the reactions in mitochondria are in the direction of serine to glycine whereas they are in the direction of glycine to serine in the cytosol [Pawelek & McKenzie, 1998; Patel *et al.*, 2003]. This suggests that the cytosolic one-carbon units including 10-CHO-THF originate mainly from mitochondrial formate production.

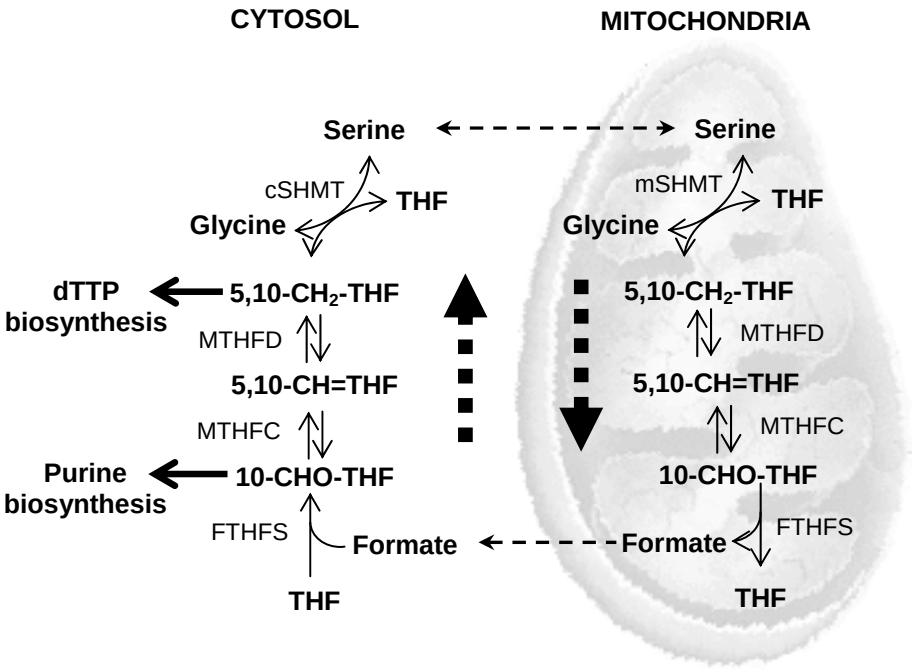

Figure 12
One-carbon metabolism in cytosol and mitochondria. Enzyme abbreviations: cSHMT, cytosolic serine hydroxymethyltransferase; mSHMT, mitochondrial serine hydroxymethyltransferase; MTHFD, 5,10-methylenetetrahydrofolate dehydrogenase; MTHFC, 5,10-methenyltetrahydrofolate cyclohydrolase; FTHFS, 10-formyltetrahydrofolate synthetase. Abbrevitaions of intermediates: THF, tetrahydrofolate; 5,10-CH_2-THF, 5,10-methylenetetrahydrofolate; 5,10-CH = THF, 5,10-methenyltetrahydrofolate; 10-CHO-THF, 10-formyltetrahydrofolate. The large arrows on the left and right denote the preferred direction of the reactions in the cytosol and in the mitochondria, respectively.

The second step in production of formate from mitochondrial serine is catalyzed by methylenetetrahydrofolate dehydrogenase converting 5,10-methylene-THF (5,10-CH_2-THF) to 5,10-CH=THF in a NAD^+ dependent reaction. Furthermore, the reaction has been suggested to be sensitive to the mitochondrial ATP/ADP ratio [Desler, 2009]. Mitochondrial dysfunction leads to decreased ATP levels and possibly changes in NAD^+/NADH levels, and can therefore influence methylenetetrahydrofolate dehydrogenase activity which depends upon NAD^+ and the ATP/ADP ratio. Hence, dysfunctional mitochondria can reduce mitochondrial formate production and thereby affect cytosolic 10-CHO-THF production which again affects purine biosynthesis.

A disruption of the one-carbon metabolism could possibly also influence the *de novo* synthesis of dTMP and consequently affect the dTTP pool. dTMP is formed from methylation of dUMP. In this reaction the methyl moiety is transferred from 5,10-methylene-THF to dUMP catalyzed by the cytosolic enzyme thymidylate synthase (figure 1).

A third effector of dNTP pools is the mitochondrial nitric oxide synthase (mtNOS). mtNOS is located in the mitochondrial inner membrane where it produces NO in a Ca^{2+} dependent reaction [Tatoyan & Guilivi, 1998]. Within the mitochondria NO can influence pyrimidine metabolism by indirectly inhibiting DHODH through inhibition of cytochrome c oxidase [Beuneu *et al.*, 2000]. NO can also be exported out of the mitochondria, and in the cytosol it can inhibit RNR [Roy *et al.*, 2004]. The NO induced inhibition of RNR was demonstrated to induce decreased dATP pools, and due to an activation of pyrimidine salvage it furthermore led to increased dTTP and dCTP pools. The dGTP pools were unchanged, perhaps due the high dTTP levels activating GDP reduction in RNR [Roy *et al.*, 2004].

The efflux of NO from mitochondria has been found to correlate with the mitochondrial membrane potential, suggesting that mtNOS is a voltage regulated enzyme. A high membrane potential leads to increased NO efflux whereas a lower membrane potential reduces the NO efflux [Valdez *et al.*, 2006]. Hence, mitochondrial dysfunction causing an increased membrane potential is able to increase NO production and thereby induce imbalanced dNTP pools.

SUMMARY OF RESULTS AND DISCUSSION

Looking at the wide range of diseases caused by imbalanced dNTP pools and dysfunctional enzymes involved in deoxynucleotide metabolism there is no doubt that a strictly regulated deoxynucleotide metabolism is pivotal for a healthy cellular environment. A detailed knowledge of the enzymes involved in regulating the cellular dNTP pools is necessary for understanding and treating some of the diseases caused by disturbances in DNA metabolism. The papers at the end of this thesis present research related to different topics within this field. The research is centered on two main themes. One is obtaining a detailed knowledge of structure function relations of thymidine kinase 1 with the purpose of using it as a suicide gene. The other is an investigation of the relation between dNTP pools, thymidine kinase 1 deficiency and mitochondrial function. A summary of these results is presented below and discussed in relation to past and present research.

Deoxynucleoside Kinases as Suicide Enzymes

The HSV1TK/ganciclovir system is one of the most well characterized systems in 'suicide' gene therapy and has been applied in clinical trials against solid tumours since the 1980's [Moolten, 1986, Ram *et al.*, 1997, Klatzmann *et al.*, 1988a; Klatzmann *et al.*, 1988b]. In order to improve the phosphorylation efficiency of the nucleoside analogue and thereby increase cell killing HSV1TK has been subjected to semi-random mutagenesis [Black *et al.*, 2001].

More recently other deoxynucleoside kinases have been considered for application in 'suicide' gene therapy. Deoxynucleoside kinases from *D. melanogaster*, *C. elegans* and human have been investigated by mutational and structural analysis [Knecht *et al.*, 2000; Welin *et al.*, 2005 (Paper I); Skovgaard & Munch-Petersen, 2006 (Paper II); Skovgaard *et al.*, submitted (Paper IV)].

In a directed evolution study the *Dm*dNK N45D/N64D double mutant was demonstrated to increase the sensitivity of transformed bacteria to several

cytotoxic nucleoside analogues. Kinetic investigation of the double mutant showed that the improved cytotoxicity was due to decreased activities with the four natural substrates and unchanged activity with the nucleoside analogue AZT compared to wild type *Dm*dNK. Besides, the double mutant had decreased feedback inhibition with dTTP [Knecht *et al.*, 2000].
Further kinetic investigation of the *Dm*dNK N45D/N64D double mutant and the two N45D and N64D single mutants proved that the mutation responsible for these changes is N64D. Additionally, the crystal structure of *Dm*dNK-N64D in complex with dTTP revealed a local destabilization preventing a hydrogen bond to the 3'-OH of dTTP. This structural change is increasing the space near the large 3'-azidogroup of AZT and at the same time it is responsible for the decreased affinity for the natural substrates and feedback inhibitors [Welin *et al.*, 2005 (Paper I)]. Transduction of human cancer cell lines with the N45D/N64D double mutant was later found to increase the sensitivity toward several cytotoxic nucleoside analogues [Knecht *et al.*, 2007]. These findings suggest that *Dm*dNK-N45D/N64D is a suitable candidate for 'suicide' gene therapy with AZT.

A new thymidine kinase from *C. elegans* has been characterized [Skovgaard & Munch-Petersen, 2006 (Paper II)] and is used along with human TK1 as the basis for a detailed structure function study [Skovgaard *et al.*, submitted (Paper IV)]. *C. elegans* thymidine kinase is special in the sense that it appears to be the only deoxynucleoside kinase present in the nematode despite its narrow substrate specificity. It is has a high sequence similarity with human TK1 but besides from phosphorylating dThd it also has a weak ability to phosphorylate dGuo. *Ce*TK1 also has a different pattern of ATP activation than observed for HuTK1 [Skovgaard & Munch-Petersen, 2006 (Paper II); Munch-Petersen *et al.*, 1993]. According to the first TK1 crystal structures all amino acid interactions with the thymine base are mediated by hydrogen bonds to main chain atoms explaining the narrow substrate specificity for TK1-type kinases [Welin *et al.*, 2004; Birringer *et al.*, 2005]. Sequence and structure analysis has revealed that the majority of the amino acids in the phosphate acceptor site are the same in HuTK1 and *Ce*TK1. Only Thr163 in HuTK1 is replaced by a Ser in *Ce*TK1 (Ser 182, *Ce*TK1 numbering). In the HuTK1 structure Thr163 is positioned in a small hydrophobic pocket near the methyl group of the thymine base [Welin *et al.*, 2004]. Site-directed mutagenesis of Thr163/Ser182 and surrounding amino acids in HuTK1/*Ce*TK1 led to the creation of new mutant enzymes with new or changes substrate activities. Some *Ce*TK1 mutants gained the ability to phosphorylate dCyd or displayed increased dGuo phosphorylation. Most interesting was the creation of HuTK1-T163S having a 70-fold higher AZT/dThd ratio in catalytic efficiency compared to the wild type human kinase [Skovgaard *et al.*, submitted (Paper IV)].

The crystal structure of the T163S mutant in complex with the feedback inhibitor dTTP did not reveal the structural background for the

changed AZT specificity. But, a modelled structure of *Ce*TK1 gave insight into the difference in substrate specificity between the two enzyme species. It is noteworthy, that none of the HuTK1 mutant enzymes were able to phosphorylate dGuo or dCyd and by close inspection of the *Ce*TK1 modelled structure it was revealed that it is likely a proline not far from the active site which is responsible for the different specificity.

The highly increased AZT specificity of the HuTK1-T163S mutant makes it a suitable candidate for 'suicide' gene therapy. Besides, the increased understanding of the TK1 active site will be of importance for designing new nucleoside analogues or development of new improved TK1 enzymes for use in 'suicide' gene/chemo therapy.

DNA Damage and Changes in dNTP Pools

Several studies have proven that dysfunction of a number of enzymes involved in nucleotide metabolism can cause imbalanced dNTP pool which in turn leads to increased sensitivity to DNA damaging agents, higher mutation rates and even cell death [Weinberg *et al.*, 1981; Meuth, 1983; Meuth, 1989; Li *et al.*, 2005; Collins *et al.*, 1988; Cohen & Thompson, 1986; Saada-Reisch, 2004; Marti *et al.*, 2002]. Additionally, the enzyme deficiencies are associated with numerous different diseases.

Despite being the key enzymes in the salvage of deoxynucleosides, TK1 deficiency has no known phenotype in humans. However, TK1 knock-out mice were found to have increased serum thymidine levels. Besides, they suffer from sclerosis of kidney glomeruli and have an average life span of only 166 days before they die of kidney failure [Dobrovolsky *et al.*, 2003]. Whereas deficiencies for many other enzymes in nucleotide metabolism increase the susceptibility to DNA damaging agents it was found that human osteosarcoma cells deficient for TK1 had a 2-fold higher survival rate after UV-induced DNA damage compared to TK1 positive control cells. The dTTP pool in the TK negative cells was only half the size of the pool in TK1 positive cells and it did not increase following DNA damage [Skovgaard *et al.*, submitted (Paper III)]. It was suggested that higher thymidine levels in the TK negative osteosarcoma cells increase the UV-resistance due to a higher absorption of UV rays by free thymidine [Skovgaard *et al.*, submitted (Paper III)]. This is based on the increased serum thymidine levels observed in the TK1 deficient mice models [Dobrovolsky *et al.*, 2003].

Several research groups have studied the effect of DNA damage on dNTP pools in mammalian cells, but with varying results. Some groups report large and rapid changes in one to two pools after DNA damage whereas others observe no changes [reviewed by Kunz and Kohalmi, 1991]. In a recent study on human osteosarcoma cells subjected to UV-induced DNA damage no change was found in any of the dNTP pool when monitored for 30 hours

after irradiation. These results were demonstrated in normal osteosarcoma cells (HOS) and in TK1 deficient osteosarcoma cells (143B TK^-) [Skovgaard *et al.*, in preparation (Paper V)], and agree with the results obtained for mouse fibroblasts [Håkansson *et al.*, 2006]. 143B TK^- cells that were also deficient for mitochondrial DNA (143B ρ^0) responded differently from the other two cell lines though, and all four dNTP pools increased 2-3-fold over a period of 30 hours after DNA damage. Inhibition of the ATP synthase with oligomycin in 143B ρ^+ cells reduced the cellular ATP concentration to the levels observed in ρ^0 cells and resulted in similar increases in dNTP pools. At the time of irradiation the 143B ρ^0 cells and the oligomycin treated 143B ρ^+ cells are distinguished by having lower dATP pools than the two untreated ρ^+ cell lines (all four pools are reduced in the oligomycin treated cells) and it is suggested that the low dATP levels are responsible for the increased dNTP pools following DNA damage [Skovgaard *et al.*, in preparation (Paper V)]. In two yeast strains it was found that the UV mimicking 4-nitroquinoline-N-oxide induced 2-7-fold increased dNTP pools, which is believed to be due to a relaxed dATP feedback of yeast ribonucleotide reductase. In order to supply the cells with dNTPs up-regulation of RNR has been demonstrated to take place upon DNA damage [Guittet *et al.*, 2001; Tanaka *et al.*, 2000]. It is likely that the dATP levels in ρ^0 and oligomycin treated ρ^+ cells are not sufficiently high to restrain RNR activity after DNA damage, which results in increased dNTP levels as observed in yeast cells.

This raises the question of why the dATP pool is low in ρ^0 cells? A previous study on human ρ^0 cell lines also reported decreased levels of some or all dNTPs [Desler *et al.*, 2007], but there is no systematic decrease of any particular dNTP pool.

Mitochondrial function (or dysfunction) has been suggested to affect cellular dNTP pools by three different paths [reviewed by Desler, 2009]. Dihydroorotate (DHODH) is located in the inner mitochondrial membrane and links mitochondrial function to *de novo* pyrimidine biosynthesis due to the simultaneous conversion of dihydroorotate to orotate and ubiquinone to ubiquinol. DHODH function and cell growth is impaired by inhibition of the electron transport chain, but the effect is reversed by addition of pyrimidines [Löffler, 1980; Grégoire *et al.*, 1984].

De novo synthesis of purines is also linked to mitochondrial function via the mitochondrial NAD^+ dependent and ATP/ADP sensitive methylenetetrahydrofolate dehydrogenase, which is one of the enzymes involved in mitochondrial formate production [Desler, 2009]. The majority of the formate used to produce 10-formyltetrahydrofolate, an important methyl donor in purine metabolism, is believed to originate from the mitochondria [Pawelek & McKenzie, 1998; Patel *et al.*, 2003]. Hence, disturbance of NAD^+ levels or the ATP/ADP ratio in the mitochondria may affect purine metabolism.

Finally, the mitochondrial nitric oxide synthase (mtNOS), located in the inner mitochondrial membrane can affect deoxynucleotide metabolism due to its production of NO. NO can affect pyrimidine metabolism within the mitochondria by indirect inhibition of DHODH [Beuneu *et al.*, 2000] or it can be exported out in the cytosol where it inhibits RNR [Roy *et al.*, 2004]. mtNOS is suggested to be a voltage regulated enzyme and the NO export increases upon increased membrane potential [Valdez *et al.*, 2006].

Due to the multiple ways in which mitochondrial dysfunction can influence the cellular dNTP pools the correlation between imbalanced dNTP pools and mitochondrial dysfunction is not so straight forward, explaining the variations in dNTP levels in different ρ^0 cells lines. It was suggested that the low initial dNTP pools observed in oligomycin treated 143B ρ^+ cells may be caused by hyperpolarization of the inner mitochondrial membrane leading to increasing NO efflux and inhibition of RNR [Skovgaard *et al.*, in preparation (Paper V)].

REFERENCES

Akman HO, Dorado B, López LC, García-Cazorla A, Vilà MR, Tanabe LM, Dauer WT, Bonilla E, Tanji K, Hirano M. Thymidine kinase 2 (H126N) knockin mice show the essential role of balanced deoxynucleotide pools for mitochondrial DNA maintenance. Hum Mol Genet. **2008** Aug 15;17(16):2433-40.

Arnér ES, Eriksson S. Mammalian deoxyribonucleoside kinases. Pharmacol Ther. **1995**;67(2):155-86.

Bauer CB, Fonseca MV, Holden HM, Thoden JB, Thompson TB, Escalante-Semerena JC, Rayment I. Three-dimensional structure of ATP:corrinoid adenosyltransferase from Salmonella typhimurium in its free state, complexed with MgATP, or complexed with hydroxycobalamin and MgATP. Biochemistry. **2001** Jan 16;40(2):361-74.

Beltinger C, Fulda S, Kammertoens T, Meyer E, Uckert W, Debatin KM. Herpes simplex virus thymidine kinase/ganciclovir-induced apoptosis involves ligand-independent death receptor aggregation and activation of caspases. Proc Natl Acad Sci U S A. 1999 Jul 20;96(15):8699-704.

Berenstein D, Christensen JF, Kristensen T, Hofbauer R, Munch-Petersen B. Valine, not methionine, is amino acid 106 in human cytosolic thymidine kinase (TK1). Impact on oligomerization, stability, and kinetic properties. J Biol Chem. 2000 Oct 13;275(41):32187-92

Bestwick RK, Moffett GL, Mathews CK. Selective expansion of mitochondrial nucleoside triphosphate pools in antimetabolite-treated HeLa cells. J Biol Chem. **1982** Aug 25;257(16):9300-4.

Beuneu C, Auger R, Löffler M, Guissani A, Lemaire G, Lepoivre M. Indirect inhibition of mitochondrial dihydroorotate dehydrogenase activity by nitric oxide. Free Radic Biol Med. **2000** Apr 15;28(8):1206-13.

Birringer MS, Claus MT, Folkers G, Kloer DP, Schulz GE, Scapozza L. Structure of a type II thymidine kinase with bound dTTP. FEBS Lett. **2005** Feb 28;579(6):1376-82.

Björklund S, Skog S, Tribukait B, Thelander L. S-phase-specific expression of mammalian ribonucleotide reductase R1 and R2 subunit mRNAs. Biochemistry. **1990** Jun 12;29(23):5452-8.

Black ME, Kokoris MS, Sabo P. Herpes simplex virus-1 thymidine kinase mutants created by semi-random sequence mutagenesis improve prodrug-mediated tumor cell killing. Cancer Res. **2001** Apr 1;61(7):3022-6.

Bourdon A, Minai L, Serre V, Jais JP, Sarzi E, Aubert S, Chrétien D, de Lonlay P, Paquis-Flucklinger V, Arakawa H, Nakamura Y, Munnich A, Rötig A. Mutation of RRM2B, encoding p53-controlled ribonucleotide reductase (p53R2), causes severe mitochondrial DNA depletion. Nat Genet. **2007** Jun;39(6):776-80.

Bradshaw HD Jr, Deininger PL. Human thymidine kinase gene: molecular cloning and nucleotide sequence of a cDNA expressible in mammalian cells. Mol Cell Biol. **1984** Nov;4(11):2316-20.

Braess J, Wegendt C, Feuring-Buske M, Riggert J, Kern W, Hiddemann W, Schleyer E. Leukaemic blasts differ from normal bone marrow mononuclear cells and CD34+ haemopoietic stem cells in their metabolism of cytosine arabinoside.Br J Haematol. **1999** May;105(2):388-93.

Brown NC, Reichard P. Ribonucleoside diphosphate reductase. Formation of active and inactive complexes of proteins B1 and B2. J Mol Biol. **1969a** Nov 28;46(1):25-38.

Brown NC, Reichard P. Role of effector binding in allosteric control of ribonucleoside diphosphate reductase. J Mol Biol. **1969b** Nov 28;46(1):39-55.

Chabes A, Georgieva B, Domkin V, Zhao X, Rothstein R, Thelander L. Survival of DNA damage in yeast directly depends on increased dNTP levels allowed by relaxed feedback inhibition of ribonucleotide reductase. Cell. **2003a** Feb 7;112(3):391-401.

Chabes AL, Pfleger CM, Kirschner MW, Thelander L. Mouse ribonucleotide reductase R2 protein: a new target for anaphase-promoting complex-Cdh1-mediated proteolysis. Proc Natl Acad Sci U S A. **2003b** Apr 1;100(7):3925-9.

Chang ZF, Huang DY, Chi LM. Serine 13 is the site of mitotic phosphorylation of human thymidine kinase. J Biol Chem. **1998** May 15;273(20):12095-100.

Chang ZF, Huang DY, Hsue NC. Differential phosphorylation of human thymidine kinase in proliferating and M phase-arrested human cells. J Biol Chem. **1994** Aug 19;269(33):21249-54.

Chottiner EG, Shewach DS, Datta NS, Ashcraft E, Gribbin D, Ginsburg D, Fox IH, Mitchell BS. Cloning and expression of human deoxycytidine kinase cDNA. Proc Natl Acad Sci U S A. **1991** Feb 15;88(4):1531-5.

Cohen A, Thompson E. DNA repair in nondividing human lymphocytes: inhibition by deoxyadenosine. Cancer Res. **1986** Apr;46(4 Pt 1):1585-8.

Cohen JL, Boyer O, Salomon B, Onclercq R, Charlotte F, Bruel S, Boisserie G, Klatzmann D. Prevention of graft-versus-host disease in mice using a suicide gene expressed in T lymphocytes. Blood. **1997** Jun 15;89(12):4636-45.

Collins A, Oates DJ. Hydroxyurea: effects on deoxyribonucleotide pool sizes correlated with effects on DNA repair in mammalian cells. Eur J Biochem. **1987** Dec 1;169(2):299-305.

Collins AR, Black DT, Waldren CA. Aberrant DNA repair and enhanced mutagenesis following mutagen treatment of Chinese hamster Ade-C cells in a state of purine deprivation. Mutat Res. **1988** Mar;193(2):145-55.

Darè E, Zhang LH, Jenssen D, Bianchi V. Molecular analysis of mutations in the hprt gene of V79 hamster fibroblasts: effects of imbalances in the dCTP, dGTP and dTTP pools. J Mol Biol. **1995** Oct 6;252(5):514-21.

Das SK, Benditt EP, Loeb LA. Rapid changes in deoxynucleoside triphosphate pools in mammalian cells treated with mutagens. Biochem Biophys Res Commun. **1983** Jul 29;114(2):458-64

Desler C, Munch-Petersen B, Stevnsner T, Matsui S, Kulawiec M, Singh KK, Rasmussen LJ. Mitochondria as determinant of nucleotide pools and chromosomal stability. Mutat Res. **2007** Dec 1;625(1-2):112-24

Dobrovolsky VN, Bucci T, Heflich RH, Desjardins J, Richardson FC. Mice deficient for cytosolic thymidine kinase gene develop fatal kidney disease. Molecular Genetics and Metabolism **2003**; 78:1-10

Dolce V, Fiermonte G, Runswick MJ, Palmieri F, Walker JE. The human mitochondrial deoxynucleotide carrier and its role in the toxicity of nucleoside antivirals. Proc Natl Acad Sci U S A. **2001** Feb 27;98(5):2284-8.

Ekberg M, Sahlin M, Eriksson M, Sjöberg BM. Two conserved tyrosine residues in protein R1 participate in an intermolecular electron transfer in ribonucleotide reductase. J Biol Chem. **1996** Aug 23;271(34):20655-9.

Ellims PH, Kao AY, Chabner BA. Deoxycytidylate deaminase. Purification and some properties of the enzyme isolated from human spleen. J Biol Chem. **1981** Jun 25;256(12):6335-40.

Engström Y, Eriksson S, Jildevik I, Skog S, Thelander L, Tribukait B. Cell cycle-dependent expression of mammalian ribonucleotide reductase. Differential regulation of the two subunits. J Biol Chem. **1985** Aug 5;260(16):9114-6.

Engström Y, Rozell B. Immunocytochemical evidence for the cytoplasmic localization and differential expression during the cell cycle of the M1 and M2 subunits of mammalian ribonucleotide reductase. EMBO J. **1988** Jun;7(6):1615-20.

Engström Y, Rozell B, Hansson HA, Stemme S, Thelander L. Localization of ribonucleotide reductase in mammalian cells. EMBO J. **1984** Apr;3(4):863-7.

Eriksson M, Uhlin U, Ramaswamy S, Ekberg M, Regnström K, Sjöberg BM, Eklund H. Binding of allosteric effectors to ribonucleotide reductase protein R1: reduction of active-site cysteines promotes substrate binding. Structure. **1997** Aug 15;5(8):1077-92.

Eriksson S, Gräslund A, Skog S, Thelander L, Tribukait B. Cell cycle-dependent regulation of mammalian ribonucleotide reductase. The S phase-correlated increase in subunit M2 is regulated by de novo protein synthesis. J Biol Chem. **1984** Oct 10;259(19):11695-700 .

Eriksson S, Munch-Petersen B, Johansson K, Eklund H. Structure and function of cellular deoxyribonucleoside kinases. Cell Mol Life Sci. **2002** Aug;59(8):1327-46.

Eriksson S, Thelander L, Akerman M. Allosteric regulation of calf thymus ribonucleoside diphosphate reductase. Biochemistry. **1979** Jul 10;18(14):2948-52.

Ferraro P, Nicolosi L, Bernardi P, Reichard P, Bianchi V. Mitochondrial deoxynucleotide pool sizes in mouse liver and evidence for a transport mechanism for thymidine monophosphate. Proc Natl Acad Sci U S A. **2006** Dec 5;103(49):18586-91.

Furman PA, Fyfe JA, St Clair MH, Weinhold K, Rideout JL, Freeman GA, Lehrman SN, Bolognesi DP, Broder S, Mitsuya H, *et al.* Phosphorylation of 3'-azido-3'-deoxythymidine and selective interaction of the 5'-triphosphate with human immunodeficiency virus reverse transcriptase. Proc Natl Acad Sci U S A. 1986 Nov;83(21):8333-7.

Gan TE, Brumley JL, Van der Weyden MB. Human thymidine kinase. Purification and properties of the cytosolic enzyme of placenta. J Biol Chem. **1983** Jun 10;258(11):7000-4.

Grégoire M, Morais R, Quilliam MA, Gravel D. On auxotrophy for pyrimidines of respiration-deficient chick embryo cells. Eur J Biochem. **1984** Jul 2;142(1):49-55.

Guittet O, Håkansson P, Voevodskaya N, Fridd S, Gräslund A, Arakawa H, Nakamura Y, Thelander L. Mammalian p53R2 protein forms an active ribonucleotide reductase in vitro with the R1 protein, which is expressed both in resting cells in response to DNA damage and in proliferating cells. J Biol Chem. **2001** Nov 2;276(44):40647-51

Hatzis P, Al-Madhoon AS, Jüllig M, Petrakis TG, Eriksson S, Talianidis I. The intracellular localization of deoxycytidine kinase. J Biol Chem. 1998 Nov 13;273(46):30239-43.

Hochster HS, Oken MM, Winter JN, Gordon LI, Raphael BG, Bennett JM, Cassileth PA. Phase I study of fludarabine plus cyclophosphamide in patients with previously untreated low-grade lymphoma: results and and long-term follow-up--a report from the Eastern Cooperative Oncology Group. J Clin Oncol. 2000 Mar;18(5):987-94.

Håkansson P, Hofer A, Thelander L. Regulation of mammalian ribonucleotide reduction and dNTP pools after DNA damage and in resting cells. J Biol Chem. **2006** Mar 24;281(12):7834-41.

Ingemarson R, Thelander L. A kinetic study on the influence of nucleoside triphosphate effectors on subunit interaction in mouse ribonucleotide reductase. Biochemistry. **1996** Jul 2;35(26):8603-9.

Jensen HK, Munch-Petersen B. Altered kinetic properties of recombinant human cytosolic thymidine kinase (TK1) as compared with the native form. Adv Exp Med Biol. **1994**;370:637-40.

Johansson K, Ramaswamy S, Ljungcrantz C, Knecht W, Piskur J, Munch-Petersen B, Eriksson S, Eklund H. Structural basis for substrate specificities of cellular deoxyribonucleoside kinases. Nat Struct Biol. **2001** Jul;8(7):616-20.

Johansson M, Brismar S, Karlsson A. Human deoxycytidine kinase is located in the cell nucleus. Proc Natl Acad Sci U S A. **1997** Oct 28;94(22):11941-5.

Johansson M, Karlsson A. Cloning and expression of human deoxyguanosine kinase cDNA. Proc Natl Acad Sci U S A. **1996** Jul 9;93(14):7258-62.

Johansson M, Karlsson A. Cloning of the cDNA and chromosome localization of the gene for human thymidine kinase 2 J Biol Chem. **1997** Mar 28;272(13):8454-8.

Jun AS, Brown MD, Wallace DC. A mitochondrial DNA mutation at nucleotide pair 14459 of the NADH dehydrogenase subunit 6 gene associated with maternally inherited Leber hereditary optic neuropathy and dystonia. Proc Natl Acad Sci U S A. **1994** Jun 21;91(13):6206-10.

Jüllig M, Eriksson S. Mitochondrial and submitochondrial localization of human deoxyguanosine kinase. Eur J Biochem. **2000** Sep;267(17):5466-72.

Kauffman MG, Kelly TJ. Cell cycle regulation of thymidine kinase: residues near the carboxyl terminus are essential for the specific degradation of the enzyme at mitosis. Mol Cell Biol. **1991** May;11(5):2538-46.

Ke PY, Chang ZF. Mitotic degradation of human thymidine kinase 1 is dependent on the anaphase-promoting complex/cyclosome-CDH1-mediated pathway. Mol Cell Biol. **2004** Jan;24(2):514-26.

Ke PY, Kuo YY, Hu CM, Chang ZF. Control of dTTP pool size by anaphase promoting complex/cyclosome is essential for the maintenance of genetic stability. Genes Dev. **2005** Aug 15;19(16):1920-33.

Klatzmann D, Cherin P, Bensimon G, Boyer O, Coutellier A, Charlotte F, Boccaccio , Salzmann JL, Herson S. A phase I/II dose-escalation study of herpes simplex virus type 1 thymidine kinase "suicide" gene therapy for metastatic melanoma. Hum Gene Ther. **1998a** Nov 20;9(17):2585-94.

Klatzmann D, Valery CA, Bensimon G, Marro B, Boyer O, Mokhtari K, Diquet B, Salzmann JL, Philippon J. A phase I/II study of herpes simplex virus type 1 thymidine kinase "suicide" gene therapy for recurrent glioblastoma. Hum Gene Ther. **1998b** Nov 20;9(17):2595-604.

Knecht W, Munch-Petersen B, Piskur J. Identification of residues involved in the specificity and regulation of the highly efficient multisubstrate deoxyribonucleoside kinase from Drosophila melanogaster. J Mol Biol. **2000** Aug 25;301(4):827-37.

Knecht W, Rozpedowska E, Le Breton C, Willer M, Gojkovic Z, Sandrini MP, Joergensen T, Hasholt L, Munch-Petersen B, Piskur J. Drosophila deoxyribonucleoside kinase mutants with enhanced ability to phosphorylate purine analogs. Gene Ther. **2007** Sep;14(17):1278-86

Kosinska U, Carnrot C, Eriksson S, Wang L, Eklund H. Structure of the substrate complex of thymidine kinase from Ureaplasma urealyticum and investigations of possible drug targets for the enzyme. FEBS J. **2005** Dec;272(24):6365-72.

Kosinska U, Carnrot C, Sandrini MP, Clausen AR, Wang L, Piskur J, Eriksson S, Eklund H. Structural studies of thymidine kinases from Bacillus anthracis and Bacillus cereus provide insights into quaternary structure and conformational changes upon substrate binding. FEBS J. **2007** Feb;274(3):727-37.

Kucera R, Paulus H. Localization of the deoxyribonucleotide biosynthetic enzymes ribonucleotide reductase and thymidylate synthase in mouse L cells. Exp Cell Res. **1986** Dec;167(2):417-28.

Kunz BA. Genetic effects of deoxyribonucleotide pool imbalances. Environ Mutagen. **1982**;4(6):695-725.

Kunz BA, Kohalmi SE. Modulation of mutagenesis by deoxyribonucleotide levels. Annu Rev Genet. **1991**;25:339-59.

Kuzin, A.P., Abashidze, M., Forouhar, F., Vorobiev, S.M., Acton, T.B., Ma, L.C., Xiao, R., Montelione, G.T., Tong, L., and Hunt, J.F.. X-ray structure of Clostridium acetobutylicum thymidine kinase with ADP. Northeast Structural Genomics Target Car26. **2004**.

Lai Y, Tse CM, Unadkat JD. Mitochondrial expression of the human equilibrative nucleoside transporter 1 (hENT1) results in enhanced mitochondrial toxicity of antiviral drugs. J Biol Chem. **2004** Feb 6;279(6):4490-7.

Larsen NB, Rasmussen M, Rasmussen LJ. Nuclear and mitochondrial DNA repair: similar pathways? Mitochondrion. **2005** Apr;5(2):89-108.

Larsson A, Reichard P. Enzymatic synthesis of deoxyribonucleotides. IX. Allosteric effects in the reduction of pyrimidine ribonucleotides by the ribonucleoside diphosphate reductase system of Escherichia coli. J Biol Chem. **1966a** Jun 10;241(11):2533-9.

Larsson A, Reichard P. Enzymatic synthesis of deoxyribonucleotides. X. Reduction of purine ribonucleotides; allosteric behavior and substrate specificity of the enzyme system from Escherichia coli B. J Biol Chem. **1966b** Jun 10;241(11):2540-9.

Lee LS, Cheng YC. Human deoxythymidine kinase. I. Purification and general properties of the cytoplasmic and mitochondrial isozymes derived from blast cells of acute myelocytic leukemia. J Biol Chem. **1976a** May 10;251(9):2600-4.

Lee LS, Cheng YC. Human deoxythymidine kinase II: substrate specificity and kinetic behavior of the cytoplasmic and mitochondrial isozymes derived from blast cells of acute myelocytic leukemia. Biochemistry. **1976b** Aug 24;15(17):3686-90.

Leeds JM, Slabaugh MB, Mathews CK. DNA precursor pools and ribonucleotide reductase activity: distribution between the nucleus and cytoplasm of mammalian cells. Mol Cell Biol. **1985** Dec;5(12):3443-50.

Li CL, Lu CY, Ke PY, Chang ZF. Perturbation of ATP-induced tetramerization of human cytosolic thymidine kinase by substitution of serine-13with aspartic acid at the mitotic phosphorylation site. Biochem Biophys Res Commun. **2004** Jan 16;313(3):587-93.

Li L, Connor EE, Berger SH, Wyatt MD. Determination of apoptosis, uracil incorporation, DNA strand breaks, and sister chromatid exchanges under conditions of thymidylate deprivation in a model of BER deficiency. Biochem Pharmacol. **2005** Nov 15;70(10):1458-68.

Lin ZP, Belcourt MF, Cory JG, Sartorelli AC. Stable suppression of the R2 subunit of ribonucleotide reductase by R2-targeted short interference RNA sensitizes p53(-/-) HCT-116 colon cancer cells to DNA-damaging agents and ribonucleotide reductase inhibitors. J Biol Chem. **2004** Jun 25;279(26):27030-8.

Liu X, Zhou B, Xue L, Shih J, Tye K, Qi C, Yen Y. The ribronucleotide reductase subunit M2B subcellular localization and functional importance for DNA replication in physiological growth of KB cells. Biochem Pharmacol. **2005** Nov 1;70(9):1288-97.

Löffler M. On the role of dihydroorotate dehydrogenase in growth cessation of Ehrlich ascites tumor cells cultured under oxygen deficiency. Eur J Biochem. **1980**;107(1):207-15.

Mandel H, Szargel R, Labay V, Elpeleg O, Saada A, Shalata A, Anbinder Y, Berkowitz D, Hartman C, Barak M, Eriksson S, Cohen N. The deoxyguanosine kinase gene is mutated in individuals with depleted hepatocerebral mitochondrial DNA. Nat Genet. **2001** Nov;29(3):337-41. Erratum in: Nat Genet 2001 Dec;29(4):491.

Mao SS, Holler TP, Bollinger JM Jr, Yu GX, Johnston MI, Stubbe J. Interaction of C225SR1 mutant subunit of ribonucleotide reductase with R2 and nucleoside

diphosphates: tales of a suicidal enzyme. Biochemistry. **1992b** Oct 13;31(40):9744-51.

Mao SS, Holler TP, Yu GX, Bollinger JM Jr, Booker S, Johnston MI, Stubbe J. A model for the role of multiple cysteine residues involved in ribonucleotide reduction: amazing and still confusing. Biochemistry. **1992a** Oct 13;31(40):9733-43.

Mao SS, Yu GX, Chalfoun D, Stubbe J. Characterization of C439SR1, a mutant of Escherichia coli ribonucleotide diphosphate reductase: evidence that C439 is a residue essential for nucleotide reduction and C439SR1 is a protein possessing novel thioredoxin-like activity. Biochemistry. **1992c** Oct 13;31(40):9752-9.

Marti R, Spinazzola A, Nishino I, Andreu AL, Naini A, Tadesse S, Oliver JA, Hirano M. Mitochondrial neurogastrointestinal encephalomyopathy and thymidine metabolism: results and hypotheses. Mitochondrion. **2002** Nov;2(1-2):143-7.

Mathews CK, Song S. Maintaining precursor pools for mitochondrial DNA replication. FASEB J. **2007** Aug;21(10):2294-303.

McKenzie M, Liolitsa D, Hanna MG. Mitochondrial disease: mutations and mechanisms. Neurochem Res. **2004** Mar;29(3):589-600.

Meuth M. Sensitivity of a mutator gene in Chinese hamster ovary cell to deoxynucleoside triphosphate pool alterations. Mol Cell Biol. **1981** Jul;1(7):652-60.

Meuth M. Deoxycytidine kinase-deficient mutants of Chinese hamster ovary cells are hypersensitive to DNA alkylating agents. Mutat Res. **1983** Aug;110(2):383-91.

Meuth M. The molecular basis of mutations induced by deoxyribonucleoside triphosphate pool imbalances in mammalian cells. Exp Cell Res. **1989** Apr;181(2):305-16.

Meuth M, L'Heureux-Huard N, Trudel M. Characterization of a mutator gene in Chinese hamster ovary cells. Proc Natl Acad Sci U S A. **1979** Dec;76(12):6505-9.

Moolten FL. Tumor chemosensitivity conferred by inserted herpes thymidine kinase genes: paradigm for a prospective cancer control strategy. Cancer Res. **1986** Oct;46(10):5276-81.

Munch-Petersen B. Differences in the kinetic properties of thymidine kinase isoenzymes in unstimulated and phytohemagglutinin-stimulated human lymphocytes. Mol Cell Biochem. **1984** Sep;64(2):173-85.

Munch-Petersen B. Reversible tetramerization of human TK1 to the high catalytic efficient form is induced by pyrophosphate, in addition to tripolyphosphates, or high enzyme concentration. FEBS J. **2009** Jan;276(2):571-80.

Munch-Petersen B, Cloos L, Jensen HK, Tyrsted G. Human thymidine kinase 1. Regulation in normal and malignant cells. Adv Enzyme Regul. **1995a**;35:69-89.

Munch-Petersen B, Cloos L, Tyrsted G, Eriksson S. Diverging substrate specificity of pure human thymidine kinases 1 and 2 against antiviral dideoxynucleosides. J Biol Chem. **1991** May 15;266(14):9032-8.

Munch-Petersen B, Piskur J, Sondergaard L. The single deoxynucleoside kinase in Drosophila melanogaster, Dm-dNK, is multifunctional and differs from the mammalian deoxynucleoside kinases. Adv Exp Med Biol. **1998**;431:465-9.

Munch-Petersen B, Tyrsted G, Cloos L. Reversible ATP-dependent transition between two forms of human cytosolic thymidine kinase with different enzymatic properties. J Biol Chem. **1993** Jul 25;268(21):15621-5.

Munch-Petersen B, Tyrsted G, Cloos L, Beck RA, Eger K. Different affinity of the two forms of human cytosolic thymidine kinase towards pyrimidine analogs. Biochim Biophys Acta. **1995b** Jul 19;1250(2):158-62.

Munch-Petersen B, Tyrsted G, Dupont B. The deoxyribonucleoside 5'-triphosphate (dATP and dTTP) pool in phytohemagglutinin-stimulated and non-stimulated human lymphocytes. Exp Cell Res. **1973** Jun;79(2):249-56.

Murthy S, Reddy GP. Replitase: complete machinery for DNA synthesis. J Cell Physiol. **2006** Dec;209(3):711-7.

Nakano K, Bálint E, Ashcroft M, Vousden KH. A ribonucleotide reductase gene is a transcriptional target of p53 and p73. Oncogene. **2000** Aug 31;19(37):4283-9.

Nevo Y, Soffer D, Kutai M, Zelnik N, Saada A, Jossiphov J, Messer G, Shaag A, Shahar E, Harel S, Elpeleg O. Clinical characteristics and muscle pathology in myopathic mitochondrial DNA depletion. J Child Neurol. **2002** Jul;17(7):499-504.

Newman CN, Miller JH. Mutagen-induced changes in cellular deoxycytidine triphosphate and thymidine triphosphate in Chinese hamster ovary cells. Biochem Biophys Res Commun. **1983** Jul 18;114(1):34-40.

Nishigaki Y, Martí R, Copeland WC, Hirano M. Site-specific somatic mitochondrial DNA point mutations in patients with thymidine phosphorylase deficiency. J Clin Invest. **2003** Jun;111(12):1913-21.

Nishino I, Spinazzola A, Hirano M. Thymidine phosphorylase gene mutations in MNGIE, a human mitochondrial disorder. Science. **1999** Jan 29;283(5402):689-92.

Nordlund P, Reichard P. Ribonucleotide reductases. Annu Rev Biochem. **2006**;75:681-706.

Nordlund P, Sjöberg BM, Eklund H. Three-dimensional structure of the free radical protein of ribonucleotide reductase. Nature. **1990** Jun 14;345(6276):593-8.

Olivero OA, Ming JM, Das S, Vazquez IL, Richardson DL, Weston A, Poirier MC. Human inter-individual variability in metabolism and genotoxic response to zidovudine. Toxicol Appl Pharmacol. **2008** Apr 15;228(2):158-64.

Patel H, Pietro ED, MacKenzie RE. Mammalian fibroblasts lacking mitochondrial NAD+-dependent methylenetetrahydrofolate dehydrogenase-cyclohydrolase are glycine auxotrophs. J Biol Chem. **2003** May 23;278(21):19436-41.

Pawelek PD, MacKenzie RE. Methenyltetrahydrofolate cyclohydrolase is rate limiting for the enzymatic conversion of 10-formyltetrahydrofolate to 5,10-methylenetetrahydrofolate in bifunctional dehydrogenase-cyclohydrolase enzymes. Biochemistry. **1998** Jan 27;37(4):1109-15.

Perry PE. Induction of sister-chromatid exchanges (SCEs) by thymidine and the potentiation of mutagen-induced SCEs in Chinese hamster ovary cells. Mutat Res. **1983** May;109(2):219-29.

Peters JM. SCF and APC: the Yin and Yang of cell cycle regulated proteolysis. Curr Opin Cell Biol. **1998** Dec;10(6):759-68.

Pfleger CM, Kirschner MW. The KEN box: an APC recognition signal distinct from the D box targeted by Cdh1. Genes Dev. **2000** Mar 15;14(6):655-65.

Pfleger CM, Lee E, Kirschner MW. Substrate recognition by the Cdc20 and Cdh1 components of the anaphase-promoting complex. Genes Dev. **2001** Sep 15;15(18):2396-407.

Piskur J, Sandrini MP, Knecht W, Munch-Petersen B. Animal deoxyribonucleoside kinases: 'forward' and 'retrograde' evolution of their substrate specificity. FEBS Lett. 2004 Feb 27;560(1-3):3-6.

Pontarin G, Fijolek A, Pizzo P, Ferraro P, Rampazzo C, Pozzan T, Thelander L, Reichard PA, Bianchi V. Ribonucleotide reduction is a cytosolic process in mammalian cells independently of DNA damage. Proc Natl Acad Sci U S A**. 2008** Nov 18;105(46):17801-6.

Pontarin G, Gallinaro L, Ferraro P, Reichard P, Bianchi V. Origins of mitochondrial thymidine triphosphate: dynamic relations to cytosolic pools. Proc Natl Acad Sci U S A. **2003** Oct 14;100(21):12159-64..

Qasim W, Gaspar HB, Thrasher AJ. T cell suicide gene therapy to aid haematopoietic stem cell transplantation. Curr Gene Ther. **2005** Feb;5(1):121-32.

Ram Z, Culver KW, Oshiro EM, Viola JJ, DeVroom HL, Otto E, Long Z, Chiang Y, McGarrity GJ, Muul LM, Katz D, Blaese RM, Oldfield EH. Therapy of malignant brain tumors by intratumoral implantation of retroviral vector-producing cells. Nat Med. **1997** Dec;3(12):1354-61.

Rampazzo C, Ferraro P, Pontarin G, Fabris S, Reichard P, Bianchi V. Mitochondrial deoxyribonucleotides, pool sizes, synthesis, and regulation. J Biol Chem**. 2004** Apr 23;279(17):17019-26.

Rawls J, Knecht W, Diekert K, Lill R, Löffler M. Requirements for the mitochondrial import and localization of dihydroorotate dehydrogenase. Eur J Biochem**. 2000** Apr;267(7):2079-87.

Reichard P. Interactions between deoxyribonucleotide and DNA synthesis. Annu Rev Biochem. **1988**;57:349-74.

Riva CM, Rustum YM.1-beta-D-arabinofuranosylcytosine metabolism and incorporation into DNA as determinants of in vivo murine tumor cell response. Cancer Res. **1985** Dec;45(12 Pt 1):6244-9

Roy B, Guittet O, Beuneu C, Lemaire G, Lepoivre M. Depletion of deoxyribonucleoside triphosphate pools in tumor cells by nitric oxide. Free Radic Biol Med. **2004** Feb 15;36(4):507-16.

Rustum YM, Raymakers RA. 1-Beta-arabinofuranosylcytosine in therapy of leukemia: preclinical and clinical overview. Pharmacol Ther. **1992** Dec;56(3):307-21.

Sabini E, Ort S, Monnerjahn C, Konrad M, Lavie A. tructure of human dCK suggests strategies to improve anticancer and antiviral therapy. Nat Struct Biol. 2003 Jul;10(7):513-9.

Sahlin M, Gräslund A, Petersson L, Ehrenberg A, Sjöberg BM. Reduced forms of the iron-containing small subunit of ribonucleotide reductase from Escherichia coli. Biochemistry. **1989** Mar 21;28(6):2618-25.

Sawaya MR, Guo S, Tabor S, Richardson CC, Ellenberger T. Crystal structure of the helicase domain from the replicative helicase-primase of bacteriophage T7. Cell. **1999** Oct 15;99(2):167-77.

Segura-Peña D, Lichter J, Trani M, Konrad M, Lavie A, Lutz S. Quaternary structure change as a mechanism for the regulation of thymidine kinase 1-like enzymes. Structure. **2007b** Dec;15(12):1555-66.

Segura-Peña D, Lutz S, Monnerjahn C, Konrad M, Lavie A. Binding of ATP to TK1-like enzymes is associated with a conformational change in the quaternary structure. J Mol Biol. **2007a** May 25;369(1):129-41.

Sherley JL, Kelly TJ. Regulation of human thymidine kinase during the cell cycle. J Biol Chem. 1988 Jun 15;263(17):8350-8.

Shields AF, Grierson JR, Dohmen BM, Machulla HJ, Stayanoff JC, Lawhorn-Crews JM, Obradovich JE, Muzik O, Mangner TJ. Imaging proliferation in vivo with [F-18]FLT and positron emission tomography. *Nat. Med*. **1998** 4, 1334-1336.

Skoog KL, Nordenskjöld BA, Bjursell KG. Deoxyribonucleoside-triphosphate pools and DNA synthesis in synchronized hamster cells. Eur J Biochem. **1973** Mar 15;33(3):428-32.

Skoog L, Bjursell G. Nuclear and cytoplasmic pools of deoxyribonucleoside triphosphates in Chinese hamster ovary cells. J Biol Chem. **1974** Oct 25;249(20):6434-8.

Skovgaard T, Munch-Petersen B. Purification and characterization of wild-type and mutant TK1 type kinases from Caenorhabditis elegans. Nucleosides Nucleotides Nucleic Acids. **2006**;25(9-11):1165-9

Song S, Wheeler LJ, Mathews CK. Deoxyribonucleotide pool imbalance stimulates deletions in HeLa cell mitochondrial DNA. J Biol Chem. **2003** Nov 7;278(45):43893-6.

Spinazzola A, Marti R, Nishino I, Andreu AL, Naini A, Tadesse S, Pela I, Zammarchi E, Donati MA, Oliver JA, Hirano M. Altered thymidine metabolism due to defects of thymidine phosphorylase. J Biol Chem. **2002** Feb 8;277(6):4128-33.

Spyrou G, Reichard P. Dynamics of the thymidine triphosphate pool during the cell cycle of synchronized 3T3 mouse fibroblasts. Mutat Res. **1988** Jul-Aug;200(1-2):37-43

Stewart CJ, Ito M, Conrad SE. Evidence for transcriptional and post-transcriptional control of the cellular thymidine kinase gene. Mol Cell Biol. **1987** Mar;7(3):1156-63.

Stuart P, Ito M, Stewart C, Conrad SE. Induction of cellular thymidine kinase occurs at the mRNA level. Mol Cell Biol. **1985** Jun;5(6):1490-7.

Saada A, Shaag A, Mandel H, Nevo Y, Eriksson S, Elpeleg O. Mutant mitochondrial thymidine kinase in mitochondrial DNA depletion myopathy. Nat Genet. **2001** Nov;29(3):342-4.

Saada-Reisch A. Deoxyribonucleoside kinases in mitochondrial DNA depletion. Nucleosides Nucleotides Nucleic Acids. **2004** Oct;23(8-9):1205-15.

Tanaka H, Arakawa H, Yamaguchi T, Shiraishi K, Fukuda S, Matsui K, Takei Y, Nakamura Y. A ribonucleotide reductase gene involved in a p53-dependent cell-cycle checkpoint for DNA damage. Nature. **2000** Mar 2;404(6773):42-9.

Tang Y, Schon EA, Wilichowski E, Vazquez-Memije ME, Davidson E, King MP. Rearrangements of human mitochondrial DNA (mtDNA): new insights into the regulation of mtDNA copy number and gene expression. Mol Biol Cell. **2000** Apr;11(4):1471-85.

Tatoyan A, Giulivi C. Purification and characterization of a nitric-oxide synthase from rat liver mitochondria.J Biol Chem. **1998** May 1;273(18):11044-8.

Tatuch Y, Christodoulou J, Feigenbaum A, Clarke JT, Wherret J, Smith C, Rudd N, Petrova-Benedict R, Robinson BH. Heteroplasmic mtDNA mutation (T----G) at 8993 can cause Leigh disease when the percentage of abnormal mtDNA is high. Am J Hum Genet. **1992** Apr;50(4):852-8.

Thelander L. Physicochemical characterization of ribonucleoside diphosphate reductase from Escherichia coli. J Biol Chem. **1973** Jul 10;248(13):4591-601.

Thelander L, Reichard P. Reduction of ribonucleotides. Annu Rev Biochem. 1979;48:133-58.

Trounce I, Neill S, Wallace DC. Cytoplasmic transfer of the mtDNA nt 8993 T-->G (ATP6) point mutation associated with Leigh syndrome into mtDNA-less cells demonstrates cosegregation with a decrease in state III respiration and ADP/O ratio. Proc Natl Acad Sci U S A. **1994** Aug 30;91(18):8334-8.

Trudel M, Van Genechten T, Meuth M. Biochemical characterization of the hamster thy mutator gene and its revertants. J Biol Chem. **1984** Feb 25;259(4):2355-9.

Tyrsted G. The pool size of deoxyguanosine 5'-triphosphate and deoxycytidine 5'-triphosphate in phytohemagglutinin-stimulated and non-stimulated human lymphocytes. Exp Cell Res. **1975** Mar 15;91(2):429-40.

Uhlin U, Eklund H. Structure of ribonucleotide reductase protein R1. Nature. **1994** Aug 18;370(6490):533-9.

Uhlin U, Eklund H. The ten-stranded beta/alpha barrel in ribonucleotide reductase protein R1. J Mol Biol. **1996** Sep 27;262(3):358-69.

Uppsten M, Färnegårdh M, Jordan A, Eliasson R, Eklund H, Uhlin U. Structure of the large subunit of class Ib ribonucleotide reductase from Salmonella typhimurium and its complexes with allosteric effectors. J Mol Biol. **2003** Jun 27;330(1):87-97.

Valdez LB, Zaobornyj T, Boveris A. Mitochondrial metabolic states and membrane potential modulate mtNOS activity. Biochim Biophys Acta. **2006** Mar;1757(3):166-72.

Wang L, Eriksson S. Mitochondrial deoxyguanosine kinase mutations and mitochondrial DNA depletion syndrome. FEBS Lett. **2003** Nov 20;554(3):319-22.

Wang L, Hellman U, Eriksson S. Cloning and expression of human mitochondrial deoxyguanosine kinase cDNA. FEBS Lett. **1996** Jul 15;390(1):39-43.

Wang L, Munch-Petersen B, Herrstrom Sjoberg A, Hellman U, Bergman T, Jornvall H, Eriksson S. Human thymidine kinase 2: molecular cloning and characterisation of the enzyme activity with antiviral and cytostatic nucleoside substrates. FEBS Lett. **1999** Jan 25;443(2):170-4.

Wang L, Saada A, Eriksson S. Kinetic properties of mutant human thymidine kinase 2 suggest a mechanism for mitochondrial DNA depletion myopathy. J Biol Chem. **2003** Feb 28;278(9):6963-8.

Weinberg G, Ullman B, Martin DW Jr. Mutator phenotypes in mammalian cell mutants with distinct biochemical defects and abnormal deoxyribonucleoside triphosphate pools. Proc Natl Acad Sci U S A. **1981** Apr;78(4):2447-51.

Welin M, Kosinska U, Mikkelsen NE, Carnrot C, Zhu C, Wang L, Eriksson S, Munch-Petersen B, Eklund H. Structures of thymidine kinase 1 of human and mycoplasmic origin. Proc Natl Acad Sci U S A. **2004** Dec 28;101(52):17970-5.

Welin M, Skovgaard T, Knecht W, Zhu C, Berenstein D, Munch-Petersen B, Piskur J, Eklund H. Structural basis for the changed substrate specificity of Drosophila melanogaster deoxyribonucleoside kinase mutant N64D. FEBS J. **2005** Jul;272(14):3733-42.

Wiewrodt R, Amin K, Kiefer M, Jovanovic VP, Kapoor V, Force S, Chang M, Lanuti M, Black ME, Kaiser LR, Albelda SM. Adenovirus-mediated gene transfer of enhanced Herpes simplex virus thymidine kinase mutants improves prodrug-mediated tumor cell killing. Cancer Gene Ther. **2003** May;10(5):353-64.

Xue L, Zhou B, Liu X, Qiu W, Jin Z, Yen Y. Wild-type p53 regulates human ribonucleotide reductase by protein-protein interaction with p53R2 as well as hRRM2 subunits. Cancer Res. **2003** Mar 1;63(5):980-6.

Zheng X, Johansson M, Karlsson A. Retroviral transduction of cancer cell lines with the gene encoding Drosophila melanogaster multisubstrate deoxyribonucleoside kinase. J Biol Chem. 2000 Dec 15;275(50):39125-9

Zheng X, Johansson M, Karlsson A. Bystander effects of cancer cell lines transduced with the multisubstrate deoxyribonucleoside kinase of Drosophila melanogaster and synergistic enhancement by hydroxyurea. Mol Pharmacol. 2001 Aug;60(2):262-6.

Zhou X, Solaroli N, Bjerke M, Stewart JB, Rozell B, Johansson M, Karlsson A. Progressive loss of mitochondrial DNA in thymidine kinase 2-deficient mice. Hum Mol Genet. **2008** Aug 1;17(15):2329-35.

Zhu C, Harlow LS, Berenstein D, Munch-Petersen S, Munch-Petersen B. Effect of C-terminal of human cytosolic thymidine kinase (TK1) on in vitro stability and enzymatic properties. Nucleosides Nucleotides Nucleic Acids. **2006**;25(9-11):1185-8.

Åberg A, Hahne S, Karlsson M, Larsson A, Ormö M, Åhgren A, Sjöberg BM. Evidence for two different classes of redox-active cysteines in ribonucleotide reductase of Escherichia coli. J Biol Chem. **1989** Jul 25;264(21):12249-52.

I

the FEBS Journal

Structural basis for the changed substrate specificity of *Drosophila melanogaster* deoxyribonucleoside kinase mutant N64D

Martin Welin[1], Tine Skovgaard[2], Wolfgang Knecht[3,*], Chunying Zhu[2], Dvora Berenstein[2], Birgitte Munch-Petersen[2], Jure Piškur[3,†] and Hans Eklund[1]

1 Department of Molecular Biology, Swedish University of Agricultural Sciences, Biomedical Center, Uppsala, Sweden
2 Department of Life Sciences and Chemistry, Roskilde University, Denmark
3 BioCentrum-DTU, Technical University of Denmark, Lyngby, Denmark

Keywords
crystal structure; feedback inhibition; gene therapy; pro-drug activation

Correspondence
H. Eklund, Department of Molecular Biology, Swedish University of Agricultural Sciences, Box 590, Biomedical Center, S-751 24 Uppsala, Sweden
Fax: +46 18 53 69 71
Tel: +46 18 475 4559
E-mail: hasse@xray.bmc.uu.se

***Present address**
AstraZeneca R & D, Mölndal, Sweden

†Present address
Cell and Organism Biology, Lund University, Sweden

(Received 12 April 2005, revised 30 May 2005, accepted 3 June 2005)

doi:10.1111/j.1742-4658.2005.04803.x

The *Drosophila melanogaster* deoxyribonucleoside kinase (*Dm*-dNK) double mutant N45D/N64D was identified during a previous directed evolution study. This mutant enzyme had a decreased activity towards the natural substrates and decreased feedback inhibition with dTTP, whereas the activity with 3′-modified nucleoside analogs like 3′-azidothymidine (AZT) was nearly unchanged. Here, we identify the mutation N64D as being responsible for these changes. Furthermore, we crystallized the mutant enzyme in the presence of one of its substrates, thymidine, and the feedback inhibitor, dTTP. The introduction of the charged Asp residue appears to destabilize the LID region (residues 167–176) of the enzyme by electrostatic repulsion and no hydrogen bond to the 3′-OH is made in the substrate complex by Glu172 of the LID region. This provides a binding space for more bulky 3′-substituents like the azido group in AZT but influences negatively the interactions between *Dm*-dNK, substrates and feedback inhibitors based on deoxyribose. The detailed picture of the structure–function relationship provides an improved background for future development of novel mutant suicide genes for *Dm*-dNK-mediated gene therapy.

Deoxyribonucleoside kinases (dNKs; EC 2.7.1.145) catalyze the initial, and usually rate-determining step in the synthesis of the four DNA precursors (dNTPs) through the salvage pathway. These enzymes transfer the γ-phosphoryl group from ATP to deoxyribonucleosides (dN) and form the corresponding dNMPs [1]. In the cell, dNMPs are quickly phosphorylated to dNDPs and dNTPs by ubiquitous mono- and diphosphate deoxyribonucleoside kinases.

Deoxyribonucleoside kinases are also responsible for activation (initial phosphorylation) of nontoxic nucleoside analogs such as azidothymidine (AZT) and acyclovir (ACV) used in the treatment of cancer and viral diseases. After further phosphorylation by other cellular kinases the triphosphorylated nucleoside analogs are incorporated into DNA and cause chain termination and cell death [2]. Alternatively, they inhibit the DNA synthesizing machinery or initiate apoptosis [3].

Abbreviations
ACV, acyclovir; AZT, 3′-azidothymidine; dNK, deoxyribonucleoside kinase; *Dm*-dNK, *Drosophila melanogaster* deoxyribonucleoside kinase; dCK, deoxycytidine kinase; dGK, deoxyguanosine kinase; dN, deoxyribonucleosides; dT, deoxythymidine; dU, deoxyuridine; dC, deoxycytidine; dA, deoxyadenosine; dG, deoxyguanosine; hTK1, human thymidine kinase 1; HSV1-TK, Herpes simplex virus 1 thymidine kinase; LID region, residues 167–176; MuD, double mutant N45D/N64D; TK, thymidine kinase.

Thus, the deoxyribonucleoside kinases are of medical interest both in chemotherapy of cancer and viral diseases and in suicide gene therapy of tumors with nucleoside analogs [4,5].

Gene therapy based on deoxyribonucleoside kinases is a method of therapeutic intervention to treat various cancers and also has applications in transplantation technology. The basis of this therapy is that a heterologous kinase gene, such as viral Herpes simplex virus 1 thymidine kinase (HSV1-TK) or insect dNK, is introduced into target cells (for example, neoplastic cells), where the gene is expressed. The introduced kinase can then specifically multiply the activation of pro-drugs, like nucleoside analogs, and lead to cell death [12,21–23].

Deoxyribonucleoside kinases from different species vary in their number, substrate specificity, intracellular localization and regulation of gene expression. Mammalian cells have four enzymes with overlapping specificities: thymidine kinase (EC 2.7.1.21) 1 (TK1) and 2 (TK2), deoxycytidine kinase (dCK) and deoxyguanosine kinase (dGK). TK1 has the most restricted substrate specificity and phosphorylates only thymidine (dT) and deoxyuridine (dU), whereas TK2 also phosphorylates deoxycytidine (dC). dCK phosphorylates dC, deoxyadenosine (dA) and deoxyguanosine (dG), while dGK phosphorylates dG and dA (reviewed in [1,5]). Several bacteria and viruses carry their own deoxyribonucleoside kinases [10]. The Herpes simplex virus thymidine kinase is known for its broad substrate specificity because besides dT and dU it also phosphorylates dC, several nucleoside analogs, and additionally it can phosphorylate thymidine monophosphates [11].

In the insect *Drosophila melanogaster*, only one multisubstrate deoxyribonucleoside kinase (*Dm*-dNK) is present with the unique ability to phosphorylate all four natural deoxyribonucleosides and several analogs with a high turnover rate [12–14]. *Dm*-dNK is therefore a particularly attractive candidate for the medical gene therapy applications mentioned above, as well as for industrial synthesis of d(d)NTPs and their analogs [6,15]. To further improve the ability of *Dm*-dNK to phosphorylate nucleoside analogs, Knecht *et al.* [15] mutagenized the open reading frame for *Dm*-dNK by high-frequency random mutagenesis. The mutagenized PCR fragments were expressed in the thymidine kinase deficient *Escherichia coli* strain KY895 and clones were selected for sensitivity to nucleoside analogs. Several *Dm*-dNK mutants increased the sensitivity of KY895 to at least one analog, and a double mutant N45D/N64D (MuD) decreased the LD_{100} of the transformed strain 300-fold for AZT and 11-fold for ddC when compared to wildtype *Dm*-dNK. The purified recombinant MuD had increased K_m values and decreased k_{cat} values for the four natural substrates but practically unchanged K_m and k_{cat} values for AZT. In addition, the feedback inhibition with dTTP was markedly decreased [15].

Further insight into the structure–function relationship was provided when the 3D structures of various kinases were solved. The crystallographic structures of *Dm*-dNK and human dGK were reported in 2001 [16], followed in 2003 by the crystal structure of human dCK [17]. All these kinases have very similar structures, are distantly related to the HSV1-TK structure [18,19] and profoundly different from the very recent reported crystal structure of human TK1 [20]. The crystal structures provided a rough explanation for the *Dm*-dNK substrate specificity and the feedback inhibition [16,21]. The feedback inhibitor, dTTP, was found to bind in the deoxyribonucleoside substrate site as well as parts of the phosphate donor site [21].

Of the two mutations in the double mutant MuD, N45D is in a nonconserved region whereas N64D is in a highly conserved region that is shared among *Dm*-dNK, TK2, dCK and dGK. Asn64 is located about 12 Å from the active site (Fig. 1). In this work we have expressed, purified and characterized *Dm*-dNK mutants carrying either N45D or N64D. We present data that clearly points at N64D as the residue responsible for the observed changes in the double mutant MuD. We also present the crystal structures of

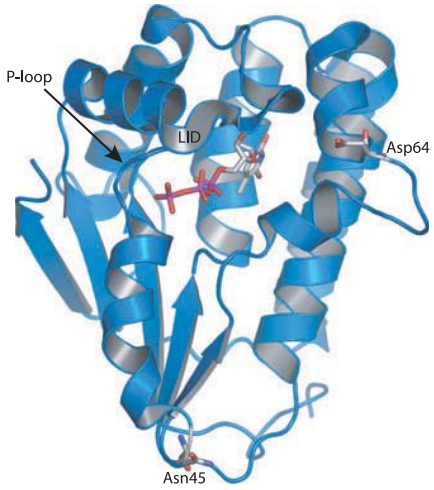

Fig. 1. Location of mutated residues. A monomer of *Dm*-dNK showing the location of Asn45 and Asp64. The feedback inhibitor dTTP is located in the active site. The P-loop and LID are labeled.

N64D in complex with its substrate dT and its inhibitor dTTP. Furthermore, our studies explain the catalytic efficiency and sensitivity of MuD over the wildtype *Dm*-dNK in terms of preference for the nucleoside analog AZT, and the decrease in feedback inhibition.

Results and Discussion

In vivo characterization of mutants

The *Dm*-dNK double mutant, N45D/N64D (MuD), was generated by random *in vitro* mutagenesis [15]. When transformed into the thymidine kinase negative *E. coli* strain KY895, the sensitivity of the cells towards four nucleoside analogs with natural nucleoside bases but modifications at the 3′-hydroxyl group increased. To examine the significance of the two amino acid exchanges for this property, we introduced either the N45D or the N64D mutation into *Dm*-dNK (lacking the 20 C-terminal residues). The resulting mutants were first tested in two plate assays, either for the presence of the TK activity or their ability to sensitize KY895 towards AZT (Table 1).

To test the effectiveness of dT conversion, the dT concentration in the TK selection plates was varied. As can be concluded from Table 1, *Dm*-dNK and mutant N45D could use dT more effectively than the double mutant N45D/N64D, followed by mutant N64D which needed the highest dT concentration to ensure the survival of the transformed bacterial strain.

In contrast, the double mutant N45D/N64D and the mutant N64D sensitized KY895 to the same degree to AZT (Table 1). Compared to *Dm*-dNK the decrease in LD_{100} for AZT was 300-fold for the double mutant N45D/N64D and mutant N64D, but only threefold for mutant N45D. Because in human cells AZT is mainly a substrate for TK1 (human TK1; hTK1) we also included this enzyme in our comparison, together with TK from human Herpes simplex 1 virus (HSV1-TK), which is currently the most widely used deoxyribonucleoside kinase in suicide-enzyme pro-drug therapy for cancer. As can be seen from Table 1, both double mutant N45D/N64D and mutant N64D were three times more efficient in killing KY895 with AZT than hTK1 or HSV1-TK.

Table 1. Growth on TK selection plates: various plasmids were transformed into KY895 and then the strains were examined for growth, +, in the presence of different concentrations of thymidine in the medium. In the last column, LD_{100} values are given (in μM) for the growth of KY895 transformed with various plasmids, on the medium containing AZT.

	dT (μg·mL^{-1})							AZT (μM)
Plasmid	0.05	1	2	10	20	50		100
pGEX-2T	–	–	–	–	–	–	–	>100
pGEX-2T-*Dm*-dNK	+	+	+	+	+	+	+	100
pGEX-2T-double mutant N45D/N64D	–	+	+	+	+	+	+	0.3
pGEX-2T-mutant N45D	+	+	+	+	+	+	+	32
pGEX-2T-mutant N64D	–	–	+	+	+	+	+	0.3
pGEX-2T-HSV1-TK								1
pGEX-2T-hTK1								1

In vitro characterization

The relationship between velocity and substrate concentration was determined for the four natural deoxyribonucleosides and AZT (Table 2). This confirmed the results from Table 1 that, according to the $k_{cat}/K_{0.5}$ values, wildtype *Dm*-dNK and mutant N45D phosphorylate dT more efficiently than the double mutant N45D/N64D, followed by mutant N64D. In general, all mutants displayed a larger decrease in catalytic efficiency ($k_{cat}/K_{0.5}$) with the natural purine deoxyribonucleosides than the pyrimidine deoxyribonucleosides, when compared to wildtype. Mutant N64D showed the largest decrease in catalytic efficiency, around 100–500-fold more than mutant N45D. The decrease in catalytic efficiency of the double mutant N45D/N64D was between N45D and N64D suggesting that the combined effect of the two mutations is not synergistic. In fact, comparing the phosphorylation of the natural substrates of the double mutant with the single mutant, it seems that the mutation N45D in the double mutant counteracts the negative effect(s) of the N64D mutation. For phosphorylation of the thymidine nucleoside analog AZT the picture is different; while the double mutation N45D/N64D has increased the efficiency for AZT, mutant N45D showed a slightly larger decrease in efficiency than mutant N64D.

If a simultaneous presence of similar concentrations of all four nucleoside substrates is assumed in the surroundings of the wildtype and the mutant enzyme, the difference in efficiencies between the two enzymes should be able to be predicted using the equation, $[k_{cat}/K_{0.5}$ (nucleoside analog)$]/[k_{cat}/K_{0.5}$ (dA) + $k_{cat}/K_{0.5}$ (dC) + $k_{cat}/K_{0.5}$ (dG) + $k_{cat}/K_{0.5}$ (dT) + $k_{cat}/K_{0.5}$ (nucleoside analog)] [22]. For the mutants N45D and N64D and the double mutant N45D/N64D this equation predicts an increase in catalytic efficiency for the phosphorylation of AZT by 2.4-, 286- and 324-fold, respectively. These values correlate quite well with the observed changes in LD_{100} for transformed KY895 in Table 1. This suggests that the more important mutation for the observed and desired phenotype,

Table 2. Kinetic parameters of wildtype and mutant *Dm*-dNKs for various native nucleoside subtrates and AZT. The k_{cat} values were calculated using the equation $V_{max} = k_{cat} \times [E]$ where [E] = total enzyme concentration and is based on one active site/monomer. Overall, in independent kinetic experiments, the coefficient of variation (standard deviation/mean) is less than 12% for V_{max} values and less than 15% for K_m values.

Dm-dNK	$K_{0.5}$ (μM)	V_{max} (U/mg)	h	k_{cat} (s^{-1})	$k_{cat}/K_{0.5}$ (M^{-1} s^{-1})	Decrease in $k_{cat}/K_{0.5}$ of the mutants compared to $k_{cat}/K_{0.5}$ of *Dm*-dNK (-fold)
dT						
N45D	0.9	5.3	1	2.6	2.9×10^6	4.1
N64D	23.2	1.7	0.8	0.82	35344	473
N45D/N64D[a]	24.2	2.5	1	1.22	50000	240
Wildtype[b]	1.2	29.5	1	14.2	1.2×10^7	1
dC						
N45D	0.9	3.4	1	1.6	1.8×10^6	4
N64D	118	3.4	0.8	1.6	13559	531
N45D/N64D[a]	96.4	8.3	1	4.04	42000	171
Wildtype[b]	2.3	34.2	1	16.5	7.2×10^6	1
dA						
N45D	119	3.8	1	1.83	15378	6
N64D	3820	0.82	0.9	0.4	105	876
N45D/N64D[a]	3166	1.7	1	0.828	260	354
Wildtype[b]	225	42.7	1	20.6	92000	1
dG						
N45D	412	2.7	1	1.3	3155	7.3
N64D	20350	0.24	0.5	0.12	5.9	3898
N45D/N64D[a]	2004	0.156	1	0.076	38	605
Wildtype[b]	665	31.3	1	15.1	23000	1
AZT						
N45D	11.7	0.06	1	0.03	2564	1.7
N64D	11.1	0.074	0.8	0.037	3333	1.3
N45D/N64D[a]	7.2	0.107	1	0.052	7200	0.6
Wildtype[a]	8.3	0.073	1	0.036	4300	1

[a] Data from [15]. [b] Data from [24].

the death of KY895 at low AZT concentrations, is in fact N64D.

dTTP feedback inhibition

dTTP is an efficient inhibitor of *Dm*-dNK with an IC_{50} value of 7 μM at 10 μM dT and 2.5 mM ATP, whereas the double mutant N45D/N64D seems to have lost the feedback inhibition property as reflected by an $IC_{50} > 1000$ μM at 2.5 mM ATP [15]. When the two mutants, N45D and N64D were examined for their dTTP inhibition, the feedback inhibition of N45D is nearly unchanged ($IC_{50} = 11$ μM) whereas N64D behaved like the double mutant by having an $IC_{50} > 1000$ μM. The pattern of inhibition for the N64D mutant was determined by varying thymidine at fixed dTTP concentrations, and was found to be predominantly competitive ($K_{ic} = 829$ μM, $K_{iu} = 3520$ μM) in contrast to a predominantly uncompetitive pattern observed with the *Dm*-dNK wildtype ($K_{ic} = 16.3$ μM, $K_{iu} = 4.7$ μM) [15]. With ATP varied at fixed dTTP concentrations, the kinetics was clearly competitive with a K_{ic} value of 1 μM. For comparison, the K_{ic} value of dTTP with varied ATP for *Dm*-dNK wildtype is about 200-fold lower (5.3 nM [21]). The kinetic studies, which demonstrated that mutation of residue 64 resulted in an enzyme with changed substrate specificity and feedback inhibition, initiated crystallographic studies of the mutant enzyme in complex with substrate and feedback inhibitor to reveal the structural basis for these phenomena.

Crystal structure of the N64D–dTTP complex

The *Dm*-dNK–dTTP complex crystallizes in a monoclinic form that has two dimers in the asymmetric unit. dTTP binds as in the wildtype, as a feedback inhibitor occupying the deoxyribonucleoside substrate site and a part of the phosphate donor site [21]. The phosphates of the inhibitor are tightly bound by residues of the P-loop and LID region (residues 167–176). A Mg ion is present in one out of the four different subunits

according to the difference density. The interactions with dTTP are very similar to the interactions in the wildtype *Dm*-dNK–dTTP complex, and the conformational changes of Glu52 are the same [21].

In wildtype *Dm*-dNK, Asn64 forms a hydrogen bond to Glu171 as well as to the main chain amino group of Leu66. Glu171 is part of the LID region within a loop that also contains Glu172 that is hydrogen bonded to the 3′-hydroxyl group of the deoxyribose ring of dTTP. The main chain of residues 65–66 are hydrogen bonded to Tyr70, which forms a second hydrogen bond with the 3′-hydroxyl group of the substrate deoxyribose ring. In alignments of eukaryotic deoxyribonucleoside kinases, Asn64 as well as Leu66 and Glu171 are highly conserved, even among deoxyribonucleoside kinases of different substrate specificities.

Surprisingly, in the N64D mutant complex with dTTP, Asp64 forms a hydrogen bond to Glu171 (Fig. 2A) which implies that one of them is protonated in spite of a pH of 6.5 in the crystallization solution. Because Glu171 is also stabilized by a hydrogen bond from Arg58, it is probable that Asp64 is protonated.

Crystal structure of the N64D–dT complex

The N64D–dT structure contained dT and a sulphate ion bound in each of the eight different subunits in the asymmetric unit (Fig. 2B). There is well defined density for Asp64 but very poor density for Glu171 as well as for Glu172 that binds to the 3′-OH in the deoxyribose in the dTTP molecule. The LID region is obviously very flexible (Fig. 3A) and there is no hydrogen bond between Asp64 and Glu171 as in the N64D–dTTP complex. In contrast to the dTTP complex, Glu172 in the dT complex does not make a hydrogen bond with the 3′-OH group of thymidine. In the wildtype *Dm*-dNK–dT complex, Glu172 is bound to the 3′-OH group of the substrate while there is no density for that interaction in the mutant structure (Fig. 2B).

Structural basis for altered properties of the N64D mutant

The LID region in wildtype *Dm*-dNK is a flexible part of the structure that can attain slightly different positions in different complexes [16,21]. With the wildtype enzyme, in most substrate complexes and the complexes with the feedback inhibitor dTTP, the LID is closed in over the active site. In substrate complexes, LID arginines bind to a sulfate ion in the P-loop and Glu172 to the 3′-OH of the substrate. In the dTTP complex, the phosphates are bound by the LID arginines and the 3′-OH is bound to Glu172. In these cases, Glu171 in the LID region forms a hydrogen bond to Asn64.

By substitution of Asn64 to Asp in the mutant enzyme, the negative charge of Asp destabilizes the normal interactions with Glu171. In the dT complex, the negative charge of Asp64 repels Glu171 and the LID region becomes more flexible and the part around Glu171 and 172 is not visible in the electron density maps (Fig. 3A). The absence of this part of the LID region removes one of the hydrogen bonding inter-

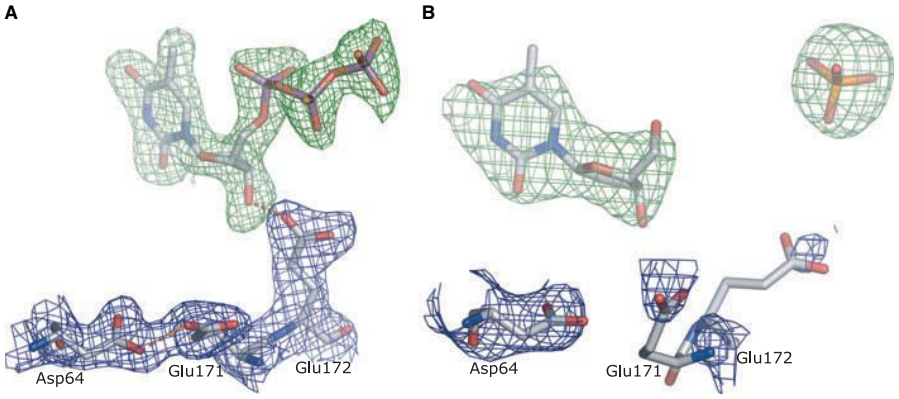

Fig. 2. Electron density maps. Final electron density maps for (A) the *Dm*-dNK N64D–dTTP complex containing the feedback inhibitor dTTP, residues Asp64, Glu171 and Glu172, and (B) the *Dm*-dNK N64D–dT structure containing the same residues, the substrate dT and a sulfate ion. The electron density maps for the protein parts (in blue) are 2Fo-Fc maps contoured at 1σ. The electron density for the ligands (in green) are Fo-Fc maps contoured at 3σ before refinement. Hydrogen bonds in (A) shown as dotted lines.

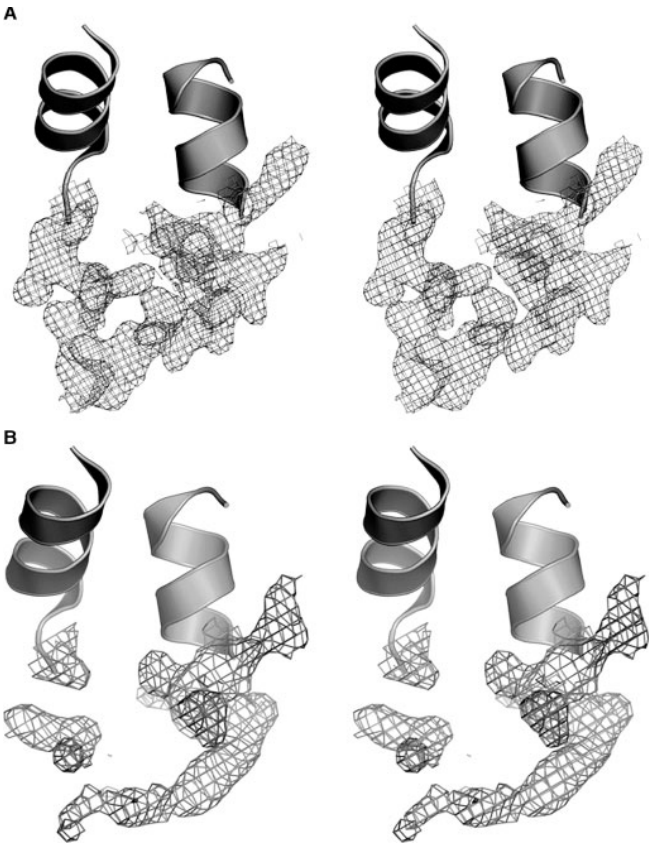

Fig. 3. The LID region in the two complexes. Stereo view of the final electron density for the LID region in (A) the *Dm*-dNK N64D–dTTP complex and (B) the *Dm*-dNK N64D–dT complex (2Fo-Fc maps contoured at 1σ).

actions with the 3′-OH of the deoxyribose of the substrate. The absence of this hydrogen bond and a flexible LID make the substrate binding pocket larger and provide space for the bulky 3′-azide group. AZT can be modeled based on the N64D–dT complex by positioning of AZT instead of dT in its binding site (Fig. 4).

In the complex of N64D and the feedback inhibitor dTTP, the LID region closes down on the inhibitor in the same way as in the wildtype complex in spite of the substitution of Asn to Asp. Because of all contacts between the phosphate groups, the LID region is held in close interaction with dTTP. Consequently, the LID region in the N64D–dTTP complex has well-defined electron density (Fig. 3B). Glu171 is thus forced into contact with Asp64 in spite of the unfavorable electrostatic situation. This is overcome by a hydrogen bonded Asp–Glu interaction that occurs similar to the Asn–Glu interaction in the wildtype enzyme. The energetic cost to bring the two carboxylates of the mutant, Asp64 and Glu171, together explains that dTTP inhibits the mutant N64D with a considerably lower efficiency than in the wildtype enzyme. The IC_{50} value for dT phosphorylation is increased more than 100-fold.

The structure of the *Dm*-dNK N64D mutant presented above and the understanding of the feedback regulation and substrate specificity in *Dm*-dNK will now help to finalize our understanding of the structure–function relationship and also have a wide impact on the following medical applications: the design of novel specific pro-drug and mutant combinations for gene therapy, the development of species-specific antiviral and antibacterial nucleoside analog based drugs, and promoting development of novel AZT-like pro-drugs.

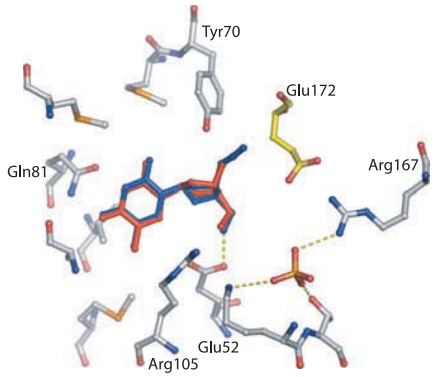

Fig. 4. Modeling of AZT. Interactions with the substrate dT, in red, and with AZT modeled in the substrate binding site, in blue. The interactions with the substrate are the same in the wildtype and the N64D mutant except for the lack of interactions between Glu172 and 3′-OH giving space for the azido-group of AZT. The position of Glu172 in the wildtype structure is given in yellow.

Experimental procedures

Materials

Unlabelled nucleosides and nucleotides were from Sigma (St Louis, MO, USA) or ICN Biochemicals (Aurora, OH). ^{3}H-labeled thymidine [Me-^{3}H]dT (925 GBq·mmol^{-1}) and deoxycytidine [6-^{3}H]dC (740–925 GBq·mmol^{-1}) were obtained from Amersham Corp., Piscataway, NJ, USA). ^{3}H-labeled deoxyadenosine [2,8-^{3}H]dA (1106 GBq), deoxyguanosine [2,8-^{3}H]dG (226 GBq·mmol^{-1}) and 3′-azido-2′,3′-dideoxythymidine [Me-^{3}H]AZT (740 GBq·mmol^{-1}) were from Moravek Biochemicals Inc. (Brea, CA, USA). When present in the radiolabeled deoxynucleosides, ethanol was evaporated before use.

Sequencing

Sequencing by the Sanger dideoxynucleotide method was performed manually, using the Thermo Sequenase radiolabeled terminator cycle sequencing kit and ^{33}P-labeled ddNTPs (Amersham Corp.).

Site directed mutagenesis and expression plasmids

Expression plasmid pGEX-2T-*Dm*-dNK is described in [24]. Expression plasmid pGEX-2T-MuD (pGEX-2T-double mutant N45D/N64D) is described in [15]. The expression vector for human TK1 (pGEX-2T-hTK1) is described elsewhere [25]. The pGEX-2T-mutant N45D and pGEX-2T-mutant N64D were constructed as follows: both mutants were constructed by site directed mutagenesis on the plasmid pGEX-2T- *Dm*-dNK with or without truncation for the C-terminal 20 amino acids [24]. The N45D mutation was created with the following primers: 45D-fw (5′-CGAG AAGTACAAG**G**ACGACATTTGCCTGC-3′) and 45D-rv (5′-GCAGGCAAATGTCGT**C**CTTGTACTTCTCG-3′), where the changed nucleotide is in bold and underlined. The N64D mutation was created with the primers 64D-fw (5′-CGTCAACGGGGTA**G**ATCTGCTGGAGC-3′) and 64D-rv (5′-GCTCCAGCAGAT**C**TACCCCGTTGACG-3′).

An expression plasmid for HSV1-TK was constructed as follows: The thymidine kinase from HSV1 was amplified using the primers HSV-for (5′-CGCGGATCCATGGCT TCGTACCCCGGCCATC-3′) and HSV-rev (5′-CCGGAA TTCTTAGTTAGCCTCCCCCATCTCCCG-3′) and using the plasmid pCMV-pacTK [26] as template. The PCR fragment was subsequently cut by *Eco*RI/*Bam*HI and ligated into pGEX-2T vector that was also cut by *Eco*RI/*Bam*HI. The resulting plasmid was named pGEX-2T-HSV1-TK (P 632).

Test for TK activity on selection plates

The thymidine kinase deficient *E. coli* strain KY895 [F^{-}, *tdk-1, ilv*] [27], was transformed with various expression plasmids. Overnight cultures of these transformants were diluted 200-fold in 10% (w/v) glycerol and 2 μL drops of the dilutions were spotted on TK selection plates [9] that contained different dT concentrations. Only enzymes complementing the TK negative *E. coli* strain KY895 gave rise to colonies on this selection medium. Growth was inspected visually after 24 h at 37 °C.

Determination of LD_{100}

Overnight cultures of single colonies were diluted 200-fold in 10% (w/v) glycerol and 2 μL of these dilutions were spotted on M9 minimal medium plates [28] supplemented with 0.2% (w/v) glucose, 40 μg·mL^{-1} isoleucin, 40 μg·mL^{-1} valin, 100 μg·mL^{-1} ampicillin and with or without AZT. Logarithmic dilutions of the nucleoside analog were used to determine the lethal dose (LD_{100}) of the nucleoside analog, at which no growth of bacteria could be seen. Growth of colonies was visually inspected after 24 h at 37 °C.

Expression and purification of recombinant enzymes

Recombinant proteins were expressed and purified as described previously [24].

Enzyme assay

Deoxyribonucleoside kinase activities were determined by initial velocity measurements based on four time samples

by the DE-81 filter paper assay using tritium-labeled nucleoside substrates. The assay was performed as described [24].

The protein concentration was determined according to Bradford with BSA as standard protein [29]. SDS/PAGE was carried out according to the procedure of Laemmli [30] and proteins were visualized by Coomassie staining.

Analysis of kinetic data

Kinetic data were evaluated by nonlinear regression analysis using the Michaelis–Menten equation $v = V_{max} \times [S]/(K_m + [S])$ or the Hill equation $v = V_{max} \times [S]^h/(K_{0.5}{}^h + [S]^h)$ as described in [31]. K_m is the Michaelis constant, $K_{0.5}$ defines the value of the substrate concentration [S] where $v = 0.5\ V_{max}$ and h is the Hill coefficient [32,33]. If $h = 1$, there is no cooperativity.

The concentration of the feedback inhibitor dTTP necessary for 50% inhibition (IC_{50}) was determined by varying dTTP at 10 μM dT and 2.5 mM ATP and plotting $\log(v_0 - v_I)/v_I$ against log[I] where v_0 and v_I are the velocities without and with inhibitor, respectively. IC_{50} was determined as the intercept with the log[I] axis, where $(v_0 - v_I)/v_I = 1$.

The pattern of inhibition was elucidated by varying dT at four fixed concentrations of dTTP and 2.5 mM ATP, and analyzing the data by the Biosoft (Cambridge, UK) program ENZFITTER for Windows.

Crystallization

The N64D mutant used for crystallization was truncated for the 20 C-terminal amino acids. The C-terminal truncated *Dm*-dNK kinases have similar enzymatic properties as the untruncated kinases but are more stable [24]. Crystals of N64D in complex with dT and dTTP were grown by counter diffusion [34] and vapor diffusion, respectively. The crystallization solution for the N64D mutant dT complex was 0.15 M Mes pH 6.5, 0.3 M lithium sulphate and 27.5% (w/v) poly(ethylene) glycol monomethyl ether 2000. The enzyme solution (20 $mg{\cdot}mL^{-1}$ including 10 mM dT) and the crystallization solution was equally mixed in a capillary and equilibrated for two weeks. For the N64D complex with dTTP the crystallization solution was 0.1 M Mes pH 6.5, 0.16 M lithium sulphate and 25% (v/v) poly(ethylene) glycol monomethyl ether 2000. The protein solution (10 $mg{\cdot}mL^{-1}$) including 5 mM dTTP and the crystallization solution were mixed equally in a hanging drop. All the crystallization trials were performed at 15 °C.

Data Collection

The N64D–dT crystals were directly flash-frozen in liquid nitrogen. The cryoprotectant for the N64D–dTTP crystals contained crystallization solution plus the addition of 20% (v/v) poly(ethylene) glycol 400. The data sets for the two complexes with dT and dTTP were collected at ID14/EH4, ESRF (Grenoble, France). The two data sets were indexed, scaled and merged with MOSFLM [35] and SCALA [36]. Both crystals belonged to the space group $P2_1$ and had a solvent content of 55%. The content in the asymmetric unit for the N64D–dT and N64D–dTTP complex corresponded to four and two dimers, respectively.

Table 3. Data collection and refinement statistics for the N64D-dT and N64D-dTTP complexes.

	N64D-dT	N64D-dTTP
Beamline	ID14/EH4, ESRF	ID14/EH4, ESRF
Wavelength (Å)	0.9393	1.0
Temperature (K)	100	100
Resolution (Å)	3.1 (3.27–3.10)	2.2 (2.32–2.20)
Reflections		
Observed	144933	189093
Unique	39562	53387
Completeness	99.9	99.9
Rmeas(%)	12.0 (45.0)	8.3 (38,9)
I/sigmal	12.5 (3.4)	14.5 (4.1)
Space group	$P2_1$	$P2_1$
Cell Dimensions		
a	69.71	67.04
b	70.34	119.27
c	224.53	68.39
beta	90.69	92.59
Content of the asymmetric unit	4 dimers	2 dimers
Refinement program	Refmac5	Refmac5
R factor (%)	27.0	21.3
R_{free} (%)	28.8	23.7
Root mean square deviation		
Bond length (Å)	0.009	0.011
Bond angles (°)	1.13	1.27
Mean B-value ($Å^2$)	37.4	36.7

Structure determination and refinement

The N64D–dTTP complex was solved with rigid body in REFMAC5 [37] with *Dm*-dNK–dTTP (PDB code: 1oe0) as a search model. The N64D–dT complex was solved with MOLREP and *Dm*-dNK–dT as a search model (PDB code: 1ot3). The mutated residue Asn to Asp in the two complexes was altered in the program O (http://xray.bmc.uu.se/alwyn) [38]. After rigid body refinement the dT and the dTTP complex were refined with fourfold and eightfold noncrystallographic averaging, respectively, in REFMAC5, CCP4. The N64D–dT complex had a final *R*-value of 27.0% and an R_{free} of 28.8% while the model for N64D–dTTP complex had an *R*-value of 21.3% and an R_{free} of 23.7%. The data collection and refinement statistics are shown in Table 3. The coordinates have been deposited with PDB codes: 1zmx and 1zm7.

Acknowledgements

We would like to thank Marianne Lauridsen for excellent technical assistance. This work was supported by grants from the Swedish Research Council (to H.E. and J.P.), the Swedish Cancer Foundation (to H.E.), and Danish Research Council (to B.M.-P., W.K. and J.P.).

References

1 Arnér ESJ & Eriksson S (1995) Mammalian deoxyribonucleoside kinases. *Pharmacol Ther* **67**, 155–186.
2 Plunkett W & Gandhi V (2001) Purine and pyrimidine nucleoside analogs. *Cancer Chemother Biol Response Modif* **19**, 21–45.
3 Klopfer A, Hasenjager A, Belka C, Schulze-Osthoff K, Dorken B & Daniel PT (2004) Adenine deoxynucleotides fludarabine and cladribine induce apoptosis in a CD95/Fas receptor, FADD and caspase-8-independent manner by activation of the mitochondrial cell death pathway. *Oncogene* **23**, 9408–9418.
4 Furman PA, Fyfe JA, St Clair MH, Weinhold K, Rideout JL, Freeman GA *et al.* (1986) Phosphorylation of 3′-azido-3′-deoxythymidine and selective interaction of the 5′-triphosphate with human immunodeficiency virus reverse transcriptase. *Proc Natl Acad Sci USA* **83**, 8333–8337.
5 Eriksson S, Munch-Petersen B, Johansson K & Eklund H (2002) Structure and function of cellular deoxyribonucleoside kinases. *Cell Mol Life Sci* **59**, 1327–1346.
6 Zheng X, Johansson M & Karlsson A (2000) Retroviral transduction of cancer cell lines with the gene encoding *Drosophila melanogaster* multisubstrate deoxyribonucleoside kinase. *J Biol Chem* **275**, 39125–39129.
7 Rainov NG (2000) A phase III clinical evaluation of herpes simplex virus type 1 thymidine kinase and ganciclovir gene therapy as an adjuvant to surgical resection and radiation in adults with previously untreated glioblastoma multiforme. *Hum Gene Ther* **11**, 2389–2401.
8 Greco O & Dachs GU (2001) Gene directed enzyme/prodrug therapy of cancer: historical appraisal and future prospectives. *J Cell Physiol* **187**, 22–36.
9 Black ME, Newcomb TG, Wilson HM & Loeb LA (1996) Creation of drug-specific herpes simplex virus type 1 thymidine kinase mutants for gene therapy. *Proc Natl Acad Sci USA* **93**, 3525–3529.
10 Gentry GA (1992) Viral thymidine kinases and their relatives. *Pharmac Ther* **54**, 319–355.
11 Chen MS & Prusoff WH (1978) Association of thymidylate kinase activity with pyrimidine deoxyribonucleoside kinase induced by herpes simplex virus. *J Biol Chem* **253**, 1325–1327.
12 Munch-Petersen B, Piskur J & Søndergaard L (1998) The single deoxynucleoside kinase in *Drosophila melanogaster*, dNK, is multifunctional and differs from the mammalian deoxynucleoside kinases. *Adv Exp Med Biol* **431**, 465–469.
13 Munch-Petersen B, Piskur J & Søndergaard L (1998) Four deoxynucleoside kinase activities from *Drosophila melanogaster* are contained within a single monomeric enzyme, a new multifunctional deoxynucleoside kinase. *J Biol Chem* **273**, 3926–3931.
14 Johansson M, Van Rompay AR, Degreve B, Balzarini J & Karlsson A (1999) Cloning and characterization of the multisubstrate deoxyribonucleoside kinase of *Drosophila melanogaster*. *J Biol Chem* **274**, 23814–23819.
15 Knecht W, Munch-Petersen B & Piskur J (2000) Identification of residues involved in the specificity and regulation of the highly efficient multisubstrate deoxyribonucleoside kinase from *Drosophila melanogaster*. *J Mol Biol* **301**, 827–837.
16 Johansson K, Ramaswamy S, Ljungcrantz C, Knecht W, Piskur J, Munch-Petersen B *et al.* (2001) Structural basis for substrate specificities of cellular deoxyribonucleoside kinases. *Nat Struct Biol* **8**, 616–620.
17 Sabini E, Ort S, Monnerjahn C, Konrad M & Lavie A (2003) Structure of human dCK suggests strategies to improve anticancer and antiviral therapy. *Nat Struct Biol* **10**, 513–519.
18 Brown DG, Visse R, Sandhu G, Davies A, Rizkallah PJ, Melitz C *et al.* (1995) Crystal structures of the thymidine kinase from herpes simplex virus type-1 in complex with deoxythymidine and ganciclovir. *Nat Struct Biol* **2**, 876–881.
19 Wild K, Bohner T, Folkers G & Schulz GE (1997) The structures of thymidine kinase from herpes simplex virus type 1 in complex with substrates and a substrate analogue. *Protein Sci* **6**, 2097–2106.
20 Welin M, Kosinska U, Mikkelsen NE, Carnrot C, Zhu C, Wang L *et al.* (2004) Structures of thymidine kinase 1 of human and mycoplasmic origin. *Proc Natl Acad Sci USA* **101**, 17970–17975.
21 Mikkelsen NE, Johansson K, Karlsson A, Knecht W, Andersen G, Piskur J *et al.* (2003) Structural basis for feedback inhibition of the deoxyribonucleoside salvage pathway: studies of the *Drosophila* deoxyribonucleoside kinase. *Biochemistry* **42**, 5706–5712.
22 Kokoris MS, Sabo P, Adman ET & Black ME (1999) Enhancement of tumor ablation by a selected HSV-1 thymidine kinase mutant. *Gene Ther* **6**, 1415–1426.
23 Sandrini M & Piskur J (2005) Deoxyribonucleoside kinases: two enzyme families catalyze the same reaction. *Trends Biochem Sci* **30**, 225–228.
24 Munch-Petersen B, Knecht W, Lenz C, Søndergaard L & Piskur J (2000) Functional expression of a multisubstrate deoxyribonucleoside kinase from *Drosophila melanogaster* and its C-terminal deletion mutants. *J Biol Chem* **275**, 6673–6679.

25 Berenstein D, Christensen JF, Kristensen T, Hofbauer R & Munch-Petersen B (2000) Valine, not methionine, is amino acid 106 in human cytosolic thymidine kinase (TK1). Impact on oligomerization, stability, and kinetic properties. *J Biol Chem* **275**, 32187–32192.
26 Karreman C (1998) A new set of positive/negative selectable markers for mammalian cells. *Gene* **218**, 57–61.
27 Igarashi K, Hiraga S & Yura T (1967) A deoxythymidine kinase deficient mutant of *Escherichia coli*. II. Mapping and transduction studies with phage phi 80. *Genetics* **57**, 643–654.
28 Ausubel F, Brent R, Kingston RE, Moore DD, Seidman JG, Smith JA *et al.* (1995) *Short Protocols in Molecular Biology*, 3rd edn. John Wiley & Sons, Inc., USA.
29 Bradford MM (1976) A rapid and sensitive method for the quantitation of microgram quantities of protein utilizing the principle of protein-dye binding. *Anal Biochem* **72**, 248–254.
30 Laemmli UK (1970) Cleavage of structural proteins during the assembly of the head of bacteriophage T4. *Nature* **227**, 680–685.
31 Knecht W, Bergjohann U, Gonski S, Kirschbaum B & Loffler M (1996) Functional expression of a fragment of human dihydroorotate dehydrogenase by means of the baculovirus expression vector system, and kinetic investigation of the purified recombinant enzyme. *Eur J Biochem* **240**, 292–301.
32 Cornish-Bowden A (1995) *Fundamentals of Enzyme Kinetics*. Portland Press Ltd, London.
33 Liebecg C (1992) *IUIMB Biochemical Nomenclature and Related Documents*. Portland Press Ltd, London.
34 Ng JD, Gavira JA & Garcia-Ruiz JM (2003) Protein crystallization by capillary counterdiffusion for applied crystallographic structure determination. *J Struct Biol* **142**, 218–231.
35 Leslie AGW (1992) Joint CCP4 + ESF-EAMCB Newsletter on Protein Crystallography, No. 26.
36 Collaborative Computational Project, Number 4 (1994) The CCP4 Suite: Programs for Protein Crystallography. *Acta Crystallogr* **D50**, 760–763.
37 Murshudov GN, Vagin AA & Dodson EJ (1997) Refinement of macromolecular structures by the maximum-likelihood method. *Acta Crystallogr* **D53**, 240–255.
38 Jones TA, Zou JY, Cowan SW & Kjeldgaard M (1991) Improved methods for building protein models in electron density maps and the location of errors in these models. *Acta Crystallogr* **47**, 110–119.

II

Nucleosides, Nucleotides, and Nucleic Acids, 25:1165–1169, 2006

ISSN: 1525-7770 print / 1532-2335 online
DOI: 10.1080/15257770600894410

Taylor & Francis
Taylor & Francis Group

PURIFICATION AND CHARACTERIZATION OF WILD-TYPE AND MUTANT TK1 TYPE KINASES FROM *CAENORHABDITIS ELEGANS*

T. Skovgaard and B. Munch-Petersen □ *Department of Life Sciences and Chemistry, Roskilde University, Roskilde, Denmark*

□ Caenorhabditis elegans *has a single deoxynucleoside kinase-like gene. The sequence is similar to that of human TK1, but besides accepting thymidine as a substrate, the C. elegans TK1 (*Ce*TK1) also phosphorylates deoxyguanosine. In contrast to human TK1, the* Ce*TK1 exclusively exists as a dimer with a molecular mass of ~60 kDa, even if incubated with ATP. Incubation with ATP induces a transition into a more active enzyme with a higher k_{cat} but unchanged K_m. This activation only occurs at an enzyme concentration in the incubation buffer of 0.5 μg/ml (8.42 nM) or higher. C-terminal deletion of the enzyme results in lower catalytic efficiency and stability.*

Keywords Thymidine kinase; TK1; *Caenorhabditis elegans*; ATP activation; Characterization; Enzyme kinetics

INTRODUCTION

Caenorhabditis elegans thymidine kinase (*Ce*TK1) is a TK1 type deoxynucleoside kinase that catalyzes the transfer of γ-phosphate from ATP to the 5′-OH of thymidine and deoxyguanosine to form dTMP and dGMP, respectively. In humans and other mammalians TK1 is a key enzyme in the salvage of dTTP for DNA synthesis.

Deoxynucleoside kinases are also important for activation of antiviral and anticancer drugs such as the nucleoside analog AZT used for HIV treatment. A thymidine kinase from Herpes Simplex virus type 1, HSV1-TK, has been used in suicide gene therapy in an attempt to cure cancer.[1,2] In tumor cells expressing the HSV1-TK, the analog is phosphorylated to the monophosphate level. Subsequently, cellular kinases add 2 more phosphate groups to form the triphosphate analog, which after incorporation into

We would like to thank Zoran Gojkovic from ZGene for providing the *Ce*TK1-gene and Marianne Lauridsen and Lene S. Harlow for excellent technical assistance.

Address correspondence to B. Munch-Petersen, Department of Life Sciences and Chemistry, Roskilde University, DK-4000, Roskilde, Denmark. E-mail: bmp@ruc.dk

DNA prevents DNA elongation and causes cell cycle arrest or apoptosis. In order to find a better deoxynucleoside kinase with higher analog specificities for this purpose, new enzymes are continuously characterized and new analogs are created.

In the present characterization of *Ce*TK1, the enzyme is compared with human TK1 (HuTK1) with regard to native size, activation by ATP, stability and kinetic parameters for thymidine. *Ce*TK1 is truncated in the C-terminal in order to see how the truncation affects stability and activity.

MATERIALS AND METHODS

The *Ce*TK1 gene was provided from ZGene (Hoersholm, Denmark) and cloned into the expression vector pGEX-2T by PCR amplifcation (Primers: Forward: 5′-CGG CGC CCG GGC ATG GAC ATT GAA GCG GCC AAG AAT GAG ATG ACT TGC-3′; Reverse: 5′ CCG GAA TTC TTA AGT CCG AGC TGT GGC CTC CAG AGC 3′) followed by cleavage and ligation at XmaI and EcoRI restriction sites. *Ce*TK1 was expressed in *E. coli* BL21 as a GSH fusion protein and purified by GSH affinity chromatography as described.[3]

The C-terminally truncated mutant was constructed using the QuickChange site-directed mutagenesis kit from Stratagene (AH Diagnostic, Denmark) (Primers: Forward: 5′-GC AGAGAA TGT TAT GTT CAA AAG AGC TAA GAA AAA GAT GC-3′; Reverse: 5′ GC ATC TTT TTC TTA GCT CTT TTG AAC ATA ACA TTC TCT GC-3′. Mutation marked with grey). The truncated enzyme was expressed and purified as the wild type.

Effect of ATP on the enzymes was examined by incubating 5 μg/ml (84.2 nM) enzyme for 2 hours on ice in buffer A (50 mM Tris HCL pH 7.5, 5 mM $MgCl_2$, 0.1 M KCl, 2 mM 3-[(3-Cholamidopropyl)-dimethylammonium]-1-propanesulfonate (CHAPS), 10% Glycerol, 5 mM dithiothreitol (DTT)) with 2.5 mM ATP. For comparison, an aliquot of enzyme was incubated in the same buffer without ATP.

Enzyme activities were measured as initial velocities determined by 3 time samples (5, 10, and 15 minutes) with the DE-81 filter paper assay using ^{3}H labelled substrates.[3] Reaction mixture of 50 μl contained 50 mM TRIS-HCl, pH 7.5, 2.5 mM $MgCl_2$, 10 mM DTT, 0.5 mM CHAPS, 3 mM NaF, 3 mg/ml BSA, 2.5 mM ATP, and [*methyl*-^{3}H]-Thymidine (1.8 Ci mmol^{-1} Amersham Pharmacia Biotech, now GE Healthcare Bio-Sciences, Hilleroed, Denmark) and 0.074 nM enzyme.

The native size was determined by gel filtration on a superdex 200 column as described.[3]

*Ce*TK1 stability was determined by incubating the enzyme at room temperature (5 μg/ml, 84.2 nM) in buffer A with or without ATP.

RESULTS AND DISCUSSION

The entire genome of *C. elegans* is sequenced and appears to contain only a single deoxynucleoside kinase-like sequence. Humans have 4 different deoxynucleoside kinases whereas insects, such as the fruit fly *Drosophila melanogaster*, only have a single one. However, in contrast to the human deoxynucleoside kinases, the insect deoxynucleoside kinase can phosphorylate all 4 naturally occurring deoxynucleosides and differ greatly in structure from the TK1-type kinases.[4–6] A BLAST search on the *Ce*TK1 protein sequence reveals the closest similarity to HuTK1, with 46% identical and 63% positive matches. A sequence alignment of HuTK1 and *Ce*TK1 is presented in Figure 1, and it is evident from the alignment that the two enzymes have high sequence similarity with exception of the N- and C-terminal regions.

In spite of the high similarity, HuTK1 and *Ce*TK1 differ in respect to both substrate specificity and ATP-activation pattern: When HuTK1 is incubated with ATP it changes from a dimer form with a mass of ~50 kDa and a high K_m of ~15 μM into a tetramer of ~100 kDa with an approximately 20– to 30- fold lower K_m (Table 1).[7,8] k_{cat} for HuTK1 is in the same range for both the dimer and tetramer. In contrast to this, *Ce*TK1 is a dimer of ~60 kDa regardless of ATP incubation, but even so ATP has an effect on enzyme activity. The ATP incubated *Ce*TK1 has a higher k_{cat} than the enzyme incubated without ATP, but K_m is unchanged. Hence, ATP activates both enzymes, but HuTK1 is activated with regard to K_m and *Ce*TK1 with regard to k_{cat}. In general, the k_{cat} values for HuTK1 and *Ce*TK1 are in the same range, but for the enzymes not incubated with ATP, the HuTK1 k_{cat} is higher than

```
HuTK1   ---------MSCINLPT------VLPGSPSKTRGQIQVILGPMFSGKSTELMRRVRRFQI 45
CeTK1   MDIEAAKNEMTCCSSNSSLSDFNTLPRCPNR-VGSITVILGPMFSGKTTELLRLHDRQII 59
                 *:* .  :      .** .*.:  *.* **********:***:*   *  *

HuTK1   AQYKCLVIKYAKDTRYSSS-FCTHDRNTMEA--LPACLLRDVAQEALG--VAVIGIDEGQ 100
CeTK1   AKRTCVLVKYAGDTRYDADLVATHSKMTGQGRTVKAHRLSEVQSQIFNDEVQVVSIDEGQ 119
        *: .*:::*** ****.:. ..**.: * :.  : *  * :* .: :.  * *:.*****

HuTK1   FFPDIVEFCEAMANAGKTVIVAALDGTFQRKPFGAILNLVPLAESVVKLTAVCMECFREA 160
CeTK1   FFEDLAETCEELAQRGKVVCVAALNGTFERKPFPQISLLLPYANEIKQVTAVCVECGSQA 179
        ** *:.* ** :*: **.* ****:***:****  *  *:* *:.: ::****:**  :*

HuTK1   AYTKRLGTEKEVEVIGGADKYHSVCRLCYFKKASGQPAGPDNKENCP----------VPG 210
CeTK1   NFSFRSTLDKKVEVIGGSDTYTALCRECYVQKSEEKDAEEQMKTGCDKNENDITGIFLAK 239
         :: *   :*:******:*.* ::** **.:*:. : *  : * .*           :.

HuTK1   KP----GEAVAARKLFAPQQILQCSPAN-- 234
CeTK1   KEQRSDGSVSPPRKKIGLSKSMALEATART 269
        *     *.. ..** :. .: :  ..:
```

FIGURE 1 ClustalX 1.8 alignment of sequences of HuTK1 (GeneBank nr. AAH06484) and *Ce*TK1 (GeneBank nr. NM_069485). (* Indicates a conserved amino acid.) The gray boxes indicate the position for C-terminal truncation of the 2 enzymes.

TABLE 1 Kinetic Values with the Substrate Thymidine

HuTK1[a]	WT (25.5 kDa)		CΔ40 (21.1 kDa)	
Storage conditions	−ATP	+ATP	−ATP	+ATP
k_{cat} (sec^{-1})	6.3 ± 0.9	6.9 ± 0.2	9.5 ± 1.1	9.7 ± 0.2
K_m (μM)	16 ± 3.4	0.7 ± 0.2	1.4 ± 0.6	0.6 ± 0.1
k_{cat}/K_m	0.4×10^6	9.9×10^6	6.8×10^6	16.2×10^6
CeTK1	WT (29.7 kDa)		CΔ56 (23.6 kDa)	
Storage conditions	−ATP	+ATP	−ATP	+ATP
k_{cat} (sec^{-1})[b]	5.0 ± 0.1	8.8 ± 0.2	1.1 ± 0.0	3.5 ± 0.2
K_m (μM)	2.3 ± 0.3	2.6 ± 0.3	7.4 ± 0.8	5.8 ± 0.9
k_{cat}/K_m	2.2×10^6	3.4×10^6	0.1×10^6	0.6×10^6

[a]Kinetic values for HuTK1 are from.[8]

[b]k_{cat} values were calculated presuming one binding site per subunit using the theoretical MW for the enzyme. +ATP and −ATP denotes whether the enzyme has been pre-incubated in a buffer with or without 2.5 mM ATP/$MgCl_2$.

the *Ce*TK1 k_{cat}, and for the ATP incubated enzymes, *Ce*TK1 k_{cat} is slightly higher than the HuTK1 k_{cat}.

Due to a high K_m value and a low solubility of deoxyguanosine accurate kinetic values for phosphorylation of this substrate could not be achieved.

The ATP-activation of *Ce*TK1 depends on enzyme concentration in the incubation buffer. At concentrations of 0.1 μg/ml (1.68 nM) and lower there is no transition to the more active +ATP form of the enzyme, whereas at 0.5 μg/ml (8.42 nM) and higher concentrations the transition to the higher k_{cat} form takes place. The low enzyme concentration in the assay (0.074 nM) explains our linear progression curves and absence of transition during the kinase assay although there is 2.5 mM ATP in the assay mixture.

*Ce*TK1 is remarkably stable compared to the human TK1. When incubated in TRIS buffer, the half-life of *Ce*TK1 is 222 hours whereas the half-life of HuTK1 incubated in phosphate buffer (50 mM K-phosphate with 0.5 mM CHAPS) is only 58 minutes.[8] The half-lifes are not directly comparable due to the different incubation buffers, but since HuTK1 has a lower stability in TRIS buffer than in phosphate buffer (B. Munch-Petersen, personal communication) the stability of *Ce*TK1 is more than 540 fold higher than the stability of HuTK1. However, where deletion of the C-terminal of the HuTK1 increases the stability,[8] similar deletion of the C-terminal of *Ce*TK1 has a destabilizing effect. Thus, the half-life for HuTK1 deleted by 40 amino acids in the C-terminal is 256 minutes,[8] which is 32 = fold higher than the undeleted enzyme. Deletion of the corresponding amino acids (the position of deletion is marked on Figure 1) in *Ce*TK1 (*Ce*TK1-CΔ56) results in a 1.4-fold decrease in half-time from 222 hours to 156 hours. Further, the C-terminal deletion in the human kinase increases the catalytic activity,

whereas the C-terminal deletion of *Ce*TK1 decreases the catalytic activity. In general, *Ce*TK1 is a remarkably stable enzyme both with and without the C-terminal. During more than two weeks of storage at 4°C it maintains full activity.

In summary, the results presented here show that in contrast to the C-terminal of HuTK1 that decreases the stability and enzymatic activity, the C-terminal of *Ce*TK1 maintains stability and enzymatic activity.

REFERENCES

1. Klatzmann, D.; Valery, C.A.; Bensimon, G.; Marro, B.; Boyer, O.; Mokhtari, K.; Diquet, B.; Salzmann, J.L.; Philippon, J. A phase I/II study of herpes simplex virus type 1 thymidine kinase "suicide" gene therapy for recurrent glioblastoma. *Hum. Gene. Ther.* **1998**, 9, 2595–2604.
2. Ram, Z.; Culver, K.W.; Oshiro, E.M.; Viola, J.J.; DeVroom, H.L.; Otto, E.; Long, Z.; Chiang, Y.; McGarrity, G.J.; Muul, L.M.; Katz, D.; Blaese, R.M.; Oldfield, E.H. Therapy of malignant brain tumors by intratumoral implantation of retroviral vector-producing cells. *Nat. Med.* **1997**, 3, 1354–1361.
3. Frederiksen, H.; Berenstein, D.; Munch-Petersen, B. Effect of valine 106 on structure-function relation of cytosolic human thymidine kinase. Kinetic properties and oligomerization pattern of nine substitution mutants of V106. *Eur J. Biochem.* **2004**, 271, 2248–2256.
4. Munch-Petersen, B.; Piskur, J.; Sondergaard, L. Four deoxynucleoside kinase activities from Drosophila melanogaster are contained within a single monomeric enzyme, a new multifunctional deoxynucleoside kinase. *J. Biol. Chem.* **1998**, 273, 3926–3931.
5. Johansson, K.; Ramaswamy, S.; Ljungcrantz, C.; Knecht, W.; Piskur, J.; Munch-Petersen, B.; Eriksson, S.; Eklund, H. Structural basis for substrate specificities of cellular deoxyribonucleoside kinases. *Nat. Struct. Biol.* **2001**, 8, 616–620.
6. Welin, M.; Kosinska, U.; Mikkelsen, N.E.; Carnrot, C.; Zhu, C.; Wang, L.; Eriksson, S.; Munch-Petersen, B.; Eklund, H. Structures of thymidine kinase 1 of human and mycoplasmic origin. *Proc. Natl. Acad. Sci. USA.* **2004**, 101, 17970–17975.
7. Munch-Petersen, B.; Tyrsted, G.; Cloos, L. Reversible ATP-dependent transition between two forms of human cytosolic thymidine kinase with different enzymatic properties. *J. Biol. Chem.* **1993**, 268, 15621–15625.
8. Zhu, C.; Harlow, L.; Berenstein, D.; Munch-Petersen, S.; Munch-Petersen, B. Effect of C-terminal of human cytosolic thymidine kinase (TK1) on in vitro stability and enzymatic properties. *Nucleosides, Nucleotides, Nucleic Acids* (this issue).

III

THYMIDINE KINASE 1 DEFICIENT CELLS SHOW INCREASED SURVIVAL RATE AFTER UV-INDUCED DNA DAMAGE

T. Skovgaard, L. J. Rasmussen* and B. Munch-Petersen

Dept. of Science Systems and Models, Roskilde University, Roskilde, Denmark
*present address: Center for Healthy Aging, Department of Cellular and Molecular Medicine, University of Copenhagen, Copenhagen, Denmark

ABSTRACT

Balanced deoxynucleotide pools are known to be important for correct DNA repair, and deficiency for some of the central enzymes in deoxynucleotide metabolism can cause imbalanced pools which in turn can lead to mutagenesis and cell death. Here we show that cells deficient for the thymidine salvage enzyme thymidine kinase 1 (TK1) are more resistant to UV-induced DNA damage than TK1 positive cells although they have thymidine triphosphate (dTTP) levels of only half the size of control cells. Our results suggest that higher thymidine levels in the TK- cells caused by defect thymidine salvage to dTTP protects against UV irradiation.

Keywords: Thymidine kinase 1; Survival; DNA damage; UV; dTTP pools.

INTRODUCTION

When mammalian cells are subjected to DNA damage by UV-radiation they respond by cell cycle arrest and initiation of DNA repair, and if the damage is too extensive they enter apoptosis.[1] Balanced deoxynucleotide (dNTP) pools are important for correct DNA repair and replication, and pool imbalances can lead to severe mutagenesis and even cell death.[2]

The most common form of UV-induced DNA damage is the formation of pyrimidine dimers of which T-T dimers formed between two thymines are the most abundant. It has been shown that elevation of thymidine (dThd) levels in the micromolar range stimulated the rejoining of UV-induced DNA-strand breaks in quiescent lymphocytes.[3] dThd is phosphorylated by thymidine kinase 1 (TK1) in cycling cells and by TK2 in resting cells, and two subsequent phosphorylations lead to thymidine triphosphate (dTTP).[4] dTTP is a regulator of ribonucleotide reductase (RNR) switching the specificity from pyrimidine to purine nucleotide reduction.[5] It

was suggested that the increased DNA repair observed in lymphocytes is caused by a conversion of dThd to dTTP and a subsequent dTTP induced increase of purine dNTPs.[3]

In this study we examine the connection between cellular dTTP pools and cell survival upon UV irradiation in cycling cells. We compare survival and dTTP pools upon UV irradiation in two osteosarcoma cell lines, one of which has disturbed dTTP metabolism due to TK1 deficiency. An increased survival rate of TK1 deficient (TK^-) cells compared to TK1 proficient (TK^+) control cells is observed, and we suggest that the increased survival is due to increased levels of dThd absorbing some of the UV-radiation in TK^- cells.

MATERIALS AND METHODS

Cell cultures – HOS and 143B are human osteosarcoma cells originating from the same host. 143B is TK^- and originates indirectly from HOS which is TK^+. 143B cells (ATCC no.: CRL-8303™) were grown in DMEM with Glutamax (GIBCO) supplemented with 10% FBS (Biochrom AG), 1% penicillin/streptomycin (GIBCO). HOS cells (ATCC no.: CRL-1543™) were grown as 143B cells but with 7.5 % FBS.

UV irradiation of cells – Prior to UV irradiation the cells were washed twice with 37ºC 1x Dulbecco's Phosphate Buffered Saline (1xDPBS) containing magnesium and calcium (GIBCO or Lonza). The DPBS was removed and the dishes irradiated at varying time periods with 254 nm UVC light from a 20 $\mu W/cm^2$ source. Unless the cells were harvested immediately after irradiation they were supplemented with preheated medium and stored in the 37 ºC incubator until harvest.

Cell survival assay with Giemsa staining – 1000 and 5000 cells are seeded in 8.8 cm^2 petri dishes and irradiated on the following day with varying UV doses. The medium is changed every 2-3 days and after 4-6 days, when non-irradiated control plates contain 170-300 colonies of approx. 50 cells, the cells are dried, fixed and stained as described in [6]. Colonies containing 10-50 cells are counted.

Measuring dTTP pools – Cells for cell cycle analysis or dTTP assays were set up in 145 cm^2 dishes, and after UV irradiation dTTP pools were measured with the DNA polymerase assay as described in [7] with the following modifications: four times 10 µl assay solution aliquots were spotted on Whatman DE81 paper discs, and after being

washed the filters were eluted with 0.5 ml 0.5 M HCl and 0.2 M KCl. Radioactivity was counted in a Wallac Trilux 1450 Microbeta liquid scintillation counter.

Cell cycle analysis – Cell cycle distribution was determined with a Becton Dickinson FACS Calibur fluorescence activated cell sorter as described in [6]. Data were analyzed with Cell QuestPro and ModFit software.

RESULTS AND DISCUSSION

Cell survival at varying doses of UV light was determined for the two osteosarcoma cell lines HOS and 143B (figure 1). HOS and 143B originate from the same tumour but 143B is deficient for the dTTP salvage enzyme TK1. Interestingly, the TK1 deficient cells were more resistant to cell killing by UV than the TK^+ cells, as evident from LD_{50} values of 8 J/m^2 and 4 J/m^2 for 143B and HOS cells, respectively.

Micromolar concentrations of thymidine have previously been reported to increase the repair efficiency of UVC induced DNA strand breaks in quiescent lymphocytes, and it was suggested that this may be due to allosteric regulation of RNR by dTTP.[3]

In order to see if the difference in survival rate between the TK^+ and TK^- cells is caused by different dTTP pools the cellular dTTP levels are measured immediately after irradiation and 24 hours after irradiation (figure 2). The cells are irradiated with a UV dose corresponding to their LD_{50}. At the time of irradiation the TK1 deficient cells have a dTTP pool of half the size of the TK^+ cells. This indicates that TK1 is important for maintaining cellular dTTP pools in cycling cells. The two important regulators of dTTP pools TK1 and RNR are both tightly cell cycle regulated and are only expressed in S-phase. In order to ensure that the differences in dTTP levels are not due to a different number of cells in S-phase and hence different levels of RNR expression, the cell cycle distribution was determined along with the dTTP levels. At the time of UV irradiation the percentage of cells in S-phase was 45±2 and 43±2 for 143B and HOS cells, respectively (n=2, ±S.D.), concluding that the difference in dTTP levels is not due to different percentages of S-phase cells.

The dTTP pools did not change in either of the cell lines when measured 24 hours after UV irradiation. This is in agreement with results previously obtained for TK^+ mouse fibroblasts.[8] Since TK^+ and TK^- cells behave similarly in the period after UV irradiation it is evident that TK1 deficiency does not influence the dTTP pool after DNA damage with UV.

We conclude that the increased survival rate of TK1 deficient cells is not caused by increased dTTP levels, but it is likely that the lack of TK1 in these cells leads to increased levels of dThd since it cannot be phosphorylated. Increased dThd levels have previously been observed in TK1 deficient mice models.[9] It may be that a high level of dThd and not dTTP is the cause of increased repair efficiency in the study on lymphocytes[3] and the increased survival rate in the present study. Since the thymine base of free dThd is able to absorb part of the UV radiation inflicted on the cells, another possibility is that a high level of dThd in TK^- cells compared to TK^+ cells increases their UV resistance due to higher absorption of UV rays by free dThd.

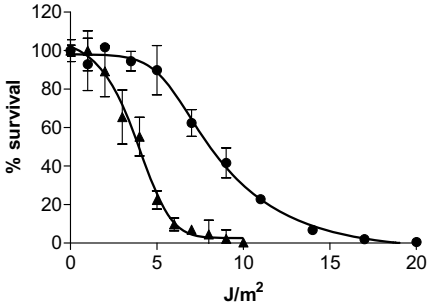

Figure 1: Cell survival increase in TK1 deficient osteosarcoma cells. Cell survival at varying doses of UV light. (▲) HOS cells (TK^+) and (●) 143B (TK^-). The LD_{50} values for HOS and 143B cells are 4 J/m^2 and 8 J/m^2, respectively. Error bars are ±S.D. of three independent measurements.

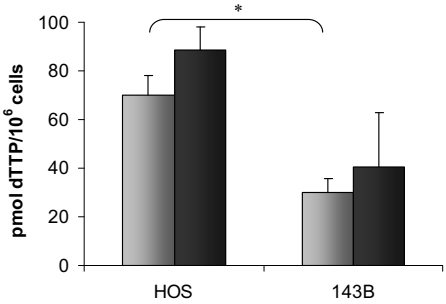

Figure 2: dTTP pools are lower in TK- cells but are not affected by UV irradiation of TK^+ and TK^- osteosarcoma cells. Cellular dTTP levels measured immediately after (grey bars) and 24 hours after (black bars) UV irradiation with a single pulse of 254 nm 20 μW/cm^2 UV light corresponding to the cells LD50. * dTTP levels at the time of irradiation are significantly different in the two cell lines ($p<0.05$ with students t-test). The error bars show ±S.D. of two independent measurements.

ACKNOWLEDGEMENTS AND CORRESPONDENCE

We would like to thank Chiara Rampazzo for providing the HOS cells.

Address correspondence to B. Munch-Petersen, Department of Science, Systems and Models, Roskilde University, 4000 Roskilde, Denmark. E-mail: bmp@ruc.dk

REFERENCES

1. Latonen L, Laiho M. Cellular UV damage responses – functions of tumor suppressor p53. Biochim Biophys Acta. **2005**, *1755(2)*, 71-89.
2. Kunz BA, Kohalmi SE. Modulation of mutagenesis by deoxyribonucleotide levels. Annu Rev Genet. **1991**, *25*, 339-59.
3. Munch-Petersen B. Thymidine in the micromolar range promotes rejoining of UVC-induced DNA strand breaks and prevents azidothymidine from inhibiting the rejoining in quiescent human lymphocytes. Mutat Res. **1997**, *383(2)*, 143-53.
4. Arnér ES, Eriksson S. Mammalian deoxyribonucleoside kinases. Pharmacol Ther. **1995**, *67(2)*, 155-86.
5. Eriksson S, Thelander L, Akerman M. Allosteric regulation of calf thymus ribonucleoside diphosphate reductase. Biochemistry. **1979**, *18(14)*, 2948-52.
6. Lützen A, Bisgaard HC, Rasmussen LJ. Cyclin D1 expression and cell cycle response in DNA mismatch repair-deficient cells upon methylation and UV-C damage. Exp Cell Res. **2004**, *292(1)*, 123-34.
7. Desler C, Munch-Petersen B, Stevnsner T, Matsui S, Kulawiec M, Singh KK, Rasmussen LJ. Mitochondria as determinant of nucleotide pools and chromosomal stability. Mutat Res. **2007**, *625(1-2)*, 112-24.
8. Håkansson P, Hofer A, Thelander L. Regulation of mammalian ribonucleotide reduction and dNTP pools after DNA damage and in resting cells. J Biol Chem. 2006, *281(12)*, 7834-41.
9. Dobrovolsky VN, Bucci T, Heflich RH, Desjardins J, Richardson FC. Mice deficient for cytosolic thymidine kinase gene develop fatal kidney disease. Molecular Genetics and Metabolism. **2003**, *78*, 1-10.

IV

Mutation of Thr163 to Ser in Human Thymidine Kinase 1 Shifts the Specificity from Thymidine towards the Nucleoside Analogue Azidothymidine

Tine Skovgaard[1], Ulla Uhlin[2] and Birgitte Munch-Petersen[1]

[1] Department of Science, Systems and Models, Roskilde University, Universitetsvej 1, 4000 Roskilde, Denmark (tinehans@ruc.dk, bmp@ruc.dk).

[2] Department of Molecular Biology, Swedish University of Agricultural Sciences, Uppsala, Box 590, Biomedical Centre, Sweden (ulla@xray.bmc.uu.se)

Corresponding author: Birgitte Munch-Petersen, +45 46742418

Abbreviations*

Abstract:

The rate-limiting step for the absorption of several anticancer or antiviral nucleoside analogues is thymidine kinase. Thymidine kinase 1 has recently been crystallized and characterized with different ligands. Here, a detailed comparative structure-function study of the active site of the thymidine kinases HuTK1 and *Ce*TK1 (from *Caenorhabditis elegans*) is presented. These kinases are compared via mutational analysis to improve our understanding of thymidine kinase 1 substrate specificity.

* Abbreviations: dNTP, deoxynucleoside triphopshate; dThd, thymidine; dNK, deoxynucleoside kinase; HuTK1, human cytosolic thymidine kinase 1; *Ce*TK1, *Caenorhabditis elegans* thymidine kinase 1.

Specifically, mutations were introduced in the hydrophobic pocket surrounding the substrate base. In *Ce*TK1, some mutations led to increased activity with deoxycytidine and deoxyguanosine, two unusual substrates for TK1-like kinases. Mutation of Thr163 to Ser in HuTK1 resulted in a kinase with 140-fold lower K_m for the antiviral nucleoside analogue AZT (compared to the natural substrate thymidine). The crystal structure of the T163S mutated HuTK1 reveals a less ordered conformation of the ligand dTTP compared to the wild type structure but the cause of the changed specificity towards AZT is not obvious. Based on its highly increased AZT activity (relative to dThd activity) this TK1 mutant could be suitable for suicide gene therapy.

Key words: Thymidine kinase 1, nucleoside analogue, mutagenesis, crystal structure, enzyme kinetics.

Mammals have four different deoxynucleoside kinases (dNK's) with overlapping substrate specificities. Two are cytosolic, thymidine kinase 1 (TK1) and deoxycytidine kinase (dCK), and two are mitochondrial, thymidine kinase 2 (TK2) and deoxyguanosine kinase (dGK). Based on sequence and structure analyses TK1 has a different evolutionary origin than TK2, dCK and dGK and consequently, the kinases can be divided into TK1-like and non-TK1-like groups.[1-3] In addition to the mammalian TK2, dCK and dGK, the non-TK1-like group includes insect dNK's and herpes simplex type 1 thymidine kinase. Vaccinia virus thymidine kinase belongs to the TK1-like kinases.[1,4] TK1 is a key enzyme in the salvage of thymidine for DNA synthesis. It catalyzes the first of three phosphate

transfers from ATP to thymidine, following which dTMP is quickly phosphorylated to dTDP and dTTP by di- and triphosphate kinases. The hydration sphere imparted by the first phosphate traps thymidine (and its analogues) into cells, and given its passive transport across cell membranes TK1, in effect, serves as a thymidine pump.

The end product of the thymidine salvage pathway, dTTP, is a feedback inhibitor of TK1, but it is also an allosteric effector of ribonucleotide reductase (RNR) where it shifts RNR specificity from pyrimidine to purine nucleotide reduction.[5] Hence, an imbalance in the dTTP pool can cause an imbalance in both the purine and pyrimidine pools and thus a broader disturbance in DNA metabolism and repair.

Apart from phosphorylation of naturally occurring deoxynucleosides, deoxynucleoside kinases are also important for the activation of anticancer and antiviral nucleoside analogue pro-drugs such as 1-β-D-arabinofuranosylcytosine (Cytarabine, AraC) and 3'-azido-3'-deoxythymidine (Zidovudine, AZT). TK1 in particular is known for its activation of AZT, the cancer diagnostic positron emission tomography imaging agent 3'-[(18)F]fluoro-3'- deoxythymidine,[6] and the anti-cancer experimental radiosensitizer iodinated deoxyuridine.[7] In general, absorption of nucleoside analogues, such as AZT, is rate-limited by its first phosphorylation step by deoxynucleoside kinases, and the toxic triphosphorylated nucleoside analogues can cause DNA-chain termination, inhibit DNA polymerase and induce apoptosis.[8,9]

Thymidine kinase 1 from Human and *Caenorhabditis elegans*

Similar to insects that have only one multisubstrate deoxynucleoside kinase, *C. elegans* also has only one. However, the *C. elegans* kinase belongs to the TK1 type family and has no homology to the multisubstrate insect dNK's and the other non-TK1-like kinases. Like human TK1 (HuTK1) *C. elegans* thymidine kinase (*Ce*TK1) uses thymidine as its preferred substrate, and it also displays a low capacity to phosphorylate deoxyguanosine (with an estimated specificity of 81.7 $M^{-1}s^{-1}$, see Table 1).[10]

The structure of HuTK1 has been shown to fundamentally differ from other human deoxynucleoside kinases. It has been crystallized with the feedback inhibitor dTTP[3,11] and with the bisubstrate inhibitor P1-(5′-adenosyl)P4-(5′-(2′-deoxy-thymidyl)) tetraphosphate (TP4A).[12] The latter is bound in the deoxynucleoside part of the active site which is located between the α/β-domain and the lasso domain. The base and sugar moiety of dTTP is buried in the interior of the protein between the two domains while the phosphates extend into the p-loop of the α/β-domain. In other dNK's the thymine base is stabilized by different side chain interactions, and the variability of the side chains lead to different substrate specificities in the non-TK1-like deoxynucleoside kinases.[13,14] In HuTK1 the thymine base is stabilized by main chain interactions along the edge of the ring, explaining the narrow substrate range of TK1-like enzymes.

With the exception of the N- and C-terminal regions *Ce*TK1 is similar in sequence to HuTK1 with 43% amino acid identity and 63% similarity.[10] Despite the similarity *Ce*TK1 is a dimer also in presence of ATP, as determined by gel filtration at concentrations of

250 nM or lower. In contrast, HuTK1 at the same concentrations occurs as a tetramer when eluted in the presence of ATP and a dimer in the absence of ATP. The tetramer has a low Km (0.5 μM) and the dimer has a high Km (15-17 μM) but both forms have the same k_{cat}.[10,15,16]

A 3D model of *Ce*TK1 was constructed with the SWISS-MODEL Protein Modelling Server[17-19] based on a crystal structure of HuTK1 (PDB ID: **1XBT**) (Figure 1). The modelled structure shows that the majority of the amino acids surrounding the dTTP molecule are identical in the two enzymes. One exception is Thr163 in HuTK1 which is a Ser182 in *Ce*TK1. Thymidine kinase from Vaccinia virus also have a Ser in this position, and unlike HuTK1 it is known to accept (south)methanocarbathymidine as a substrate.[11] Considering this and since Thr163 is the only apparent difference between the deoxynucleoside binding sites of the two enzymes, the significance of Thr163/Ser182 and some of the nearby amino acids was investigated in order to elucidate the effect on substrate specificity.

In HuTK1 Thr163 is part of an otherwise hydrophobic pocket around the methyl group of thymine. Besides from Thr163 the methyl group is surrounded by Leu124, Tyr181 and Met28. The latter is also in close proximity to the 5'-oxygen of the ribose moiety where it stabilizes the position of the oxygen forcing it into proximity of Glu98. The Glu98 carboxy group is believed to act as the base that abstracts a proton from the deoxyribose 5'-OH leading the 5'-oxygen to act as a nucleophile in the phosphor transfer reaction.[3,11]

(Figure 1)

Drosophila melanogaster dNK (*Dm*dNK) has been the subject of intensive mutation studies. Random mutagenesis has led to a mutant kinase with increased specificity towards the antiviral nucleoside analogue AZT[20,21], and site directed mutagenesis has revealed details about *Dm*dNK catalytic function and substrate specificity.[22,23] Here we present the first active site structure-function study of TK1-type enzymes.

A detailed comparison of the active site of the two TK1 enzymes presented in this study will provide an increased understanding of the substrate specificity of TK1, and that could help the development of new and more efficient nucleoside analogues. It also opens up possibilities of creating new mutated HuTK1 enzymes with increased nucleoside analogue specificity that could be used in suicide gene therapy. The advantage of using a mutated human kinase over foreign kinases like HSV1TK or *Dm*dNK is avoiding antigenic response to foreign protein expression.

With the purpose of directing the substrate specificity from thymidine towards other deoxynucleosides and nucleoside analogues, the HuTK1 amino acids Thr163, Met28 and Leu124 and the corresponding *Ce*TK1 amino acids, Ser182, Met42 and Leu143, were subjected to one or more mutations using site-directed mutagenesis. In order to facilitate crystallization of HuTK1 the 41 or 40 C-terminal amino acids were removed.[3,11] Removal of 41 amino acids (HuTK1-CΔ41, named HuTK1-CΔ40 in Zhu *et al*., 2006) has also been shown to increase the stability of the kinase compared to the untruncated enzyme.[24] However, a similar truncation in *Ce*TK1 has been proven to

destabilize the enzyme,[10] and therefore all HuTK1 mutants are made on HuTK1-CΔ41, and all *Ce*TK1 mutants are made on *Ce*TK1-WT.

The mutated TK1 genes were expressed in *E. coli* as glutathione transferase tagged enzymes which are purified by glutathione sepharose chromatography. The purified enzymes are tested for activity with 100 μM of the natural substrates, dThd, dGuo, deoxycytidine (dCyd), and deoxyadenosine (dAdo) and the two nucleoside analogues AZT and AraC. Kinetic parameters were determined for all enzymes with dThd and for those enzyme/substrate combinations where the activities were no more than 3000-fold lower than the activity with dThd. None of the kinases displayed activity with AraC but a few showed low dGuo and dCyd activity (Table 1). One promising candidate, HuTK1-T163S, with improved activity towards the nucleoside analogue AZT, was crystallized in order to understand the structural basis of the improved AZT specificity.

(Table 1)

HuTK1-M28 and *Ce*TK1-M42

Met28 in HuTK1 corresponds to Met42 in *Ce*TK1. The methionine is positioned at the side of the thymine ring with the tip of the amino acid side chain above the 2'- and 3'-carbon of the deoxyribose and the sulphur pointing towards the 6-carbon atom of thymine at a distance of 3.8 Å. The mutation M28I results in an increased space above the deoxyribose but only a slight increase near the thymine base. The short branch of Ile extends towards the β-phosphate of dTTP in the structure and could possibly influence the phosphate transfer between ATP and dThd (Figure 1). In both HuTK1 and *Ce*TK1 the

mutation from Met to Ile has a negative impact on enzyme activity with dThd, affecting both K_m and k_{cat}. K_m is increased 250-fold relative to wild type for both mutated enzymes, and k_{cat} is reduced by 2- and 6-fold for *Ce*TK1 and HuTK1, respectively. Assuming that the catalytic or a preceding step is rate determining for the reaction of TK1-like kinases, as it is for *Dm*dNK (Browne, R., Andersen, G., Le, G., Munch-Petersen, B. & Grubmeyer, C., unpublished results), a change in k_{cat} can be interpreted as an effect on catalysis and a change in K_m as an effect on substrate binding. A lowered dThd activity is not unexpected for HuTK1-M28I and *Ce*TK1-M42I, since this particular Met is conserved in all TK1-like proteins, and this amino acid is believed to constrain the 5'-hydroxyl of thymidine into position near the catalytic Glu (Glu98 in HuTK1 and Glu117 in *Ce*TK1).[12] A spatial increase in this region will cause the 5'-hydroxyl group of ribose to move away from the putative catalytic residue which should affect k_{cat} the most. However, with M28I the effect on k_{cat} is minor whereas it is high on K_m. This may be caused by other steric changes of the enzyme-substrate contact.

The activity with AZT is even more reduced for the Ile mutants compared to the two wild types. This is likely due to the fact that Met28 and Met42 are positioned just above the 3'-azido group in AZT. The impact on k_{cat} is an 11-fold decrease for *Ce*TK1 and 15-fold for HuTK1, and for *Ce*TK1 the impact on K_m is an increase in the vicinity of 200-fold whereas it is approx. 500-fold for HuTK1. This reflects a strong negative effect on substrate binding and some effect on catalysis. Overall, the effect on catalytic efficiency (k_{cat}/K_m) is an approximately 2000-7000-fold reduction for both of the mutated enzymes.

*Ce*TK1-M42I also displayed some extent of activity with dCyd, and the kinetic parameters showed a very low k_{cat} but also a K_m that is 150- and 650-fold lower than

those for dThd and AZT, respectively. HuTK1-M28I did not display any activity with dCyd.

The mutation of Met28 to Ala in HuTK1 results in a larger open pocket above the ribose which can explain the decreased enzymatic activity with both dThd and AZT. The effect on K_m and k_{cat} is similar to that of M28I, indicating a stronger effect of this mutation on substrate binding than on catalysis, but it is slightly less destructive with respect to AZT phosphorylation than the M28I mutation.

HuTK1-L124 and *Ce*TK1-L143

Like Met28 amino acid Leu124 in HuTK1 (corresponding to Leu143 in *Ce*TK1) is positioned near the 6-carbon atom of thymine with a 3.7 Å distance, but Leu124 is located on the α/β-domain side above the thymine ring plane in proximity to the ring oxygen in the sugar moiety (3.8 Å). Mutation of Leu124 to Ala in HuTK1 results in an opening of the space on the α/β-domain side of dTTP above the thymine and the deoxyribose. The mutation leads to a 5-fold decrease in k_{cat} and a 25-fold increase in K_m with dThd, resulting in a 100-fold reduction in catalytic efficiency compared to wild type. k_{cat} for AZT is only slightly affected by the mutation but K_m is increased more than 50-fold so overall, the catalytic efficiency with AZT is lower in the L124A mutant than in wild type. This indicates that the mutation affects substrate binding more than catalysis of both dThd and AZT.

By introducing the same mutation L143A in *Ce*TK1 the space around the thymine ring becomes slightly larger than in HuTK1-L124A due to the presence of Ser182 in *Ce*TK1 (Thr163 in HuTK1) (Figure 1). With dThd as substrate the presence of an Ala instead of Leu results in a 190-fold decrease in k_{cat}/K_m due to a 150-fold increase in K_m and 1.3-fold decrease of k_{cat}. Hence, the decreased activity is mainly caused by a less efficient substrate binding. The strong effect on K_m also accounts for the nucleoside analogue AZT where the increase in K_m is so pronounced that complete saturation was not obtained. k_{cat}/K_m is therefore estimated from the linear slope of initial velocity vs. substrate concentration at low concentrations of substrate (the slope approaches k_{cat}/K_m when $[S]<<K_m$). The *Ce*TK1-L143A mutant displays over 1500-fold decrease in catalytic efficiency with AZT compared to wild type. Why the Leu to Ala mutation has such a drastic impact on AZT phosphorylation is unclear since the azido group of AZT is located at the opposite side of the active site. It is likely that the change from a large and bulky amino acid to the small Ala creates a space that is too large for proper positioning of the substrate and/or induces minor changes in other amino acids in the active site. Changes may occur around the 4th and 5th positions of the substrate base since *Ce*TK1-L143A has gained the ability to phosphorylate dCyd which differs from dThd in those positions. The k_{cat}/K_m with dCyd is, however, very low compared to that of dThd and AZT. Since none of the HuTK1 mutants are able to phosphorylate dCyd, this ability could be caused by the increased space near the 5-methyl of thymine that is occupied by a Ser in *Ce*TK1 (replaced by the slightly larger Thr in HuTK1) in combination with increased space around the sugar moiety and carbon 6 of thymine where Leu143 and Met42 are positioned in *Ce*TK1. The increased space leaves room for a slight shift in

substrate position that could provide space for the amino group of cytosine. Such a shift could also explain the poor catalysis with dCyd since it would likely affect the position of the 5'-oxygen that receives the phosphate upon catalysis. Met42 and Leu143 (Met28 and Leu124 in HuTK1) are both in position to keep the 5'-oxygen in close proximity to the catalytic glutamate (Glu98 in HuTK1) but mutation of those residues to shorter amino acids will leave the oxygen more flexible. In order to fit dCyd into the active site the 5'-oxygen will likely be moved further away from the catalytic glutamate, resulting in poor catalysis which is reflected by the decreased k_{cat} values with dCyd for *Ce*TK1-M42I. *Ce*TK1-L143A also displays high K_m, suggesting poor binding of dCyd. Since dThd fits into the active site pocket, the 5'-oxygen of the deoxyribose is not shifted away from the catalytic glutamate, and the deleterious effect on activity is likely due to poor substrate binding as reflected by increased K_m values with dThd for both *Ce*TK1-M42I and *Ce*TK1-L143A.

***Ce*TK1-S182**

In the modeled structure of *Ce*TK1 amino acid Ser182 is positioned on the side of the base ring plane pointing Cβ towards the 5-methyl group of thymine at a distance of 3.5 Å. In HuTK1 the amino acid in the corresponding location is the slightly larger Thr163. Since this is the only amino acid around the thymidine binding site that differs between the two enzymes, Ser182 in *Ce*TK1 was mutated to Thr in order to mimic the HuTK1 active site. Mutating Ser to Thr reduced the space around the 5-methyl group of thymine.

In order to elucidate the effect of increased space in this area Ser was also mutated to the smaller residue Ala.

The S182T mutation results in a minor decrease of K_m for dThd from 2.3 µM in *Ce*TK1-WT to 1.3 µM. However, k_{cat} for S182T is more decreased (about 7-fold), resulting in a catalytic efficiency that is 3-4-fold lower compared to *Ce*TK1-WT.
With AZT the catalytic efficiency is also reduced compared to wild type. The 8-fold decrease in k_{cat}/K_m is mainly due to a 6-fold decrease in k_{cat}, suggesting that the mutation affected the turnover of AZT and dThd into products more than substrate binding.

The S182T mutant is able to phosphorylate dGuo with higher catalytic efficiency than *Ce*TK1-WT. Due to the limited solubility of dGuo and high K_m values with both enzymes it was not possible to obtain saturating dGuo concentrations. Therefore, k_{cat}/K_m was estimated as a single parameter from the linear slope at low concentrations of dGuo (Table 1).

Ser182 was also mutated to Ala, and this yielded an enzyme that had even more reduced activity with dThd than S182T. The catalytic efficiency was reduced nearly 300-fold compared to wild type but unlike S182T, this reduction was not only due to a 9-fold decrease in k_{cat} but also a 30-fold increase in K_m. The S182A mutation appears to have a larger impact on substrate binding whereas the S182T mutation mainly affects the turnover of dThd. The same picture accounts for AZT. The S182T mutation mainly affects AZT turnover as reflected by a decrease in k_{cat} whereas *Ce*TK1-S182A has 30-fold increased K_m with AZT compared to wild type reflecting a marked impact on

substrate binding. A 16-fold decrease in k_{cat} is also observed for *Ce*TK1-S182A with AZT, indicating that the mutation also affects AZT turnover.

*Ce*TK1-S182A also phosphorylates dGuo but with a specificity lower than for the *Ce*TK1-WT and S182T. Hence, the additional space created by introducing the small amino acid Ala does not improve the activity with dGuo. However, a reduction of space resulting from the introduction of Thr instead of Ser gives rise to a small increase in catalytic efficiency with dGuo, making S182T the best dGuo phosphorylating enzyme presented here.

The reason for the loss of activity of the S182A mutant with all substrates is most likely to be found in the loss of a hydrogen bond between Ser182 and the main chain nitrogen of Met42 (figure 1). The loss of this hydrogen bond may destabilize the binding pocket and lead to poorer binding as reflected by the large impact on K_m values for the S182A mutant.

Crystal structure and activity parameters of HuTK1-T163S

Mutation of Thr163 to Ser in HuTK1 results in mimicking the active site of *Ce*TK1 since the amino acid composition around the phosphate acceptor in *Ce*TK1 only differs from HuTK1 by having a Ser in this position (Ser182). T163S displays a decrease in activity with dThd compared to wild type HuTK1 reflected by a 3-fold decrease in k_{cat} and a large 40-fold increase in K_m. With AZT the T163S-kinase displays a very low K_m value of only 0.43 μM, and k_{cat} is only reduced 2-3-fold compared to wild type and the overall catalytic efficiency for AZT has only decreased 2-fold. Most importantly, what distinguishes this mutant from all the other kinases presented is the AZT/dThd catalytic efficiency ratio.

Since the nucleoside analogue competes with dThd inside cells, this ratio is of major importance to the efficiency of the thymidine kinase as a suicide enzyme when used in conjunction with AZT. T163S is the only enzyme that displays a higher k_{cat}/K_m with the nucleoside analogue AZT than with dThd. For the wild type kinase the catalytic efficiency is nearly the same for AZT and dThd but for T163S the AZT/dThd ratio is 70. The increased activity is due to the 140-fold lower K_m with AZT compared to dThd.

The C-terminally truncated HuTK1-T163S has been crystallized in complex with the feedback inhibitor dTTP and the structure was solved with X-ray crystallography to 2.2 Å resolution with R and R_{free} being 16.7% and 21.8%, respectively (Table 2). Like the previously crystallized HuTK1 (PDB ID: **1XBT**) the T163S crystals contain two tetramers in the asymmetric unit but the unit cell dimensions are different due to a shift in the position of the two tetramers relative to one another. Due to flexible parts none of the subunits display electron density before amino acid no. 18 and after amino acid 192. Density is also absent for the loop between amino acid 64 and 73. These are the same regions lacking electron density in the 1XBT structure of HuTK1.

(Table 2)

Superposition of the T163S mutant and the wild-type HuTK1 structures revealed an rmsd of 0.21 $Å^2$ and 0.26 $Å^2$ over 642 Cα for the tetramers consisting of poly peptide chains A-D and E-H respectively. Hence, the overall structural fold is not affected by the T163S mutation. However, the position of the ligand is different in the presented structure. In the

wild-type structure published by Welin *et al*. in 2004 the three phosphates form an arch with a Mg^{2+} ion positioned beside it (PDB ID: **1XBT**). In another wild type structure (PDB ID: **1W4R**) published shortly thereafter, two different conformations of dTTP were present with an occupation ratio of 60/40 in all binding sites (Birringer *et al*., 2005). The dominant binding mode is identical to the dTTP binding described in the paper by Welin and co-workers.[3]

The structure of T163S also displays two different conformations of dTTP. One is the conformation reported by Welin *et al*, and the other has the β-phosphate in place of the magnesium ion and a water molecule in place of the β-phosphate (Figure 2a and 2b). In the present T163S structures the occupation ratio is 75/25. In three of the sites the dominant mode is the same as in the structure from 2004 by Welin *et al*., and a magnesium ion has been assigned to this conformation. In the remaining five subunits the situation is reverse but no magnesium ion could be assigned for this mode. In the three subunits containing magnesium in the active site the position of Arg60 is stable and the amino acid has hydrogen bonds to the 5'-oxygen and to an oxygen atom in the β-phosphate. In the remaining five subunits the same Arg60 is very flexible and has no hydrogen bonds to dTTP (compare figure 2a and 2b).

(figure 2)

By superposing the wild type and T163S structures, it is evident that the replacement of Thr163 by Ser does not have any major impact on the position of the amino acid in the

active site compared to the wild-type but only leaves a little more room at the 5-methyl group of the thymine ring and some minor changes in amino acids around the phosphates (Figure 2c). Only one amino acid, Arg60, appears to have different orientations in the two structures but that is likely due to a more disordered binding of dTTP in the T163S-mutant structure.

The primary reason for the improved AZT/dThd ratio in catalytic efficiency for T163S is the 40-fold increased K_m for dThd. There is no strong evidence from the structure as to what causes this increased K_m, since dTTP binds very similarly in the wild type and the T163S-mutant structures. It is, however, very possible that the change from Thr to the slightly smaller Ser can affect the positioning of dThd even if it is not visible upon binding of dTTP. The positioning of dTTP is to a high degree stabilized by a network of hydrogen bonds around the phosphates which are not present upon binding of dThd. This gives a higher degree of freedom for dThd binding and hence, it is affected more easily by small amino acid changes in the hydrophobic pocket around the base. It is possible that the large azido group of AZT reduces the movement of the analogue in the active site and thereby serves to stabilize its position. That would explain why AZT activity is not affected by the amino acid change from Thr163 to Ser.

From this perspective one could argue that *Ce*TK1 should have the same low activity with dThd as the HuTK1-T163S mutant since the Thr to Ser substitution in HuTK1 mimics the amino acid composition in the *Ce*TK1 active site. But structural examination of nearby amino acids reveals that even though the amino acids around the thymine base are the same in *Ce*TK1 and HuTK1-T163S, the positions of some amino

acids are affected by differences in residues further away. The thymine base is sandwiched between the hydrophobic Tyr181 on one side and Phe101 and Phe133 on the other. These residues are identical in the two enzymes but the neighbouring residue to Phe133 is the small flexible Gly134 in HuTK1 and a large inflexible Pro in *Ce*TK1. This difference is likely to be a cause of a changed binding pocket in *Ce*TK1 which could explain why *Ce*TK1 and HuTK1-T163S behave differently with respect to thymidine affinity, and why HuTK1-T163S displays no activity with dGuo.

Summary

In summary, the majority of the mutations introduced around the hydrophobic pocket surrounding the thymine base have a negative impact on enzyme activity with both dThd and AZT but some also produce activity with dCyd or dGuo.

Mutation of Met28/42 to the more bulky Ile in HuTK1/*Ce*TK1 has a drastically negative impact on AZT phosphorylation which can be explained by its proximity to the 3'-azido group. In *Ce*TK1 the mutations M42I or L143A produce activity with dCyd but the same mutations in HuTK1 (M28I and L124A) do not give rise to dCyd activity. dCyd and dThd differ around the 4th and 5th positions of the base which is near S182 in *Ce*TK1 and T163 in HuTK1. It is likely that dCyd can only bind to the two *Ce*TK1-M42I and *Ce*TK1-L143A mutants because the amino acid near the 5 position of the base is the small Ser182 (Thr163 in HuTK1). In *Ce*TK1 this gives room for a shift in substrate position providing space for the amino group of dCyd. The shift could, however, affect the position of the 5'-oxygen and move it away from the catalytic Glu, explaining the inefficient catalysis.

*Ce*TK1-WT displays activity with dGuo but HuTK1-T163S, which has the same amino acids in the active site as *Ce*TK1-WT, shows no dGuo activity. This indicates that dGuo phosphorylation is caused by interactions by amino acids not directly surrounding the substrate base. Most likely, Pro153 in *Ce*TK1 (corresponds to Gly134 in HuTK1) changes the hydrophobic pocket surrounding the thymine base by twisting of Phe152. The corresponding Phe133 in HuTK1 is involved in sandwiching the thymine ring. An increase in space and the loss of a hydrogen bond between S182 and M42 caused by the S182A mutation in *Ce*TK1 reduces the dGuo activity. Unexpectedly, a decrease in space resulting from the S182T mutation increases the dGuo activity compared to the *Ce*TK1-wt. This may indicate that the binding pocket in *Ce*TK1-wt is slightly too big' for dGuo, reflecting the low catalytic efficiency. Introduction of a larger side chain it might lead to more favourable binding.

HuTK1 has nearly the same catalytic efficiency with dThd and AZT but mutating Ser163 to Thr results in an enzyme with 140-fold lower K_m with AZT compared to dThd and therefore an increase in the AZT/dThd ratio of catalytic efficiency by 70. This ratio is in part due to a decreased activity with dThd in T163S. The structure of the T163S mutant shows a dTTP that is bound in a less ordered manner than in the wild type structure but due to the extensive network of hydrogen bonds between dTTP and the active site residues, the minor Thr to Ser change has no visible effect on dTTP binding. dThd is smaller and binds with more degrees of freedom and could easily be influenced by the Thr163 to Ser mutation. Crystal structures with the T163S-mutant in complex with AZT or dThd would possibly reveal the structural background for the changed AZT specificity.

Acknowledgements

We thank Nils Egil Mikkelsen and Martin Welin for technical assistance with solving the crystal structure and Andrea Telatin and Stefano Angiari for assistance in the kinetic studies. Also thanks to Tomas Radivoyevitch for commenting critically on the manuscript. This work was supported by grants from the Danish Research Council.

References

1. Eriksson, S., Munch-Petersen, B., Johansson, K. & Eklund, H. (2002). Structure and function of cellular deoxyribonucleoside kinases. *CMLS, Cell. Mol. Life Sci.* **59**, 1327–1346

2. Piskur, J., Sandrini, M., Knecht, W. & Munch-Petersen, B. (2004). Animal deoxyribonucleoside kinases: 'forward' and 'retrograde' evolution of their substrate specificity. *FEBS Letters*. **560**, 3-6.

3. Welin, M., Kosinska, U., Mikkelsen, N. E., Carnrot, C., Zhu, C., Wang, L., Eriksson, S., Munch-Petersen, B. & Eklund, H. (2004). Structures of thymidine kinase 1 of human and mycoplasmic origin. *Proc. Natl. Acad. Sci. U S A*. **101**, 17970-17975.

4. El Omari, K., Solaroli, N., Karlsson, A., Balzarini, J. & Stammers, D. K. (2006) Structure of vaccinia virus thymidine kinase in complex with dTTP: insights for drug design. *BMC Struct Biol*. **6**, 22.

5. Thelander, L. & Reichard, P. (1979). Reduction of Ribonucleotides. *Ann. Rev. Biochem.* **48**, 133-158.

6. Shields AF, Grierson JR, Dohmen BM, Machulla HJ, Stayanoff JC, Lawhorn-Crews JM, Obradovich JE, Muzik O, Mangner TJ. (1998). Imaging proliferation in vivo with [F-18]FLT and positron emission tomography. *Nat. Med.* 1998 **4**, 1334-1336.

7. Schulz CA, Mehta MP, Badie B, McGinn CJ, Robins HI, Hayes L, Chappell R, Volkman J, Binger K, Arzoomanian R, Simon K, Alberti D, Feierabend C, Tutsch KD, Kunugi KA, Wilding G, Kinsella TJ. (2004). Continuous 28-day iododeoxyuridine infusion and hyperfractionated accelerated radiotherapy for malignant glioma: a phase I clinical study.
Int. J. Radiat. Oncol. Biol. Phys. **59**, 1107-1115.

8. Beltinger, C., Fulda, S., Kammertoens, T., Meyer, E., Uckert, W. & Debatin, K. M. (1999). Herpes simplex virus thymidine kinase/ganciclovir-induced apoptosis involves ligand-independent death receptor aggregation and activation of caspases. *Proc. Natl. Acad. Sci. U S A*. **96**, 8699-8704.

9. Goody, R. S., Müller, B. & Restle, T. (1991). Factors contributing to the inhibition of HIV reverse transcriptase by chain-terminating nucleotides in vitro and in vivo. *FEBS Lett. 291*, 1-5

10. Skovgaard, T. & Munch-Petersen, B. (2006). Purification and characterization of wild-type and mutant TK1-type kinases from *Caenorhabditis elegans*. *Nucleosides Nucleotides Nucleic Acids.* **25**, 1165-1169.

11. Birringer, M. S., Claus, M. T., Folkers, G., Kloer, D. P., Schulz, G. E. & Scapozza, L. (2005). Structure of a type II thymidine kinase with bound dTTP. *FEBS Lett.* **579**, 1376-1382.

12. Segura-Peña, D., Lutz, S., Monnerjahn, C., Konrad, M. & Lavie, A. (2007). Binding of ATP to TK1-like enzymes is associated with a conformational change in the quaternary structure. *J Mol Biol.* **369**, 129-141.

13. Johansson, K., Ramaswamy, S., Ljungcrantz, C., Knecht, W., Piskur, J., Munch-Petersen, B., Eriksson, S. & Eklund, H. (2001). Structural basis for substrate specificities of cellular deoxyribonucleoside kinases. *Nat Struct Biol*. **8**, 616-620.

14. Sabini, E., Ort, S., Monnerjahn, C., Konrad, M. & Lavie, A. (2003). Structure of human dCK suggests strategies to improve anticancer and antiviral therapy. *Nat Struct Biol.* **10**, 513-519.

15. Munch-Petersen, B., Tyrsted, G. & Cloos, L. (1993). Reversible ATP-dependent transition between two forms of human cytosolic thymidine kinase with different enzymatic properties. *J. Biol. Chem.* **268**, 15621-15625.

16. Munch-Petersen, B. (2009). Reversible tetramerization of human TK1 to the high catalytic efficient form is induced by pyrophosphate, in addition to tripolyphosphates, or high enzyme concentration. *FEBS Journal*. **276,** 571-580.

17. Schwede, T., Kopp, J., Guex, N. & Peitsch, M. C. (2003). SWISS-MODEL: An automated protein homology-modeling server. *Nucleic Acids Res.* **31**, 3381-3385.

18. Guex, N. & Peitsch, M. C. (1997). SWISS-MODEL and the Swiss-PdbViewer: an environment for comparative protein modelling. *Electrophoresis.* **18**, 2714-2723.

19. Peitsch, M. C. (1995). Protein modeling by E-mail. *Bio/Technology*. **13**, 658-660

20. Knecht W, Munch-Petersen B, Piskur J. (2000). Identification of residues involved in the specificity and regulation of the highly efficient multisubstrate deoxyribonucleoside kinase from Drosophila melanogaster. *J Mol Biol.*, **301**, 827-837.

21. Welin, M., Skovgaard, T., Knecht, W., Zhu, C., Berenstein, D., Munch-Petersen, B., Piskur, J. & Eklund, H. (2005). Structural basis for the changed substrate specificity of

Drosophila melanogaster deoxyribonucleoside kinase mutant N64D. *FEBS J.* **272**, 3733-3742.

22. Knecht W, Sandrini MP, Johansson K, Eklund H, Munch-Petersen B, Piskur J. (2002). A few amino acid substitutions can convert deoxyribonucleoside kinase specificity from pyrimidines to purines. *EMBO J.* **21**, 1873-1880.

23. Egeblad-Welin L, Sonntag Y, Eklund H, Munch-Petersen B. (2007). Functional studies of active-site mutants from Drosophila melanogaster deoxyribonucleoside kinase. Investigations of the putative catalytic glutamate-arginine pair and of residues responsible for substrate specificity. *FEBS J*., **274**, 1542-1551.

24. Zhu, C., Harlow, L. S., Berenstein, D., Munch-Petersen, S. & Munch-Petersen, B. (2006). Effect of C-terminal of human cytosolic thymidine kinase (TK1) on in vitro stability and enzymatic properties. *Nucleosides Nucleotides Nucleic Acids*. **25**, 1185-1188.

25. Kristensen, T. (1996) Ph.D. thesis (Roskilde University, Roskilde, Denmark), pp. 45–50.

26. Frederiksen, H., Berenstein, D. & Munch-Petersen, B. (2004). Effect of valine 106 on structure-function relation of cytosolic human thymidine kinase, Kinetic properties and

oligomerization pattern of nine substitution mutants of V106. *Eur. J. Biochem*. **271**, 2248-2256.

27. Bradford, M. M. (1976). A rapid and sensitive method for the quantitation of microgram quantities of protein utilizing the principle of protein-dye binding. *Anal Biochem.* **72**, 248-254.

28. Leslie, A. G. W. (1992). Recent changes to the MOSFLM package for processing film and image plate data. *Joint CCP4 and ESF-EACBM Newsletter*, 26.

29. Collaborative Computational Project, Number 4 (1994). The CCP4 suite: programs for protein crystallography. *Acta Crystallog. sect. D,* **50**, 760-763.

30. Emsley, P. & Cowtan, K. (2004). Coot: Model-building tools for molecular graphics. *Acta Crystallog. sect. D*. **60**, 2126-2132.

31. DeLano, W. L. (2002). The PyMOL Molecular Graphics System. *DeLano Scientific, San Carlos, CA, USA*. http://www.pymol.org.

Table 1. Kinetic parameters

Enzyme	Substrate	K_m or $K_{0.5}$ (μM) (n)	V_{max} (nmol min^{-1} mg^{-1})	k_{cat} (s^{-1})	k_{cat}/K_m (s^{-1} M^{-1})
HuTK1					
HuTK1-CΔ41	dThd [a]	1.4 ± 0.6	26600 ± 3080	9.5 ± 1.1	6.8×10^6
	AZT	0.52 ± 0.1	10000 ± 324	3.5 ±0.11	6.7×10^6
M28I	dThd	349 ± 29	4180 ± 155	1.5 ± 0.05	4.2×10^3
	AZT	254 ± 42	675 ± 31	0.24 ± 0.01	940
M28A	dThd	317 ± 54	4032 ± 236	1.4 ± 0.08	4.5×10^3
	AZT	204 ± 41	955 ± 50	0.34 ± 0.02	1.7×10^3
L124A	dThd	36 ± 3.9	5210 ± 175	1.8 ± 0.06	5.1×10^4
	AZT	33 ± 3.7	4060 ± 142	1.4 ± 0.05	4.4×10^4
T163S	dThd	59 ± 14	7720 ± 655	2.7 ± 0.23	4.6×10^4
	AZT	0.43 ± 0.1	3740 ± 291	1.3 ± 0.10	3.1×10^6
***Ce*TK1**					
Wild type	dThd	2.3 ± 0.2	12700 ± 256	6.4 ± 0.13	2.8×10^6
	dGuo [b]				82
	AZT	12 ± 1.8	18600 ± 495	9.3 ± 0.25	7.8×10^5
M42I	dThd	565 ± 94	5590 ± 410	2.8 ± 0.21	5.0×10^3
	dCyd	3.6 ± 0.8	0.34 ± 0.02	1.7×10^{-4} ± 8.2×10^{-6}	48
	AZT	2318 ± 460	1610 ± 209	0.81 ± 0.10	350
L143A	dThd	336 ± 76	9780 ± 723	4.9 ± 0.36	1.5×10^4
	dCyd [b]				1.9
	AZT [b]				490
S182A	dThd	74 ± 13	1470 ± 111	0.74 ± 0.06	1.0×10^4
	dGuo [b]				6.6
	AZT [c]	406 ± 51	1160 ± 49	0.58 ± 0.02	1.4×10^3
S182T	dThd	1.3 ± 0.2	1930 ± 67.6	0.97 ± 0.03	7.5×10^5
	dGuo [b]				230
	AZT	18 ± 2.9	3470 ± 152	1.5 ± 0.08	9.8×10^4

Kinetic parameters are based on 2-5 independent measurements and are presented with standard deviation on the plot. k_{cat} is determined using the theoretical molecular weight of

one monomer. a) From [24]. b) The specificity is estimated from the slope of a v_0 vs. [S] plot at [S]<<K_m. c) Parameters are based on a single measurement.

Construction of the expression plasmids pGEX-2T-*Ce*TK1 and pGEX-2T-HuTK1-CΔ41 has been described previously. [10,25,3] Mutations are introduced by site-directed mutagenesis using forward and reverse primers (designated F and R, respectively). For all *Ce*TK1 mutants, the following primers are used with the template pGEX-2T-*Ce*TK1: S182T-F: 5'-gc gga tcg caa gca aac ttc **a**ca ttc cgc agc-3'. S182T-R: 5'-gct gcg gaa tg**t** gaa gtt tgc ttg cga tcc gc-3'. S182A-F: 5'-gc gga tcg caa gca aac ttc **g**ca ttc cgc agc-3'. S182A-R: 5'-gct gcg gaa tg**c** gaa gtt tgc ttg cga tcc gc-3'. L143A-F: 5'-gct gca **gc**c aat gga aca ttc gag aga aag ccg ttc c-3'. L143A-R: 5'-g gaa cgg ctt tct ctc gaa tgt tcc att g**gc** tgc agc-3'. M42I-F: 5'-g ggg cca at**t** ttc agt ggc aaa acc acc g-3'. M42I-R: 5'-c ggt ggt ttt gcc act gaa **a**at tgg ccc c-3'. The template pGEX-2T-HuTK1-CΔ41, which is encoding a 41 C-terminal truncated version of HuTK1, is applied for all HuTK1 mutants in combination with the primers: T163S-F: 5'-gg gaa gcc gcc tat a**g**c aag agg ctc gg-3'. T163S-R: 5'-cc gag cct ctt g**c**t ata ggc ggc ttc cc-3'. T163A-F: 5'-gg gaa gcc gcc tat **g**cc aag agg ctc gg-3'. T163A-R: 5'-cc gag cct ctt gg**c** ata ggc ggc ttc cc-3'. L124A-F: 5'-cc gta att gtg gct gca **gc**g gat ggg acc ttc c-3'. L124A-R: 5'-g gaa ggt ccc atc c**gc** tgc agc cac aat tac gg-3'. M28I-F: 5'-g gtg att ctc ggg ccg at**c** ttc tca gga aaa agc-3'. M28I-R: 5'-gct ttt tcc tga gaa **g**at cgg ccc gag aat cac c-3'. M28A-F: 5'-g gtg att ctc ggg ccg **gc**g ttc tca gga aaa agc-3'. M28A-R: 5'-gct ttt tcc tga gaa c**gc** cgg ccc gag aat cac c-3'.

The mutated plasmids were transformed into XL10-Gold Supercompetent Cells and isolated, and the mutations were verified by sequencing at MWG Biotech in Martinsried, Germany.

The plasmids were then transformed into the expression host *E. coli* BL21, and after IPTG induction the bacteria were harvested when the thymidine kinase activity per mg total protein was at its highest. After expression the cells were disrupted by the French Press, and the proteins were purified by GST affinity chromatography with thrombin cleavage as previously described.[26] Purification quality was determined by SDS-PAGE, Experion Automated Gel electrophoresis and the Bradford method.[27]

HuTK1-CΔ41-T163S was purified on larger scale for crystallography and was subjected to additional purification steps. After GSH chromatography the protein was desalted on a G25 column with the elution buffer: 20 mM Tris pH 7.5, 5 mM $MgCl_2$, 5 mM NaF, 10 % glycerol, 0.5 mM CHAPS, 50 mM ε-amino capronic acid and 2 mM dithiotreitol, and purified on a CM cation exchange column. The column is equilibrated with 10 mM Potassium phosphate pH 6.0, 5 mM $MgCl_2$, 10 % glycerol, 0.1 % Triton X-100 and 2 mM dithiotreitol, and the protein is eluted with the same buffer, but 10 mM Potassium phosphate pH 6.0 is substituted with 50 mM Potassium phosphate pH 8.0.

Kinase activities were determined with tritium labelled substrates by the DE-81 filter paper assay.[26] Initial velocities were determined by three or four time samples at varying substrate concentrations. The standard assay conditions were: 50 mM Tris/HCl pH 7.5, 10 mM dithiotreitol, 2.5 mM $MgCl_2$, 0.5 mM CHAPS, 3 mM NaF, 0.5 mg ml^{-1} bovine serum albumin and 2.5 mM ATP.

Results were analyzed with GraphPad Prism by nonlinear regression to the Michaelis-Menten equation ($v = V_{max}\cdot[S]/(K_m + [S])$ or the Hill equation ($v = V_{max}\cdot[S]^n/(K_{0.5}{}^n + [S]^n)$. In all cases the Michaelis-Menten equation resulted in the best fit.

Table 2. Data collection and refinement statistics.

Source for data collection[1]	ESRF, ID23-1
Space group and unit cell	C2
a, Å	156.9
b, Å	123.3
c, Å	121.0
β, °	133.0
Content of the asymmetric unit	2 tetramers
Solvent content, %	43
Resolution, Å	2.2 (2.32-2.20)
Completeness, %	99.9 (99.9)
*R*merge, %	10.4 (36.7)
$I/\sigma I$	10.6 (3.4)
Redundancy	3.7 (3.7)
No. of observed reflections	310,674
No. of unique reflections	85,205
R, %	16.7
*R*free, %	21.8
rms deviation	
Bond length, Å	0.010
Bond angle, °	1.327
Mean *B* value, Å^2	21.1

[1]Data was collected at 100 K. Values in parentheses are for the outermost shell.

Crystals of HuTK1-Δ41-T163S were obtained at 15 ºC by hanging drop vapour diffusion after 3-5 days. The drops were a mixture of 2 µl protein solution (10 mg/ml in 50 mM KPO_4^{3-} pH 8.0, 2 mM DTT, 10% glycerol, 0.1% triton X-100, 5 mM $MgCl_2$ and 5 mM dTTP) and 2 µl precipitant (0.1 M Na citrate (pH 5.6), 20% 2-propanol, and 17% polyethylene glycol 4000). Before flash-freezing in liquid nitrogen the crystals were soaked in cryo-protectant consisting of precipitant containing 20% glycerol. The data set for HuTK1-Δ41-T163S in complex with dTTP was collected at beamline ID23-1 at ESRF in Grenoble, France. Data were indexed, scaled and merged with MOSFLM[28] and SCALA.[29] The structure was solved with molecular replacement with the program Molrep[29] using HuTK1-Δ41 as a search model (PDB: 1XBT) The model with waters was adjusted manually to the $2F_o$-F_c electron density in Coot[30] and refined with Refmac5.[29]

Figure 1. Comparison of the thymidine binding site in *Ce*TK1 and HuTK1. A model of *Ce*TK1 (cyan) is superposed with the crystal structure of HuTK1[3] (grey) with TTP and Mg^{2+} (light yellow-green) in the active site. The *Ce*TK1 structure model is built with the SWISS-MODEL Protein Modelling Server[17-19] with HuTK1 (PDB ID:1XBT) as a reference structure. Faded residues are deeper in the plane, and atoms in the residues are colored red (oxygen), blue (nitrogen), yellow (sulphur), orange (phosphorous) and grey or cyan (carbon). Hydrogen bonds are displayed for residues in HuTK1, and amino acid numbering is written as HuTK1/*Ce*TK1. Residues subjected to mutations, M28/42, L124/143 and T163/S182, are shown. These residues, together with Y181/200, form a snug hydrophobic pocket for the substrate's methyl group. The putative catalytic glutamine and other residues interacting with the thymine ring are also shown.

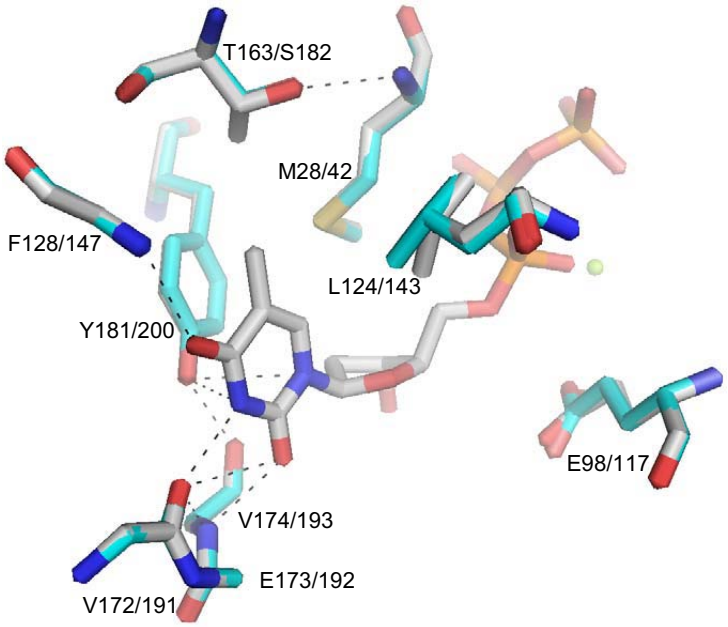

Figure 2. Protein-ligand interactions in the active site of HuTK1 structures. A and B: Active site of HuTK1-T163S with two conformations of TTP. Both conformations are present in all molecules with a ratio of approximately 75/25. Five subunits (chains A, B, C, E, F) favour the conformation in A and the remaining three subunits (chains D ,G ,H) the conformation in B. The green atom is Mg^{2+}. C: Superposition of HuTK1[3] (in black) and T163S. Hydrogen bonds between dTTP and Arg60 are shown as dark grey dotted lines. Superposition of Cα-atoms is performed in Coot. Figures are created in PyMOL.[31] Atoms are coloured as in figure 1.

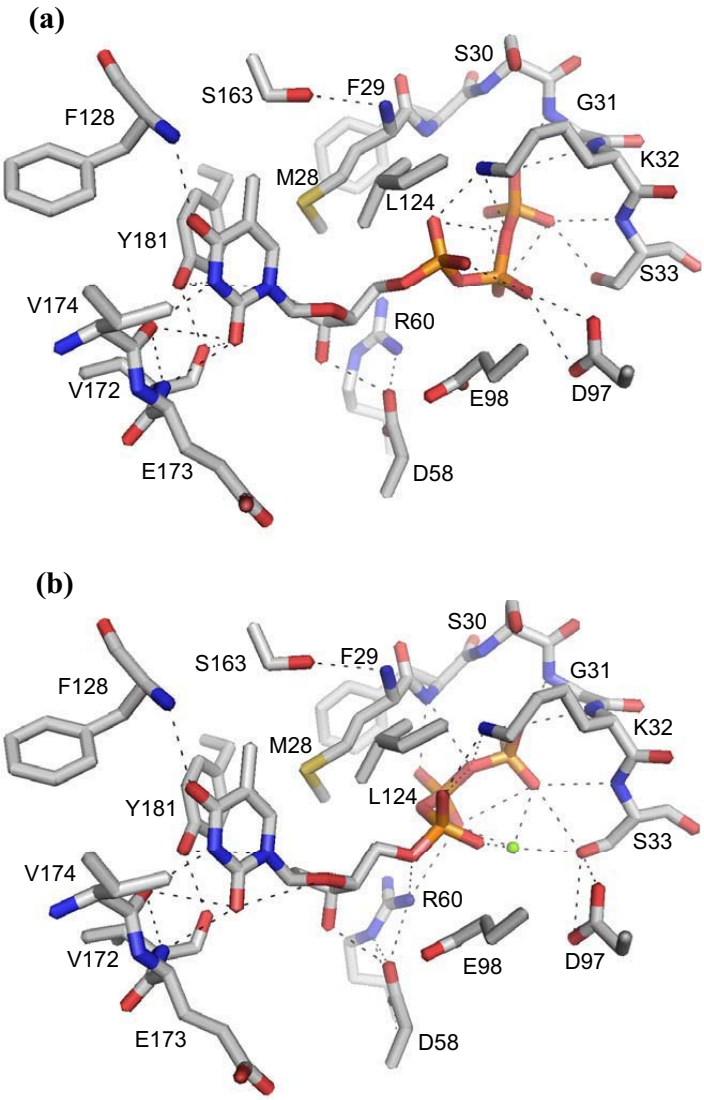

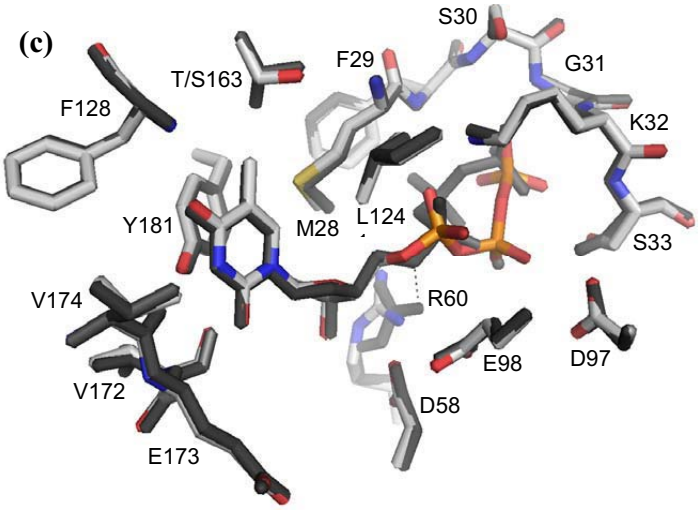
(c)
S30
F29
G31
T/S163
F128
K32
Y181
M28
L124
S33
V174
R60
E98
D97
V172
D58
E173

V

Osteosarcoma Cells Deficient for Mitochondrial DNA Increase their dNTP Pools after UV-Induced DNA Damage

T. Skovgaard, L. J. Rasmussen* and B. Munch-Petersen

Dept. of Science Systems and Models, Roskilde University, Roskilde, Denmark
*present address: Center for Healthy Aging, Department of Cellular and Molecular Medicine, University of Copenhagen, Copenhagen, Denmark

Abstract
Imbalanced dNTP pools are highly mutagenic due to a deleterious effect on DNA polymerase fidelity. One of many causes of cellular dNTP pools imbalance is mitochondrial DNA (mtDNA) deficiency, and mtDNA defects, including mutations and deletions, are commonly found in a wide variety of different cancer types.

In order to further study the interconnection between dNTP pools and mitochondrial function we have examined the effect of DNA damage on dNTP pools in human osteosarcoma cells deficient of the salvage enzyme thymidine kinase 1 (TK1) and mtDNA (143B-TK$^-$ ρ^0), and cells deficient for only TK1 (143B-TK$^-$) and normal cells (HOS). We show that DNA damage induced by UV-irradiation, in a dose corresponding to the cell's LD_{50} value, induces an S phase delay in all three cell lines. The UV pulse also has a destabilizing effect on the dNTP pools in cells deficient of mtDNA (ρ^0) but not in ρ^+ cells. In the 143B-TK$^-$ ρ^0 cells a 2.2-3.2-fold increase in all four deoxynucleotides is observed after UV-irradiation.
The mitochondrial genome is encoding 13 proteins in the electron transport chain, including 2 subunits of the ATP-synthase. As a result of this the ρ^0 cells have much lower ATP levels than ρ^+ cells. In order to mimic the ATP situation in 143B-TK$^-$ ρ^0 cells the 143B-TK$^-$ ρ^+ cells are incubated with the ATP synthase inhibitor, oligomycin. Similar to the ρ^0 cells the oligomycin incubated ρ^+ cells display increased dNTP pools upon UV-irradiation. At the time of irradiation the dATP levels are low in 143B-TK$^-$ ρ^0 cells and in oligomycin treated 143B-TK$^-$ ρ^+ cells compared to untreated ρ^+ cells, and it is suggested that the dNTP pools increase after DNA damage due to insufficient dATP feedback inhibition of ribonucleotide reductase.

Our data show that normal mitochondrial function is a prerequisite for retaining stable dNTP pools upon DNA damage. Therefore it is likely that mitochondrial deficiency defects may cause an increase in DNA mutations by disrupting dNTP pool balance.

Abbreviations: deoxynucleoside triphosphate (dNTP), thymidine kinase 1 (TK1), ribonucleotide reductase (RNR), deoxynucleoside kinase (dNK)

Introduction

Most of the proteins in human cells are encoded by nuclear DNA but a small fraction is encoded by the small circular mitochondrial genome (mtDNA): 2 rRNAs, 22 tRNAs and 13 proteins. All the mtDNA encoded proteins are subunits in four of the five large protein complexes in the electron transport chain responsible for oxidative phosphorylation. Hence, cells with dysfunctional mtDNA are highly dependent on glycolytic ATP production since oxidative phosphorylation is impaired. Dysfunctional mtDNA is believed to play a role in cancer development since mutations at various locations in mtDNA are found

in a wide range of different cancers (Penta *et al.*, 2001; Modica-Napolitano and Singh, 2004). The link between mtDNA dysfunction and cancer is still unknown but it was previously found that yeast cells lacking mtDNA showed an increased mutation frequency in nuclear DNA, and that human HeLa cells deficient of mtDNA (designated. ρ^0 cells) had a reduced ability to repair oxidative DNA damage (Rasmussen *et al.*, 2003; Delsite *et al.*, 2003). The increased mutation frequency in ρ^0 cells could be caused by either possible malfunctions in nuclear DNA repair pathways, or the mtDNA deficiency may result in increased DNA damage leading to mutations due to error-prone translesion synthesis. In two human cell lines mtDNA deficiency is shown to cause imbalanced dNTP pools (Desler *et al.*, 2007), and dNTP pool imbalance is believed to induce increased error-prone bypass of DNA lesions, especially if the nucleotide positioned 3' to the misincorporation is a nucleotide in excess (Meuth, 1989). The ρ^0 cells have two or more of the dNTP pools 2-6-fold reduced compared to the corresponding cells containing mtDNA (ρ^+). This imbalance in dNTP pools is suggested to cause DNA damage that promotes chromosomal translocations (Desler *et al.*, 2007). Both resting and dividing cells depend on balanced pools of deoxynucleoside triphosphates (dNTPs) in order to maintain DNA replication and repair. Apart from being a cause of chromosomal translocations, imbalanced dNTP pools is known to cause mutations, strand breaks and even cell death (Reichard, 1988).

dNTPs are produced via the *de novo* or the salvage pathways. In the *de novo* pathway the key enzyme, ribonucleotide reductase (RNR), is responsible for reducing nucleoside diphosphates (NDPs) to deoxynucleoside diphosphates (dNDPs). It is a tightly regulated enzyme consisting of two homodimeric proteins: The R2 subunit carries an iron centre that generates a tyrosyl free radical necessary for catalysis while the R1 subunit harbours the active site (Nordlund *et al.*, 1990; Uhlin & Eklund, 1994). In mammalian cells the tight cell cycle regulation of RNR includes specific S phase transcription of both genes encoding the R1 and R2 subunits (Björklund *et al.*, 1990) and degradation of the R2 subunit in late mitosis mediated by anaphase promoting complex/Cdh1 (Chabes *et al.*, 2003b). While the R2 protein only has a half-life of 3 hours (Eriksson *et al.*, 1984) the R1 subunit has a long half-life of 15 hours, and in proliferating cells it can be detected outside S phase (Engström *et al.*, 1985). The regulation of activity and substrate specificity is very complex and is mediated by binding of nucleoside triphosphates to allosteric sites in the R1 subunit (Thelander & Reichard, 1979; Eriksson *et al.*, 1979). ATP and dATP bind to the activity-regulating site functioning as on- and off-switches, respectively. The substrate specificity is regulated by binding of different dNTP in the specificity-regulating site which up- or down-regulates reduction of other NDPs.

The key enzymes in the salvage of deoxynucleosides for DNA synthesis are deoxynucleoside kinases (dNKs), catalyzing the first of three subsequent phosphorylations of deoxynucleosides (dNs) to dNTPs. Mammalia have four dNKs; thymidine kinase 1 (TK1) and deoxycytidine kinase (dCK) in the cytosol and deoxyguanosine kinase (dGK) and thymidine kinase 2 (TK2) in mitochondria. With the exception of TK1, the kinases are constitutively expressed. Like the R2 subunit of RNR, TK1 is targeted for degradation in late mitosis by the anaphase promoting complex/Cdh1 (Ke & Chang, 2004). As a result the dNTP pools in resting cells are maintained in part by the salvage enzymes, TK2, dGK and dCK, but low amounts of a second small subunit of RNR, the p53R2, were also found to exist throughout the cell cycle (Håkansson *et al.*, 2006). When resting cells were exposed to DNA damaging agents the demand for dNTPs increased and as a result of this, expression of R1 and p53R2 were induced (Tanaka *et al.*, 2000; Nakano *et al.*, 2000; Guittet *et al.*, 2001). Changes in dNTP pools have been measured in bacteria, yeast and mammalian cells after exposure to a variety of different mutagens, and the results with mammalian cells are found to vary between different studies (reviewed by Kunz & Kohalmi, 1991).

In logarithmically growing budding yeast a 7-fold increase in dNTP pools was observed upon addition of the UV mimetic 4-nitroquinoline-N-oxide (4-NQO) (Chabes *et al.*, 2003a), and by 4-NQO treatment of *Schizosaccharomyces pombe* cells a 2-fold increase in dNTP pools was observed (Håkansson *et al.*, 2005). However, UV-irradiation of mouse fibroblasts did not have any effect on dNTP pools (Håkansson *et al.*, 2006). This is likely due to the fact that yeast and mammalian cells have different regulation mechanisms for RNR.

The purpose of this study is to examine the role of thymidine kinase 1 and the importance of having a functional mitochondria in cells subjected to DNA damage. We demonstrated previously that osteosarcoma cells deficient for thymidine kinase 1 displayed increased survival rate in response to UV-induced DNA damage compared to thymidine kinase positive cells (Skovgaard *et al.*, submitted for publication). The TK negative cells had low dTTP pools compared to the TK positive cells, and we suggested that the increased survival rate was caused by increased levels of thymidine in the TK1 deficient cells absorbing part of the UV rays.

Here we demonstrate that, similar to the results obtained with mouse fibroblasts in the study by Håkansson *et al.*, (2006), human osteosarcoma cells, HOS, do not increase their dNTP pools after DNA damage with 254 nm UV light, and neither does the thymidine kinase negative cell line 143B-TK$^-$. If the 143B-TK$^-$ cells are deficient of mtDNA, however, they display a 2-3-fold increase of all four dNTP pools. We suggest that the low dATP levels found in ρ^0 cells are responsible for the increased dNTP pools since the cells are unable to sustain sufficient dATP feedback inhibition of RNR when RNR protein is up-regulated after DNA damage. We also suggest that the increased dNTP pools in ρ^0 cells are the cause of the mutator phenotype observed by Desler et al (2007) due to increased error-prone translesion DNA synthesis.

Results

Thymidine Kinase Negative Cells have Low dTTP Pools and mtDNA Deficient Cells have Low dATP Pools

In a recent study we found that HOS and 143B-TK$^-$ cells differ in their sensitivity to UV light as reflected by LD_{50} values of 4 J/m^2 and 8 J/m^2, respectively (Skovgaard *et al.*, submitted for publication). Applying the same method, we determine the LD_{50} for 143B-TK$^-$ ρ^0 cells to be 8 J/m^2, showing that there is no difference in survival rate between 143B-TK$^-$ ρ^+ and 143B-TK$^-$ ρ^0. At LD_{50} the UV-irradiation should inflict a significant amount of DNA damage without killing all the cells and hence, the LD_{50} values, 4 J/m^2 for HOS and 8 J/m^2 for the two 143B-TK$^-$ cell lines, are applied in all subsequent experiments involving UV-irradiation.

The cells are irradiated with one pulse of UV. At the time of irradiation and every 6 hours until 30 hours after irradiation cells are harvested, and cell size, cell cycle distribution and dNTP levels are measured. As seen in figure 1A the initial dNTP pools vary between the three cell lines. The 143B-TK$^-$ ρ^+ and ρ^- cell lines display 2-3-fold lower dTTP pools than the TK positive cell line HOS. The dCTP and dGTP pools are very similar in all three cell lines but the dATP pool in 143B-TK$^-$ ρ^0 cells is less than half of the dATP pool in HOS (ρ^+) and 143B-TK$^-$ ρ^+ cells.

Due to the S phase specific activity of RNR and TK1, dNTP pools are higher in S phase cells than in non-proliferating cells. Cell cycle analysis shows that only 36 % of the ρ^0 cells are in S phase due to the slower growth of those cells compared to the two ρ^+ cell lines having approx. 43 % cells in S phase (figure 2). In order to ensure that the differences observed in dNTP pools are not due to a difference in

number of S phase cells, the dNTP pools are normalized to the number of S-phase cells (figure 1B). This did not change the pattern.

These results show that thymidine kinase 1 is important for maintaining cellular dTTP pools and that dysfunctional mitochondria relying solely on glycolytic ATP production lead to a decrease in dATP pools.

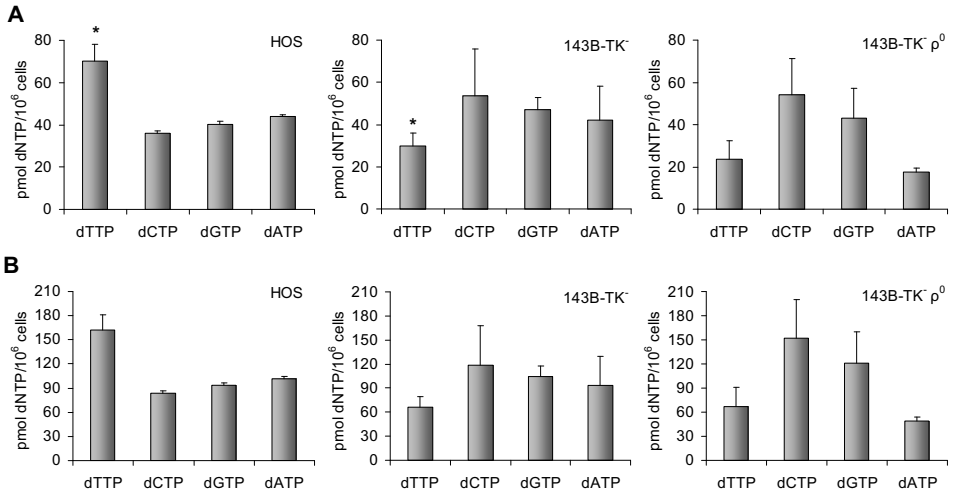

Figure 1. Initial dNTP pools at the time of DNA damage in logarithmically growing osteosarcoma cells.
A: dNTP pools were measured in cells harvested immediately after UV-irradiation with a single pulse corresponding to the cells LD50 from a 254 nm 20 μW/cm^2 UV source. Error bars are ±S.D. of two independent measurements. * From (Skovgaard *et al.*, submitted for publication) B: Results from A normalized to the number of cells in S-phase.

Cells Arrest in S phase after UV-Irradiation in all Three Osteosarcoma Cell Lines

High levels of DNA damage are known to cause cell cycle arrest but irradiation of mouse fibroblasts with a single pulse of 10 J/m^2 UV light has previously been found to have nearly no effect on cell cycle distribution and dNTP levels (Håkansson *et al.*, 2006). Here we examine the cell cycle distribution in the cell lines, HOS, 143B-TK$^-$ and 143B-TK ρ^0 following UV-irradiation with a dose corresponding to the cell's LD_{50} value. The cell cycle distribution is also examined in non-irradiated cells during the entire time span of the experiment.

The dNTP pools change with the number of cells in S phase (Rampazzo *et al.*, 2004), and the percentage of S phase cells changes with the confluence of the cells. When the cells start growing too densely the number of cells in S phase will decrease. In all experiments but cell survival determination the cells are set up in large petri dishes so that they are never more than 80-90 % confluent. This way they always have the same cell cycle distribution during the time span of the experiment if left undisturbed. In order to confirm the stability of cell cycle distribution and dNTP pools, 143B-TK$^-$ cells were followed for five days after seeding. They grew logarithmically and had approximately the same percentage of cells in S phase on day two, three and four (42.2±0.9 on day two and 40.3±0.4 on day

four; ±S.D. n=2). All four dNTP pools measured on day three and four were also the same within standard deviations (not shown), and only started do decline slightly on day five as the percentage of S phase cells decreased to 38.3±0.9 (n=2).

The cells are irradiated 2 to 3 days after they have been seeded, and for every 6 hours after UV-irradiation the cell cycle distribution was determined by flow cytometry. In all three cell lines the cell cycle changed dramatically following UV-irradiation (figure 2). The cells accumulate in S phase and are subsequently released into G2/M phase after approximately 18 hours. The HOS cells progress from S phase to G2/M phase slightly faster than the two TK$^-$ cell lines and the 143B-TK$^-$ ρ^0 cells slightly faster than the two ρ^+ cell lines which corresponds well with their growth rate. After 30 hours the cells have achieved or nearly achieved the initial cell cycle distribution.

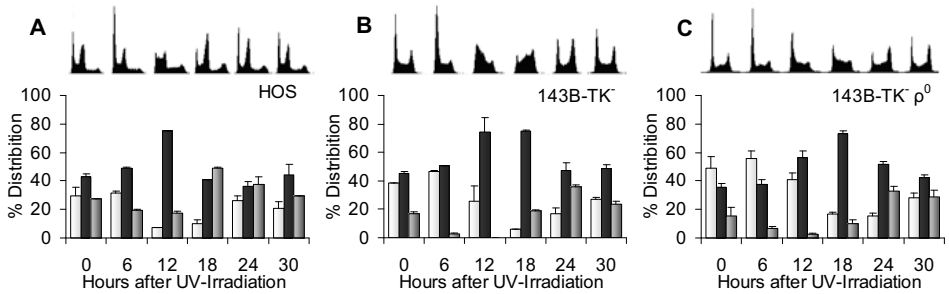

Figure 2. Logarithmically growing osteosarcoma cells enter S-phase arrest after UV-induced DNA damage.
The cell cycle distribution is measured in HOS (A), 143B-TK$^-$ (B) and 143B-TK$^-$ ρ^0 (C) cells by flow cytometry every 6 hours after a single pulse of UV-irradiation corresponding to the cells' LD_{50} (254nm, 20 μW/cm^2 UV source). G_0/G_1 phase cells: white bars, S phase cells: black bars and G_2/M phase cells: grey bars. The error bars show ±S.D. of two independent measurements.

mtDNA Deficient Cells Increase their dNTP Pools after DNA Damage

The cellular dNTP pools are determined with 6 hour intervals over a 30 hour time course after UV-irradiation.

Despite the changes in cell cycle distribution none of the two ρ^+ cell lines, HOS and 143B-TK$^-$, show any changes in dNTP pools (figure 3A and 3B) which is in agreement with the results obtained for UV-irradiated mouse fibroblasts (Håkansson *et al.*, 2006). However, during the 30 hour time course the 143B-TK$^-$ ρ^0 cells display an increase of all four dNTPs (figure 4C). The two pools that were initially the lowest (figure 1A), dTTP and dATP, display the highest relative increase (3.2- and 3.0-fold, respectively), and dCTP and dGTP a lesser increase (2.2- and 2.4-fold, respectively).

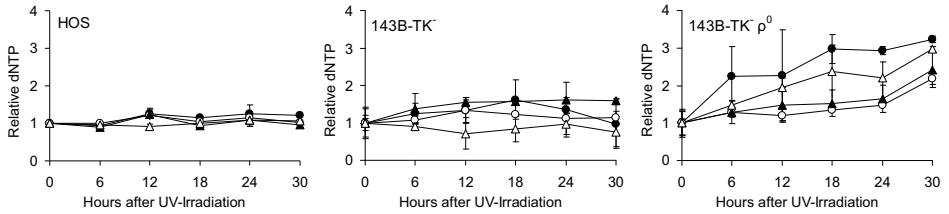

Figure 3. dNTP pools increase in ρ^0 cells after DNA damage.
Intracellular dNTP pools are measured in logarithmically growing HOS (A), 143B-TK$^-$ (B) and 143B-TK$^-$ ρ^0 (C) cells every 6 hours after UV-irradiation (254nm, 20 μW/cm^2) with a dose corresponding to the LD_{50} of the respective cell lines. (●) dTTP, (○) dCTP, (▲) dGTP and (Δ) dATP. The error bars show ±S.D. of two independent measurements.

Inhibition of ATP Synthase Lowers the ATP Level but all Cell Lines Increase their ATP levels after DNA Damage

ρ^0 cells are deficient for four of the five protein complexes involved in ATP production from oxidative phosphorylation and have previously been shown to have lower ATP levels than ρ^+ cells (Desler *et al.*, 2007). In ρ^+ cells ATP is synthesized from ADP by the last complex in the electron transport chain, ATP synthase, which is driven by the proton gradient across the inner mitochondrial membrane. In order to test if the increased dNTP pools in 143B-TK$^-$ ρ^0 cells are an effect of deficient electron transport chain, the ATP synthase in 143B-TK$^-$ ρ^+ cells is inhibited with oligomycin.

Using a luciferase-based assay, the ATP levels are measured in all three UV-irradiated cell lines at the time of DNA damage and 30 hours after damage. Furthermore, 143B-TK$^-$ ρ^+ cells are exposed to 0.25 μg/ml oligomycin for 24 hours prior to DNA damage and like unexposed cells, ATP levels are measured at the time of damage and 30 hours later (oligomycin is present in the media until harvest). Control cells are exposed to oligomycin without UV-irradiation for the same periods of time (24 hours and 54 hours).

As expected, the 143B-TK$^-$ ρ^0 cells have much lower initial ATP levels than either of the two ρ^+ cell lines since they rely solely on glycolytic ATP production (figure 4, grey bars). They only have 0.8±0.2 nmol ATP/10^6 cells whereas the ρ^+ cells, 143B-TK$^-$ and HOS, have 4.9±0.5 and 2.7±0.2 nmol ATP/10^6 cells, respectively. Addition of the ATP synthase inhibitor oligomycin reduces the ATP level in 143B-TK$^-$ ρ^+ cells to 0.9±0.2 nmol ATP/10^6 cells which is nearly the same as in 143B-TK$^-$ ρ^0 cells. The oligomycin-treated 143B-TK$^-$ ρ^+ control cells that are not subjected to UV-irradiation have approx. the same ATP levels (1.2±0.4 nmol ATP/10^6 cells) as the 143B-TK$^-$ ρ^+ cells irradiated immediately before harvest, proving that the ATP pools do not change immediately after DNA damage.

30 hours after UV-irradiation the ATP levels increase for all cells except for the non-irradiated oligomycin-treated control 143B-TK$^-$ ρ^+ cells. The lowest increase in ATP levels was observed in HOS (ρ^+) and 143B-TK$^-$ (ρ^+) cells where the ATP level increased 2.1-fold and 1.7-fold, respectively. Despite the lack of oxidative phosphorylation, the 143B-TK$^-$ ρ^0 cells and oligomycin treated 143B-TK$^-$ ρ^+ cells, having the lowest initial levels of ATP, showed the highest fold increase of 2.6 and 3.3, respectively. This suggests that glycolytic ATP up-regulation is very efficient in ρ^0 cells when the cells are damaged.

The cell size is also affected by oligomycin treatment. Using a Beckmann Coulter Counter the cell diameter of HOS, 143B-TK$^-$ ρ^+ and 143B-TK$^-$ ρ^0 cells was measured to be 16.6±0.9 μm, 16.7±1.2 μm

and 16.3±1.2 µm, respectively (n=12, ±S.D.), while it is 20.1±0.7 µm (n=6, ±S.D.) in oligomycin treated 143B-TK$^-$ ρ$^+$ cells. The cell diameter did not change significantly during the 30 hours after UV-irradiation and hence, the presented cell sizes are the average values of all time samples for each cell line. If the ATP levels presented as nmol ATP/10^6 cells are converted into cellular ATP concentrations, the slightly larger cell size of oligomycin-treated 143B-TK$^-$ ρ$^+$ cells results in ATP concentrations approximately 20 % lower compared to the 143B-TK$^-$ ρ^0 cells.

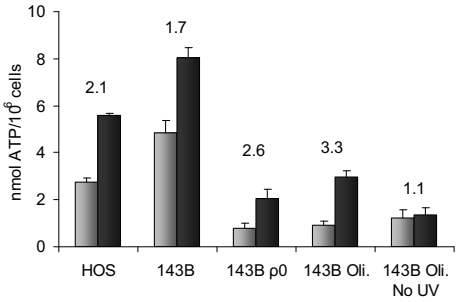

Figure 4. ATP levels are low in ρ^0 cells and in oligomycin-treated cells.
Intracellular ATP levels measured immediately after (grey bars) and 30 hours after (black bars) UV-irradiation with a single pulse of 254 nm 20 µW/cm^2 UV light corresponding to the LD_{50} of the respective cell lines. The error bars indicate the S.D. of two independent measurements, and the numbers indicate the fold difference between samples measured immediately after and 30 hours after irradiation. 143B-TK$^-$ is abbreviated 143B, and oligomycin is abbreviated Oli.

Inhibition of ATP Synthase in ρ$^+$ Cells Reduces all Four dNTP Pools and Causes Them to Increase after DNA Damage

Initial dNTP pools were also determined for the oligomycin-treated and UV-irradiated 143B-TK$^-$ ρ$^+$ cells (figure 5, grey bars), and by comparing those to the dNTP pools in figure 1 it is evident that they differ significantly from the pool levels in both untreated 143B-TK$^-$ ρ$^+$ and 143B-TK$^-$ ρ^0 cells. All four dNTPs are drastically reduced in the 143B-TK$^-$ ρ$^+$ oligomycin-treated cells, and even dTTP, which is low in both 143B-TK$^-$ cell lines, and dATP, which is only low in 143B-TK$^-$ ρ^0 cells, are reduced even further in the oligomycin-treated 143B-TK$^-$ ρ$^+$ cells. Initial levels of all four dNTPs in oligomycin-treated cells are in the range of 8-17 pmol/10^6 cells.

In figure 3 the 143B-TK$^-$ ρ^0 cells are distinguished from the two ρ$^+$ cell lines by their increase in dNTP pools varying from 2.2-fold to 3.2-fold after 30 hours, and the dNTP pools in oligomycin treated cells display similar fold changes (numbers over bars in figure 5A). Non-irradiated 143B-TK$^-$ ρ$^+$ control cells exposed to oligomycin show no changes in dNTP pools (figure 5B) but have the same low dNTP levels as 143B-TK$^-$ ρ$^+$ cells harvested immediately after irradiation.

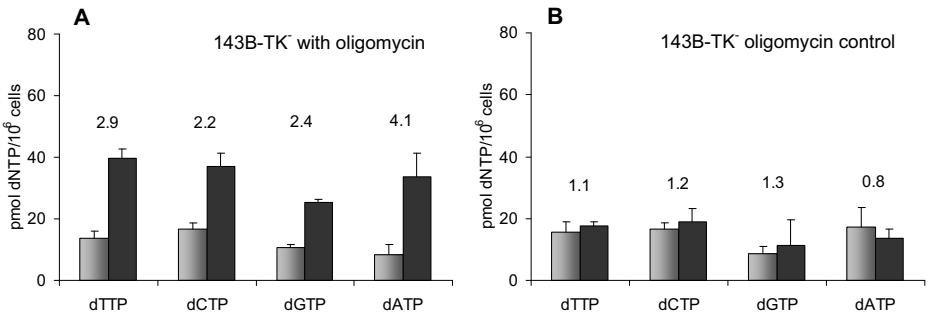

Figure 5. All four dNTP pools increase in oligomycin treated 143B-TK$^-$ (ρ^+) cells after DNA damage.
A: dNTP pools are measured in logarithmically growing 143B-TK$^-$ cells immediately after (grey bars) and 30 hours after (black bars) UV-irradiation with a single pulse of UV light corresponding to the to the LD_{50} of the respective cell lines (254nm, 20 μW/cm^2). All cells are incubated with 0.25 μg/ml oligomycin for 24 hours prior to UV exposure, and the cells represented by black bars also for 30 hours after exposure. B: The cells are treated like the cells in A but without UV-irradiation. The error bars show ±S.D. of two independent measurements.

Discussion

The purpose of the present study was to examine the effect of TK1 and mtDNA deficiency on all four dNTP pools and hence, the 143B-TK$^-$ ρ^+ and ρ^0 cell lines used are TK negative. Previously, we found that the 143B-TK$^-$ cell lines have low dTTP pools (Skovgaard *et al.*, submitted for publication), and here we see that the same is the case for 143B-TK$^-$ ρ^0 cells. Consequently, a potential effect of mtDNA deficiency on dTTP pools could be masked by the TK1 deficiency. A comparison of the dCTP, dATP and dGTP pools reveal that despite of the regulatory function of dTTP on ribonucleotide reductase, none of the other pools differ significantly between the HOS and 143B-TK$^-$ cells (figure 1).

It has recently been shown that several of the dNTP pools in HeLa cells and in MDAMB435 cells are lower in ρ^0 cells compared to the parental ρ^+ cell lines (Desler *et al.*, 2007). A comparison of the dNTP levels for the two ρ^+ cell lines, HOS and 143B-TK$^-$, with those in the 143B-TK$^-$ ρ^0 cells shows that the present work partially agrees with those results. A lower dATP level is found in 143B-TK$^-$ ρ^0 cells than in the ρ^+ HOS and 143B-TK$^-$ cells. The dTTP, dCTP and dGTP pools are the same in 143B-TK$^-$ ρ^0 and ρ^+ cells, however. In both cell lines studied by Desler et al (2007) the most prominent decrease was observed for the dTTP pools but also the dCTP pools were affected in both ρ^0 cell lines. dATP and dGTP pools were only decreased in MDAMB435 ρ^0 cells.

When the changes in dNTP pools are monitored after DNA damage our results show that unlike yeast cells, the dNTP pools in normal mammalian cells do not increase after damage. These data agree with those observed by Håkansson *et al.*, (2006). If the cells are deficient for mtDNA, however, they increase all four dNTP pools 2.2- to 3.2-fold during 30 hours after DNA damage (figure 3C). We also show that this increase in dNTP pools after DNA damage in mammalian cells is likely related to deficient oxidative phosphorylation since inhibition of the ATP synthase in 143B-TK$^-$ ρ^+ cells exhibits the same dNTP pool behaviour after damage as the 143B-TK$^-$ ρ^0 cells (figure 5). The common trait between the

oligomycin-treated cells and the ρ^0 cells are their low levels of the two adenine nucleotides ATP and dATP, both regulators of RNR.

Mammalian RNR activity is stimulated when ATP is bound to the activity site but it is inactivated when dATP is bound. When the activity site is empty the enzyme remains active but at lower activity levels than when ATP is bound (Reichard, 2000). Upon DNA damage the cells respond by up-regulating transcription and translation of R1 (Guittet *et al.*, 2001) and p53R2 (Tanaka *et al.*, 2000). In yeast cells this RNR up-regulation results in an increase of all four dNTP pools which is allowed by a relaxed feedback inhibition by dATP (Chabes *et al.*, 2003). In yeast RNR containing Rnr1 no inhibition is observed at dATP concentrations up to 50 μM, and 50 % inhibition is at approx 80-90 μM (Domkin *et al.*, 2002) whereas mammalian RNR is inhibited 50 % at around 5-20 μM dATP (Eriksson *et al.*, 1979 & Reichard et al, 2000).

We suggest that the increase in dNTP pools observed for 143B-TK$^-$ ρ^0 cells and oligomycin treated 143B-TK$^-$ cells upon DNA damage is also due to a decreased dATP feedback inhibition of RNR. In contrast to yeast cells, where the decreased dATP feedback inhibition is due to a relaxed interaction between dATP and the RNR activity site, we believe that the decreased inhibition observed in this study is caused by low dATP levels in ρ^0 and oligomycin treated cells. Assuming that dATP is evenly distributed in the cells the initial dATP concentration is only 7.8±0.8 μM in 143B-TK$^-$ ρ^0 cells and 1.9±0.8 μM in oligomycin treated 143B-TK$^-$ ρ^+ cells. In contrast, it was found to be 17±6.7 μM in 143B-TK$^-$ ρ^+ and 18±0.4 μM in HOS ρ^+ cells (based on the values presented in figure 1 and 5 and the cell diameters). These data suggest that the low dATP concentrations in the cells with deficient electron transport chain are insufficient to sustain feedback inhibition of RNR after DNA damage. When RNR protein levels are up-regulated, and the dATP feedback inhibition is insufficient, the result is increased dNTP pools as shown in the figures 4C and 6.

In yeast the elevated dNTP pools are believed to be important in order to sustain a more efficient translesion DNA synthesis during DNA damage but translesion synthesis is error-prone and leads to higher mutation rates. It is possible that the increased dNTP pools following DNA damage in ρ^0 cells is also inducing an increased translesion synthesis, explaining the mutator phenotype observed for ρ^0 cells.

The present work does not explain the reason for the decreased dATP levels observed in 143B-TK$^-$ ρ^0 cells and the decrease of all four dNTPs in oligomycin-treated 143B-TK$^-$ ρ^+ but a recent review discusses several possible mechanisms linking mitochondrial function with dNTP biosynthesis (Desler, 2009).

The multiple ways in which mitochondrial dysfunction may affect the cellular dNTP pools clarifies why there is no simple systematic change in dNTP pools in ρ^0 cells. The low initial dNTP pools observed in oligomycin-treated 143B-TK$^-$ ρ^+ cells may be caused by hyperpolarization of the inner mitochondrial membrane leading to increasing NO efflux and inhibition of RNR (Desler, 2009). In a study on murine and human lymphoblasts NO was proven to decrease all four dNTP pools in the absence of deoxynucleoside salvage but when deoxynucleoside salvage was active, NO induced an increase in pyrimidine dNTPs (Roy *et al.*, 2004). The 143B ρ^+ cells are TK1 deficient and hence, the salvage pathway may not respond to NO with a similar pyrimidine increase. The membrane potential in 143B ρ^0 cells is unlikely to be as high as in oligomycin-treated 143B ρ^+ cells, and the low dATP level in these cells may be caused by other mechanisms.

Materials and Methods

Cell Culture

All three cell lines are human osteosarcoma cells originating from the same host. 143B-TK$^-$ ρ^0 is deficient of mtDNA (ρ^0) and thymidine kinase 1 negative (TK$^-$) and originates from 143B-TK$^-$ which is thymidine kinase 1 negative. 143B-TK$^-$ originates indirectly from HOS which is TK$^+$ and ρ^+ and is the oldest of the three cell lines. The 143B-TK$^-$ ρ^0 cells was a gift form Keshav Singh's laboratory, and the HOS cells were received from Chiara Rampazzo. Both the TK$^-$ cell lines 143B-TK$^-$ (ρ^+) (American Type Culture Collection (ATCC) no.: CRL-8303) and 143B-TK$^-$ ρ^0 were grown in DMEM with Glutamax (GIBCO) supplemented with 10 % fetal bovine serum (FBS) (Biochrom AG), 1 % Penicillin/streptomycin (GIBCO) without and with 200 µM uridine, respectively. HOS cells (ATCC no.: CRL-1543) were grown as 143B-TK$^-$ ρ^+ cells but with 7.5 % FBS. When cells are harvested they are trypsinized and resuspended in ice-cold 1 x DPBS (GIBCO). In order to diminish unwanted enzymatic reactions in the cells they are kept on ice while cell concentration and size distribution are determined with a Beckman Coulter Counter Z2.

UV-Irradiation of Cells

Cells subjected to UV-irradiation were set up in 8.8 cm^2 (for cell survival assay) or 145 cm^2 (for cell cycle analysis, dNTP or ATP assays) petri dishes. Prior to UV-irradiation the cells were washed twice with 37ºC DPBS. The DPBS was removed, and the dish was irradiated at varying times with 254 nm UVC light from a 20 µW/cm^2 source. With the exception of cells that were trypsinized and harvested immediately after irradiation, the petri dishes were supplemented with pre-heated medium and stored in the 37 ºC incubator until harvest. Cells for 30 hour experiments are irradiated with 6 hour time intervals, beginning two days after the cells have been seeded, and all cells are harvested 30 hours after irradiation of the first cells (on day three) and immediately after the final irradiation. In experiments with oligomycin inhibition of ATP synthase, cells are incubated with uridine containing medium supplemented with 0.25 µg/ml oligomycin 24 hours prior to irradiation and again after irradiation until harvest. The oligomycin stock solution is 0.25 mg/ml dissolved in 96 % EtOH. Upon addition to the media it is diluted 1000 times giving a final concentration in the media of 0.25 µg/ml oligomycin and 0.096 % EtOH. Cells supplemented with the same amount of EtOH (giving a final concentration of 0.096 %) without oligomycin were set up as controls. ATP levels were unaffected by the small amounts of EtOH in the medium.

Cell Survival Assay with Giemsa Staining

1000 143B-TK$^-$ ρ^0 cells are seeded in 8.8 cm^2 cm petri dishes and irradiated after 16 hours. For UV doses in the higher range; 14-20 J/m^2 dishes with 5000 cells are also seeded. The medium is changed every 2-3 days. After 4-6 days, when non-irradiated control plates contain 170-300 colonies of app. 50 cells each, the cells are washed with DPBS and dried. The cells are fixed and stained with 5 % Giemsa's azure eosin methylene blue in 50 % methanol for 1 hour and rinsed with water. Colonies containing 10-50 cells are counted under a microscope.

Cell Cycle Analysis

0.5x10^6 cells are harvested by 5 min centrifugation at 300xG and 4 ºC, and washed in ice cold DPBS. They are resuspended by slow addition of 70 % ice-cold ethanol during whirl mixing and incubated on ice for 30 min or stored at -20 ºC. The cells are centrifuged and washed in DPBS and centrifuged again, followed by resuspension in 500 µl DPBS containing 0.1 mg/ml RNAse and 40 µg/ml propidium iodide.

The cells are incubated at room temperature in the dark for 1-1½ hours, and DNA content is measured using a Becton Dickinson FACS Calibur fluorescence activated cell sorter. Data were analyzed with Cell QuestPro software and ModFit.

Determination of dNTP Pools
dNTP pools were measured with the DNA polymerase assay (Sherman & Fyfe, 1989) as described in (Desler et al, 2007) with the following modifications: four times 10 µl assay solution aliquots were spotted on Whatman DE81 paper discs and after being washed, the filters were eluted with 0.5 ml eluent containing 0.5 M HCl and 0.2 M KCl. Radioactivity was counted in a Wallac Trilux 1450 Microbeta liquid scintillation counter.

Determination of Cellular ATP Concentration
ATP levels were measured using the luciferase-based ATPLite Luminescence ATP Detection Assay System (Perkin Elmer) according to manufacturer's instructions. The luminescence of triplicate wells containing $0.25x10^6$ cells was measured in a BioTek Synergy HT Microplate Reader at varying sensitivities. Results from sensitivity 150 are used.

References

Björklund S, Skog S, Tribukait B, Thelander L. S-phase-specific expression of mammalian ribonucleotide reductase R1 and R2 subunit mRNAs. Biochemistry. 1990 Jun 12;29(23):5452-8.

Chabes A, Georgieva B, Domkin V, Zhao X, Rothstein R, Thelander L. Survival of DNA damage in yeast directly depends on increased dNTP levels allowed by relaxed feedback inhibition of ribonucleotide reductase. Cell. 2003 Feb 7;112(3):391-401.

Delsite RL, Rasmussen LJ, Rasmussen AK, Kalen A, Goswami PC, Singh KK. Mitochondrial impairment is accompanied by impaired oxidative DNA repair in the nucleus. Mutagenesis. 2003 Nov;18(6):497-503.

Desler C, Munch-Petersen B, Stevnsner T, Matsui S, Kulawiec M, Singh KK, Rasmussen LJ. Mitochondria as determinant of nucleotide pools and chromosomal stability. Mutat Res. 2007 Dec 1;625(1-2):112-24.

Desler C. Mitochondrial dysfunction and altered dNTP levels: Insight into their possible connections. Ph.D. Thesis and mini review, Roskilde University. 2009.

Domkin V, Thelander L, Chabes A. Yeast DNA damage-inducible Rnr3 has a very low catalytic activity strongly stimulated after the formation of a cross-talking Rnr1/Rnr3 complex. J Biol Chem. 2002 May 24;277(21):18574-8.

Engström Y, Eriksson S, Jildevik I, Skog S, Thelander L, Tribukait B. Cell cycle-dependent expression of mammalian ribonucleotide reductase. Differential regulation of the two subunits. J Biol Chem. 1985 Aug 5;260(16):9114-6.

Eriksson S, Thelander L, Akerman M. Allosteric regulation of calf thymus ribonucleoside diphosphate reductase. Biochemistry. 1979 Jul 10;18(14):2948-52.

Eriksson S, Gräslund A, Skog S, Thelander L, Tribukait B. Cell cycle-dependent regulation of mammalian ribonucleotide reductase. The S phase-correlated increase in subunit M2 is regulated by de novo protein synthesis. J Biol Chem. 1984 Oct 10;259(19).

Guittet O, Håkansson P, Voevodskaya N, Fridd S, Gräslund A, Arakawa H, Nakamura Y, Thelander L. Mammalian p53R2 protein forms an active ribonucleotide reductase in vitro with the R1 protein, which is expressed both in resting cells in response to DNA damage and in proliferating cells. J Biol Chem. 2001 Nov 2;276(44):40647-51.

Håkansson P, Dahl L, Chilkova O, Domkin V, Thelander L. The Schizosaccharomyces pombe replication inhibitor Spd1 regulates ribonucleotide reductase activity and dNTPs by binding to the large Cdc22 subunit. J Biol Chem. 2006(a) Jan 20;281(3):1778-83.

Håkansson P, Hofer A, Thelander L. Regulation of mammalian ribonucleotide reduction and dNTP pools after DNA damage and in resting cells. J Biol Chem. 2006(b) Mar 24;281(12):7834-41.

Ke PY, Chang ZF. Mitotic degradation of human thymidine kinase 1 is dependent on the anaphase-promoting complex/cyclosome-CDH1-mediated pathway. Mol Cell Biol. 2004 Jan;24(2):514-26.

Modica-Napolitano JS, Singh KK. Mitochondrial dysfunction in cancer. Mitochondrion. 2004 Sep;4(5-6):755-62.

Nordlund P, Sjöberg BM, Eklund H. Three-dimensional structure of the free radical protein of ribonucleotide reductase. Nature. 1990 Jun 14;345(6276):593-8.

Penta JS, Johnson FM, Wachsman JT, Copeland WC. Mitochondrial DNA in human malignancy. Mutat Res. 2001 May;488(2):119-33.

Rampazzo C, Ferraro P, Pontarin G, Fabris S, Reichard P, Bianchi V. Mitochondrial deoxyribonucleotides, pool sizes, synthesis, and regulation. J Biol Chem. 2004 Apr 23;279(17):17019-26.

Rasmussen AK, Chatterjee A, Rasmussen LJ, Singh KK. Mitochondria-mediated nuclear mutator phenotype in Saccharomyces cerevisiae. Nucleic Acids Res. 2003 Jul 15;31(14):3909-17.

Reichard P. Interactions between deoxyribonucleotide and DNA synthesis. Annu Rev Biochem. 1988;57:349-74.

Reichard P, Eliasson R, Ingemarson R, Thelander L. Cross-talk between the allosteric effector-binding sites in mouse ribonucleotide reductase. J Biol Chem. 2000 Oct 20;275(42):33021-6.

Roy B, Guittet O, Beuneu C, Lemaire G, Lepoivre M. Depletion of deoxyribonucleoside triphosphate pools in tumor cells by nitric oxide. Free Radic Biol Med. 2004 Feb 15;36(4):507-16.

Sherman PA, Fyfe JA.Enzymatic assay for deoxyribonucleoside triphosphates using synthetic oligonucleotides as template primers. Anal Biochem. 1989 Aug 1;180(2):222-6.

Skovgaard T, Rasmussen LJ, Munch-Petersen B. Thymidine kinase 1 deficient cells show increased survival rate after UV-induced DNA damage. Submitted for publication.

Tanaka H, Arakawa H, Yamaguchi T, Shiraishi K, Fukuda S, Matsui K, Takei Y, Nakamura Y. A ribonucleotide reductase gene involved in a p53-dependent cell-cycle checkpoint for DNA damage. Nature. 2000 Mar 2;404(6773):42-9.

Thelander L, Reichard P. Reduction of ribonucleotides. Annu Rev Biochem. 1979;48:133-58.

Uhlin U, Eklund H. Structure of ribonucleotide reductase protein R1. Nature. 1994 Aug 18;370(6490):533-9.